DOCTOR OF PHILOSOPHY

Optical characterisation of suspended particulate matter in estuaries and near coastal waters

Law, Douglas J

Award date:
2001

Awarding institution:
University of Wales, Bangor

Optical Characterisation of Suspended Particulate Matter in Estuaries and Near Coastal Waters.

Douglas J Law

A thesis submitted to the University of Wales for the degree of Doctor of Philosophy

University of Wales, Bangor
School of Ocean Science
Menai Bridge
Gwynedd
LL59 5EY, UK

In collaboration with
Plymouth Marine Laboratory

June 2001

Abstract

Recent advances in focused beam reflectance technology have resulted in new instruments with the potential for particle size determination in natural waters. A commercially manufactured instrument based upon this principle has been adapted to allow the size distribution of suspended particulate matter in estuaries and coastal waters to be determined in-situ. After calibration, the standard instrument has been shown to be capable of providing accurate, undisturbed particle size distribution data over a wide range of particle concentrations (10 mg l^{-1} - 50 g l^{-1}), irrespective of current speed and, to a large extent, particle composition and density. Following modifications, the instrument underwent field trials and deployments within the Humber Estuary and Coastal zone along the East Coast of England. A further study as part of LISP (UK), upon the Intertidal mudflats of Spurn Bight demonstrates the instruments flexibility and potential in providing high-resolution data. Data obtained from these studies have revealed large temporal and spatial variations in the size distribution of suspended particles over a tidal cycle and along the estuarine salinity gradient. The largest particles occurred near the bed during periods of slack water where median diameters reached 500 μm. This was attributed to the sedimentation of large aggregates. Rapid reductions in median particle size coincided with periods of strong tidal current acceleration after low water slack current. At maximum current velocity on the flood tide, mobilisation of sediment from the bed gave rise to larger particles in the water column. Under similar conditions at low water slack in the turbidity maximum, aggregation of the much smaller flocs (90 μm) and subsequent sedimentation did not occur. Particle sizes remained low until high water slack (400 μm) when lower particle concentrations were encountered. Multivariate analysis indicated that combinations of current velocity, shear, turbulent eddy scale and particle concentration provide site-specific predictors of particle size. Despite the occurrence of small particles in the turbidity maximum, the pattern of particle size variation with particle concentration and shear stress is consistent with the conceptual model proposed by Dyer (1989).

Acknowledgements

Supervision

Throughout the course of this project I have had to draw on the support of many colleagues and in this section I would like to recognize those who have been especially influential in determining the success of the project. My joint supervisors Dr Anthony Bale and Dr Sarah Jones not only provided me with the opportunity to carry out this work but strove to make it a success. I'd also like to thank them for their thoughts and contributions throughout the project and whilst writing this thesis. My thanks also go to Colin Jago, who has on many an occasion given me the opportunity to partake in field work and has provided much in the way of support and input into the interpretation of the field results.

Fieldwork & Collaboration

Much of the fieldwork in the Humber could not have taken place without the help and guidance of Dr Reg Uncles. I must also thank him for the use of his water quality and current data in this work and for his opinions on the processes involved. My thanks also go to John Stephens and Norman Bowley for their able assistance in the carrying out of the surveys as well as for their thoughtful conversations.

There are many others who have participated in the fieldwork, to whom I am grateful for their time and effort. Mike Fennessy and Malcolm Christie deserve special thanks for their help on the Tamar and in providing data from the LISP project. Thanks also to Chris Bull and John Phillips for comparative work in the lab and field.

Technical

I am indebted to Ian Gilson and Dave Purse for their sterling work on the construction of the modified instrument, along with a host of other projects. However, much of the praise for the success of the technical adaptaion should go to Colin Barrett for his massive input into the project, from design and construction to last minute maintenance.

Having participated in several of the LOIS RACS cruises, I would also like to thank the Officers and crew of RRS Challenger as well as Peter Sergeant, the skipper of the NRA research vessel Seavigil. Taking part in the LOIS RACS (C) cruises allowed me to meet many varied characters who all contributed in some way to the success of this project, none more so than the likes of Steve Widdecombe, Tristan Sjoberg and Neil Hudson.

Lastly but by no means least I would like to thank my wife Alison, who has given me the motivation and support to complete this work. Thank you.

For Alison & our daughter Esmée.

Presentations & Conferences Attended

EC MAST Advanced Study Course : Analysis of Marine Particles, June 1993 University of Bergen, Bergen, Norway. 14 day study course / workshop. Presentation: Law D.J. Development of an optical instrument for in-situ particle sizing.

ECSA 23 Symposium : Particles in Estuaries and Coastal Waters, September 1993 Groningen, Holland. 5 day conference. Poster: Law D.J., Bale A.J. & Jones S.E. Evaluation of a laser backscattering particle sizer, for in-situ deployment in Estuarine and Coastal Waters.

INTERCOH 94 - The 4th Nearshore and Estuarine Cohesive Sediment Transport Conference, 11-15 July 1994 HR Wallingford, England. 5 day conference.

Geological Society. 1994 Burlington House, London 1 day conference. Presentation: Evaluation of FBRM for in-situ deployment in Estuarine and Coastal Waters.

LISP (UK). 1995 University of Cardiff, UK. 1 day conference. Presentation: Suspended particulate size characterisation on an intertidal mudflat using FBRM.

Publications

Law. D.J. & A.J. Bale 1998. In-situ characterisation of suspended particles using focused-beam, laser reflectance particle sizing. In: Black, K.S., Paterson, D.M. & Cramp, A. (eds) Sedimentary Processes in the Intertidal Zone. Geological Society, London, Special Publications, 139, 57-68.

Law D.J., Bale A.J. & Jones S.E. 1997. Adaptation of focused beam reflectance measurement to in-situ particle sizing in estuaries and coastal waters. Marine Geology 140, pp47-59.

Jones S.E., Bale A.J. & Law D.J. 1996. Temporal and spatial variability of in-situ suspended particle size in the Humber Estuary and Holderness coastal zone. NERC Final Report, December 1996. GR3/09469.

Jones S.E., Bale A.J. & Law D.J. 1995. Development of an instrument for in-situ particle sizing using laser backscatter spectrometry. NERC Final Report, March 1995. GST/02/665 SIDAL Special Topic.

Contents

List of Figures

List of Tables

The Characterisation of Estuarine and Coastal Suspended Particulate Matter

1.1 Introduction

In the estuarine and coastal environment, the behaviour and nature of sediment has important environmental and economic implications. Historically, estuaries in developed countries have been areas of prime industrial importance. As popular sites for large ports they allow navigable access well into the interior of countries. Estuaries also provide a seemingly direct route for inland waste and effluent disposal to escape to sea. Hence, they have attracted large-scale conurbation as well heavy as industries such as steel and petrochemicals.

The behaviour of sediment is of prime importance in the management of navigable waterways. Harbour and channel siltation are particular problems in the maintenance of a port and the cost can be financially prohibitive. Improved understanding of vertical and horizontal sediment fluxes affected by changes in particle density and size would bring about direct benefits in the management of the coastal environment (Dobereiner &

McManus, 1983; van Leussen, 1991). Natural water-borne particles are now recognised as being important in the dispersion and residence times of man made pollutants in estuaries and coastal waters, which are often, sites of industrial and domestic waste disposal. Pollutants become rapidly concentrated upon the surfaces of particles through the mechanism of physio-chemical adsorption. Alternatively, dissolved substances may become trapped in the pore waters of particle aggregates and unconsolidated bed sediment (Hart, 1982; Thorn & Burt, 1983; Abarnou, 1987; Morris, 1986). The dispersion of chemicals, such as radionuclides, PCB's (Polychlorinated Biphenyl), organic pollutants (e.g. Organophosphates) and trace metals is then linked to the fate of the contaminated bed sediment or suspended particulate matter (SPM). The aquatic food chain may also be influenced by the presence of SPM, through the attenuation of the light field in the water column. This may have significant effects upon primary production and thereby affect the upper trophic structure (Colijn, 1987). The environmental and economic impact of estuarine sediment behaviour indicates that the measurement of particle characteristics in the natural environment will not just deliver a better scientific understanding, but also bring about environmental and economic benefits.

1.2 Characterisation of Suspended Particulate Matter

1.2.1 The Importance of Particle Size in Particulate Matter Characterisation

The term suspended particulate matter (SPM) refers to material, of organic as well as inorganic origin, which occurs in suspension (permanent or transitory) in the water column. The lower end of the SPM size scale grades into dissolved matter and colloids. However, it is generally accepted that SPM is the residue left after filtering the water through a 0.45 μm glass fibre filter paper (GF/C). As an upper limit to particulate size, Sheldon (1972) considered all living (and dead) animals in the aquatic environment as

bona fide suspended particles, in an attempt to estimate fish stocks in the worlds oceans from the extrapolation of fine particle measurements with whales representing the end member. However, it is nominally the non-living particles, which are of prime importance from a sedimentological perspective. In the low particle concentrations of the open ocean, non-living particles in the form of large mucal webs, assemblages of inorganic particles and planktonic organisms tenuously held together by a web of mucus, may extend to several metres in diameter. Whilst, the more common marine snow, an aggregate of inorganic particles and organic debris, exists on the scale of centimetres (Aldredge & Silver, 1988). However in the more turbulent coastal and estuarine waters where particle concentrations may be up to 200,000 times greater, the size range is apparently more limited, between 0.45 μm and 5 mm, but includes planktonic species as well as mixed assemblages (aggregates). The composition of particles in such waters may vary greatly to include inorganic particles of clay to sand sized grains, of varying mineralogy. It may also include organic bi-products such as faecal pellets and mucus, organic detritus such as fragments of calcareous and siliceous tests, terrigenous debris such as humus and plant debris as well as dead or living phyto and zooplanktonic organisms, such as algae and copepods. The composition of particulates has the potential to greatly affect the characteristics of particle size and density. In doing so, it affects particle settling velocity and thus the transport behaviour of particles in suspension. However, it is only one factor in what is a complex set of relationships between sediment behaviour and physical, chemical and biological controls.

Much recent *in-situ* work has been undertaken primarily in Northern European and North American estuaries, in order to elucidate the spatial variability in size and settling characteristics of suspended particles. The type of surveys carried out for this purpose have included sampling along the salinity gradient of an estuary (Eisma et al, 1991a; Gibbs

et al, 1989), vertical sampling at way points (Gentien et al, 1995) and over a tidal cycle whilst at anchor (Bale et al, 1989; Eisma et al, 1991b; McCabe et al , 1992). The dominant objective being, to bring about a clearer understanding of the relative importance of turbulent shear, salinity, pH and particle composition/mineralogy to changes in SPM character, their transport and thus, the fate of associated trace metals and pollutants.

1.2.2 The Fundamentals of Particle Sizing

1.2.2.1 Problems Associated with Particle Size Measurement

When the size of a particle is to be characterised by one singular value, there are several factors which need to be taken into account before an accurate and valid representation can be provided. It is necessary not only to take into account the particles shape, but also the orientation of the particle within a particular frame of reference. The frame of reference describes the interaction between the method of measurement and the particle. In the case of the Focussed Beam Reflectance (FBRM) technique it is the provision of a chord measurement from a focussed beam passing over the surface of the particle. For Electrozone resistive measurements it is the relationship between volume and resistance within the sensing zone that describes the frame of reference. If a sphere is to be measured, it can simply be described by it's diameter, this is a unique measurement which describes the particle exactly. It is independent of it's orientation to the frame of reference due to it's symmetry in all directions. When we consider particles that are not spherical, it becomes impossible to characterise a particle size in terms of one value. For example, a cube which has equal dimensions of 50 μm along six sides, the diagonal measurement on a face would be 70.7 μm whilst the internal diagonal would be 86.6 μm. For other regular shapes the number of possible dimensions used to describe a particle is greater and for irregular shapes, the situation is considerably more complex. Given that natural water borne particles generally have complex irregular shapes some means of relating dimensional measurements to a unique value is required, most commonly this is the technique of Spherical Equivalency.

1.2.2.2 Providing a basis for measurement – Spherical Equivalency

If the volume of a particle was known, in some cases this can be provided by direct measurement, such as in Electrozone counting, then it is possible to describe that particle's dimensions with one unique value. This is done by calculating the equivalent spherical diameter of the particle volume (V). If we assume that the volume measured equates to spherical particle, then the diameter (D) of the particle can then be calculated from:

$$D = 2 \times (3V / 4\pi)^{-3} \qquad [1.1]$$

This method provides a diameter for irregularly shaped particles, which is the equivalent of a sphere of the same volume, hence the term Spherical Equivalent (SpEq). This method does not provide an absolute measurement of particle size; rather it provides a basis for comparative measurement. The technique is not only applied to measurements of particle volume, particle sizing methods employing chord measurement such as FBRM and 'Time of Flight' (TOF – Galai CIS-1), which initially produce particle chord distributions, through mathematical algorithms can generate an SpEq distribution. Whilst differing techniques of measurement appear to provide unanimity in terms of a value to describe a particles size, care must be exercised in the direct comparison of the results. Not only do techniques vary in their response to particle shape, the generation of spherically equivalent diameters will not come about in exactly the same manner. This is because the particle property that is being measured and the way they interact with the measuring device differ from one technique to another. For instance FBRM directly measures chords, whilst Low Angle Laser Scattering (LALS) or Laser Diffraction use and algorithm to generate weight distributions based upon the diffraction pattern. Electrozone resistance measurements generate distributions based upon the resistivity of a particle and equate this to its volume. Simple measurements involving sieving effectively calculate a distribution based upon the minimum diameter as particles pass through a mesh. Because each technique is measuring a different aspect of the particles size, each technique will treat the particle differently, this will result in discrepancies between the calculated spherical equivalent diameters

generated. The scale of the differences will depend upon the size and the property of the particle measured.

1.2.2.3 The Relationship between Particle Volume and Number Distributions

Before a suitable method of particle sizing can be implemented it is necessary that the requirements of the size analysis are fully understood, in particular whether it is the number of particles in a given size class which is of interest or rather their volume contribution. This is essential due to the differences in the bias for number and volume distributions, number favouring smaller particles whilst volume favours larger particles. This is easily demonstrated when we consider as an example the number of 10 μm particles that would go to make up the volume of a 100 μm particle, it would be 1000. Table 1.1 illustrates this relationship between particle number, size and their contribution to the population volume.

Diameter	Particle Number	% of Particle Number	% of Particle Volume
4	15000	77.58	0.02
15	3040	15.72	0.26
50	1033	5.34	3.29
150	245	1.27	21.05
400	15	0.08	24.44
1000	2	0.01	50.93

Table 1.1 Illustration of the relative volume contribution of particle number versus particle size.

1.2.2.4 Basic Mathematical Representation of Particle Size Distributions

If we are looking to easily describe and represent the evolution of particle populations in the natural environment, then some form of tool is necessary which allows the particle population at any given instant to be simply characterised. Several basic mathematical descriptors are available which to varying degrees provide a representation of the particle population with a single number. At a very basic level we have the Population Mean, Median and Mode. For a normal or Gaussian population distribution each of these values will be identical. For more complex or multimodal distributions there will be discrepancies between each of the descriptors as they describe differing mathematical characteristics of the particle population (Figure 1.1).

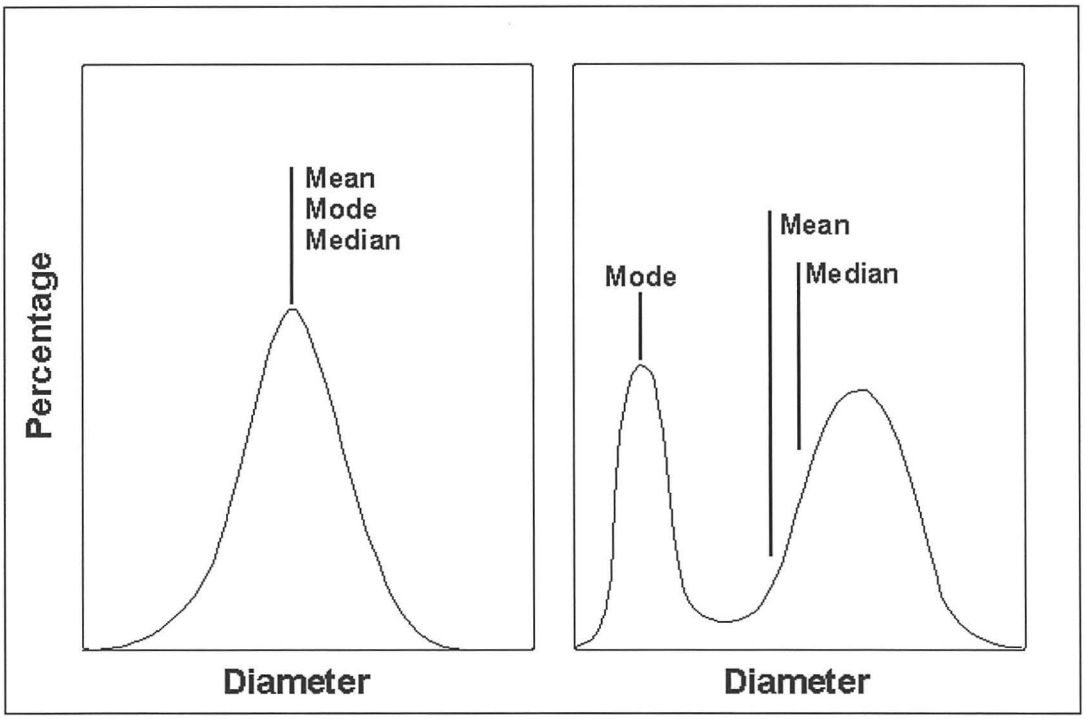

Figure 1.1 Illustration of the relationship between the distribution descriptors and the type of distribution, for a Normal (Gaussian) distribution and a Multimodal distribution.

The Mode is simply the highest point on the curve, or rather, the size class with the highest frequency of particles. The Median marks the 50^{th} percentile, the point at which

50% of the population fall above and below this value, whether by number or volume. The Mean is the mathematical average of the particle population. The Mode and Median are calculated from the particle size distribution, whether that distribution is based upon a particle number frequency or as a percentage of total volume or surface area. When the Mean or average is calculated from a frequency distribution it is necessary to understand in what way the population would be best represented given the ultimate use for the data. If surface area or volumes are important in the understanding of particle dynamics then the Mean (as well as Median and Mode) of the population can be calculated simply from the following (Rawle, 2000):

$$\text{Number Frequency Mean} = \frac{\Sigma d}{N} = D(1,0) \qquad [1.2]$$

$$\text{Surface Area Mean} = \frac{\Sigma d^2}{N} = D(2,0) \qquad [1.3]$$

$$\text{Volumetric Mean} = \frac{\Sigma d^3}{N} = D(3,0) \qquad [1.4]$$

Equations 1.3 and 1.4 are derived from the dependence of the surface area upon the square of the radius ($4\pi r^2$) and volume upon the cube of the radius ($4/3\ \pi r^3$). The average is calculated from the sum of diameters (d) divided by the number of particles (N). This method of calculation requires that a large number of particles are measured, hence another form of averaging may be used, that of moment means. In this case a second diameter term is used to provide an average or mean which provides an indication as to the central point of the frequency, in effect the centre of gravity for the distribution, thus alleviating the need for particle counting. These equations are described below for surface area and volumetric distributions:

$$\text{Surface Area Moment Mean} = \frac{\Sigma d^3}{\Sigma d^2} = D(3,2) \qquad [1.5]$$

$$\text{Volumetric Moment Mean} = \frac{\Sigma d^4}{\Sigma d^3} = D(4,3) \qquad [1.6]$$

The distribution descriptor which we choose to use, is to a large extent dependent upon the method of measurement, for example Optical Microscopy generates a Number Frequency Distribution (D(1,0)) mean. It is also necessary to bear in mind that should a non moment mean be provided (D(1,0), D(2,0) & D(3,0)), that a sufficient number of measurements should be taken, a recommendation by Gibbs (1985) being 3000 samples in the modal class.

1.2.3 Techniques and Instrumentation used in Particle Size Analysis.

In order to understand sediment behaviour and thus quantify its effect upon the chemical, biological and physical environment it is of prime importance to obtain measurements of the particle characteristics, which influence this behaviour. Sediments in estuarine and coastal waters may be physically characterised in several ways, for example size, density, strength, porosity or settling velocity. These properties exhibit considerable temporal and spatial variability which, combined with the inherently fragile nature of water-borne particles, greatly complicates their measurement (Chanut & Poulet, 1982; Gibbs, 1983; Dobereiner & McManus, 1983; Eisma, 1986; Bale et al, 1989; McCabe, 1992; van Leussen, 1993). SPM in estuarine and coastal waters is largely comprised of aggregates of finer material such as clay particles and organic material. These aggregates, which may grow to several millimetres in size, may be easily disrupted and broken down into smaller more resistant particles. Methods of particle characterisation which involve physical manipulation (bucket, pump or water bottle sampling) have been shown to bias the analysis in favour of particle fragments (Gibbs, 1983; Eisma, 1986; Bale & Morris, 1987). For this reason, several workers have attempted to measure the size distribution of suspended particles using in-situ optical techniques in order to avoid or minimise the disruption of fragile particle aggregates.

Current methods of in-situ particle size determination, such as Photography (Eisma, 1986; Gibbs et al, 1989; Kranck & Milligan, 1992), Laser Diffraction (Bale et al, 1984; Agrawal & Pottsmith, 1994; Gentien, 1995), Video microscopy (van Leussen, 1993)

and Holography (Costello, 1989) have provided limited information relating the size and settling velocity of particles. The limitations of such techniques preclude deployment in environments with either high particle concentrations, large current velocities or a rapidly changing dynamic environment. UNESCO (1988) identified the need for improved in-situ particle size characterisation combined with the study of aggregation processes. New in-situ methods are required to encompass a greater range of particle sizes (primary particles to macro aggregates which range from 125 μm to several mm), a wider range of suspended particulate loads (10s to 1000s mg l^{-1}) and at greater current velocities (>1 m s^{-1}) (UNESCO, 1988).

Rapid improvements in laser optical techniques have resulted in an extensive choice of particle size analysers which have been made commercially available to the researcher, such as CILAS, GALAI CIS-1, Malvern 2200 and the Lasentec PAR-TEC series. However, these instruments possess varying degrees of effectiveness in coping with sudden or wide ranging changes in SPM. With the exception of the CILAS 925 (IFREMER & CILAS inc.) few are capable of operating in-situ, being available only as laboratory based instruments. Modification to such laboratory instruments for use in-situ have been carried out, most notably to the Malvern 2200 laser diffraction system (Bale & Morris, 1987) and more recently to the Par-tec100 FBRM system (Law et al., 1997). Modifications to existing non-optical laboratory systems have also included the Coulter Counter (Maddux & Kanwisher, 1965). As there is a wide variety of particle sizing techniques currently available to the researcher, only those directly relevant to this study will be explained in detail below. However, more scope will be given to the application of techniques to in-situ particle sizing.

After initial doubts expressed concerning its treatment of fine particles (McCave, 1991), laser diffraction or Low Angle Light Scattering (LALS), has now gained wide acceptance in the study of naturally occurring sediments (Bale & Morris, 1987; Gentien,

1995; Agrawal & Pottsmith, 1994). Laser diffraction instruments generally utilise a Helium Neon laser to size particles according to the diffraction pattern produced by the suspended population, when illuminated by the laser beam. The particles, which are assumed to be spherical, pass through the laser beam scattering light at angles that are inversely proportional to their size. Undiverted light is focussed by a Fourier lens onto the centre of an array of photosensitive detectors (Figure 1.2). The central detector, known as the obscuration detector, registers only undiverted light. As particles diffract light from the central beam it falls onto the semicircular arrangement of photodiodes, each increasing in size from the centre. The smaller the particle population then the greater will be the degree of diffraction. Diodes on the outer edge of the semicircle will then register increased radiation. In using a Fourier lens in conjunction with the spacing of the photodiodes, light scattered from a particle will always fall on the same part of the detector array irrespective of it's position in the laser beam (Figure 1.2). This allows the particle size distribution to be produced from the distribution of radiation across the photodiodes. The particle size distribution is modelled from the distribution of radiation and calculated in a heuristic manner using Mie theory. Reporting of size distribution takes the form of the percentage of total weight over 16 size classes on a logarithmic scale, by assuming a constant particle density this may be equated to volume.

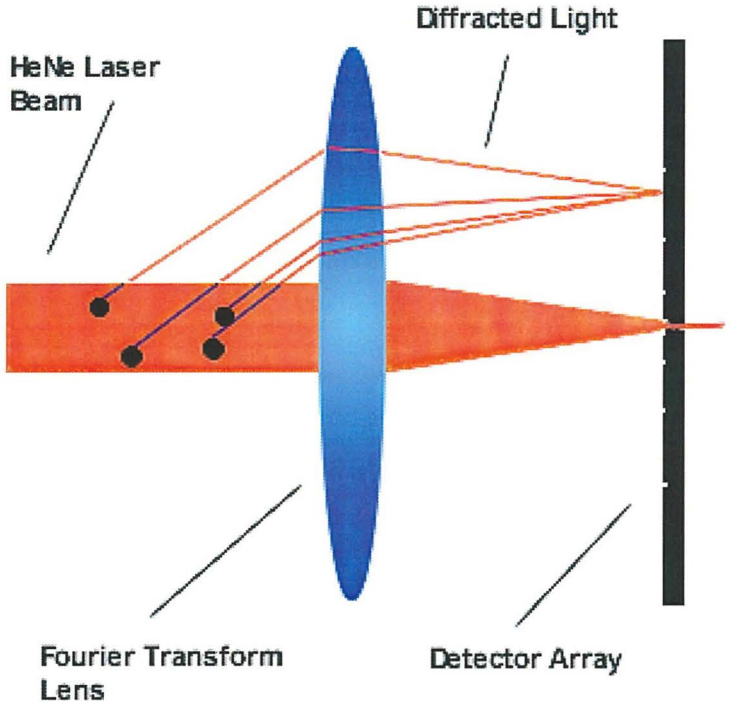

Figure 1.2 Principal of LALS (Low Angle Light Scattering) particle sizing technique, illustrating the paths of scattered light through a Fourier lens upon their illumination by a He/Ne laser.

Electro-resistive particle sizing has gained widespread acceptance in the marine community after its initial use for cell counting in the medical sciences. It has been successfully used in plankton studies and lends itself well to primary particle analysis. It is based upon changes in the electrical resistance of a volume of electrolyte, due to the presence of non-conductive materials, namely particles. The material under analysis is suspended in an electrolyte, a known volume is then displaced from the containing vessel into the instrument probe. As the particles pass through the small sampling orifice in the probe, they change the electrical resistance of the gap between two electrodes in the orifice wall. The increase in resistance seen as a voltage pulse / peak is related to the particle volume. Although the method is largely independent of particle shape, particle composition may cause significant variation, particularly as the size is measured not as an absolute, but rather in comparison to a latex standard. One advantage concerning particle

shape is it's independence of particle orientation, this is accounted for by measuring the volume under the peak rather than the height of the peak itself. The particle size distribution is then derived as a volume distribution and may also be measured as a number or surface area distribution. Although with modern Electro-zone particle counters, a size range of 0.4μm to 1200μm is achievable, the use of set orifice sizes means that this can only be achieved in several measurements by changing orifices. The effective size range measured is proportional to the orifice diameter, such that the minimum and maximum sizes measured are 20% (2% in later models) and 60% of the orifice size, respectively. Channel resolution is high, nominally being capable of 256-channel resolution, although improvements in digital technology now allow greater then 25,600-channel resolution.

The use of time of flight (TOF) particle size analysis has grown in use since the development of solid state lasers. There are effectively two forms of TOF, that of laser reflectance which will be dealt with in the next chapter and laser interruption, used in instruments such as the Galai CIS-1 (Jantschik, 1992). Laser interruption uses a laser diode to produce a beam of light that is scanned to describe a circle. Particles intercepting the beam reduce the incident light detected by the photo detection system, situated directly in line with the laser. The duration of the reduction will depend upon the speed of the beam across the particle and the size of the particle. As the scanning velocity of the beam is known, the size of the particle may be derived from the duration of the reduced light and the scanning speed ($d = v / t$, d=particle diameter, v=scanning speed, t=duration of flight (TOF)). Resolution of the Galai CIS-1 is comparable to that of the Coulter Counter, with 2 μm sizing channel widths over a range dependent upon the optical set-up. By altering the optical set-up the upper size limit may be varied between 200 μ and 2500 μm.

1.3 Size classification of suspended particulates

1.3.1 Natural State of Suspended Particulates

By its very nature the characterisation of natural SPM is problematic. Particles in the natural environment are in a state of flux, as they possess the potential to aggregate and disaggregate according to the dominant physical and biological conditions. This process of change is reflected in the fundamental physical characteristics of particles such as; size, density, strength and shape. Natural particles exist across a broad range for each of these properties, yet three general particle classes have been characterised in estuaries (Eisma, 1986), principally through the comparison of in-situ and discrete particle size measurements. The classifications are:

Primary particles: These are singular entities consisting chiefly of mineral grains, although plant debris may be considered a primary particle. As clay particles form the major component in turbid estuaries (seconded by quartz), the typical particle size is generally accepted as being around 1 μm, a density of $2.2gcm^{-3}$ or $2.65gcm^{-3}$ is used depending upon whether clay or quartz, respectively, is present.

Microflocs: Primary particles aggregate under suitable conditions with organic matter, to form tightly bound, highly stable microflocs. They have excellent resistance to turbulent shear, with high net binding strengths (Ani et al, 1991), a size range of 5-125 μm and a generally spherical shape.

Macroflocs: These are large, up to 4mm, voluminous aggregates of microflocs or smaller macroflocs, with inherently low net binding strengths (Ani et al, 1991), owing to their formation under conditions of viscous flow or in quiescent waters. Their density approaches that of water, with 90% of the particles volume consisting of pore space (Gibbs et al, 1983b). In general macroflocs have been defined as sickle shaped, irregular or cylindrical (Gibbs, 1985), in detail, however they are highly fractal (Jiang & Logan, 1991).

Suspended particles, especially macroflocs, are often fragile entities, which may be easily disrupted by the method of entrapment (Gibbs, 1983) or analysis (Bale & Morris, 1987). Methods resulting in the breakage of suspended particles will bias subsequent analyses in favour of the fragments and will not represent the characteristics of particles in their natural state. Therefore, to accurately assess particle characteristics in the natural environment, *in-situ* methods of analysis, resulting in a minimum of disruption, are vital.

1.3.2 Non Disruptive In-situ Particle Sizing Techniques

Systematic comparisons of different sizing techniques are generally rare, where they have taken place it has involved laboratory based instrumentation (Syvitski, 1991), with the exception of a recent inter-calibration exercise carried out on the Elbe (Eisma et. al., in press). Given that natural particles differ greatly from calibration materials, which are extensively used to assess the accuracy of instruments. The accuracy of particle sizing instrumentation is commonly evaluated using calibration standards. Whilst these represent an excellent benchmark for laboratory comparison, the considerable differences between these and naturally occurring particles requires that con-current operation of *in-situ* instrumentation is necessary in evaluating the validity of new instrumentation.

As one of the more commonly used techniques in Marine Science, LALS provides rapid analyses, a relatively low level of sample disruption and an measuring range covering microflocs to small macroflocs (<600 μm). Because of this it has been used widely and successfully in riverine, estuarine and coastal environments (Bale et al, 1984, 1987; 1989; 1991; McCabe et al, 1992; Agrawal & Pottsmith, 1994; Gentien et al, 1995). However, its effectiveness at extremes of particle concentration, where SPM concentration falls below $1mgl^{-1}$ or rises above $450mgl^{-1}$, has come into question (Bale & Morris, 1987; Barton et al, 1991). Also, the working range is limited at any time through the choice of lens to 5.8 - 564 μm (Malvern2200) or 1 - 500 μm (CILAS 925), also doubts have been expressed over its application of Fraunhofer diffraction to particle sizes approaching the wavelength of light (Agrawal et al, 1991; Eisma, 1990).

Widely used in the deep sea environments, *In-Situ* Photography (Benthos plankton camera) is severely limited by SPM concentration and was initially confined to particles >50 μm, owing to the limitations of particle resolution (Eisma, 1986; Gibbs et al, 1989; Kranck, 1992). More recently Eisma et al (1990) has developed a camera system employing 3 lenses covering a range of 3.6 μm to 644 μm. Beyond 644 μm qualitative imaging of larger particles is possible. Image blur at high current velocities is avoided by allowing the rig to drift with the current. This also helps to avoid induced turbulence as the net shear is very low, although this is limited to $1.5ms^{-1}$, whereupon floc breakage is reported to occur. This is because the particles have to pass between the light source and the camera lens, the funnelling effect of the water between these two interfaces inducing a higher shear than is present in the water mass, resulting in floc breakage. As with other camera systems it is limited by high SPM concentrations, as particles become obscured on the photographic image. At low SPM concentrations there maybe an insufficient number of particles on one frame to provide statistically meaningful results. Another limitation being the number of exposures available, with 250 generally being the maximum (Eisma et al (1990)) reducing the capability for long term deployment. Although systems allowing up to 6000 exposures, specifically designed for long term deployments in the deep ocean are under development (Volker Ratmeyer (pers. comm.)).

Recent developments in video and image analysis software have allowed the use of Video systems in the determination of in-situ particle settling velocities. Particles are allowed to settle under controlled conditions after carefully trapping or removing them from the dynamic environment. Particles maybe trapped by allowing them to settle into a submerged chamber and then into a lower settling column (van Leussen, 1993). Alternatively, the mechanical entrapment of a body of water allowing particles to settle out into a lower column containing water of similar salinity (Fennessy et al, 1994). Images of settling particles in the column are recorded on videotape for subsequent determination of settling velocities through image analysis. Both methods of entrapment involve separation of particles from the natural turbulent energy field, possibly creating significant changes to the frequency and mechanism of collision. For van Leussen's system the lower size limit

is determined by the image pixel size, 10-15 μm, with an upper limit approaching 4mm. Maximum turbidity is stated as being $600mgl^{-1}$, although a loss of clarity and particle masking effects may induce significant errors.

Optical Backscatter Sensors (OBS) and Beam Transmissometers, instruments commonly used for *in-situ* SPM concentration determination, have also received attention for their potential in particle sizing (Benns, pers. comm.), although their dependence upon particle nature, shape, refractive index as well as SPM concentration makes for difficult calibration.

Holography (Gibbs et al, 1989) has been little used for in-situ particle sizing. Whilst it provides detailed images of flocs in-situ (2D or 3D) beneficial to shape characterisation, like photography and video it is limited by particle masking effects caused by high SPM concentration. In common with most systems employing an orifice or two analytical interfaces such as photography, there is also the probability of floc breakage resulting from changes to the velocity field between the two interfaces. This problem is inherent in the application of electro-resistance techniques to in-situ particle size analysis, due to the requirement for very small orifice (of the order of μm's to mm's). Whilst adaptations to a Coulter Counter (Maddux & Kanwisher, 1965) may have provided size information on primary particles, the need for a small orifice and an electrolytic medium make this method unsuitable for fragile aggregates and regions of low salinity.

1.4 In-situ observations of particle size distributions

1.4.1 Variation in Particulate Sizes Observed using Non-Disruptive Techniques

The size of particles observed *in-situ* varies according to coastal location and method of analysis. Spectra with particles ranging from a few microns to 0.5-4mm are common in estuaries (Eisma et al, 1991b, Table 1.2). In some cases the size is limited by the instrumentation used and even larger flocs may exist.

Author	System	Maximum floc size
Bale & Morris (1987)	Tamar estuary	500 μm
Eisma et al (1991a)	Scheldt estuary	500 μm
Kranck & Milligan (1992)	San Fransisco bay	> 500 μm
Gibbs et al (1989)	Gironde estuary	500 μm flocs, consisting of 100 - 200 μm aggregates.
Eisma (1983) & van Leussen (1993)	Ems estuary	1 - 4 mm

Table 1.2 Maximum floc sizes measured in-situ by various authors.

In oceanic waters, marine snow consisting of largely biogenic material, such as diatom tests, detritus and faecal pellets, in many cases bound by mucal filaments, appear to be most abundant in the 1 to 2.5mm range. Although larger than 10mm particles are less abundant, they do commonly occur (Asper, 1987) and it is such large particles that are important in the vertical flux of nutrients to bottom dwelling communities on the sea floor. The shape of marine snow varies greatly, including shapes such as irregular, comets, spheroids and oblate spheres; hence diameters range from 0.5 to 25.5mm with lengths of 2.4 to 75.5mm (Alldredge, 1988). Large mucal structures of around 1m have been

observed and successfully entrapped with the aid of ROV's (remote operated vehicles) and manned submersibles.

1.4.2 Particle Sizes within the Estuarine Environment

The size distribution of SPM along the salinity gradient exhibits considerable spatial and temporal variation. It is perhaps because of this and the fact that electrolytes promote aggregation of clean clay suspensions (without organic coatings) by suppressing the electrical double layer, that salinity was held to be a key factor in the aggregation of riverine particles at the salt/fresh water interface. Early particle size measurements in the Tamar estuary by Bale & Morris (1987) which employed discrete sampling methods, indicated an increase in the floc fragment size into the fresh riverine waters. This was seen as 70 μm (at 0‰) with 25 μm (at 21.5‰), suggesting that riverine particles were already aggregated prior to salt-water contact. Data acquired from observations using an *in-situ* floc camera in the Ems, Gironde and Scheldt, also gives no indication of the coagulation of riverine particles in the low salinity region (Eisma et al, 1991a). However, an alternative study of the Gironde by Gibbs et al (1989), also using a floc camera, places the point of salt induced flocculation at 0.2‰ (from laboratory and field studies).

In the Gironde, Gibbs (1989) observed fine material in the fresh water of the Garone, which along with the Dordogne feeds the Gironde estuary, with particle diameters largely <5 μm. Increases were observed in the 50-100 μm and >100 μm fractions upon entering the low salinity region. The absence of particles >200 μm as seen in studies of other estuaries (Eisma et al, 1991a; Bale & Morris, 1987) including the Gironde, suggests that floc breakage may have occurred. Eisma et al (1991a) also presents results for the Garone, at a minimum of 0.2‰ salinity, stating that no flocculation occurred at the salt water interface. Indeed, the median particle diameter at 0.2‰ was seen to greater than at 4‰ & 10‰. Given that flocculation may occur as low as 0.2‰, it may be possible that the samples observed by Eisma et al (1991a) were already flocculated after passing from 0‰ to 0.2‰.

Evidence for salinity induced flocculation was observed by Bale et al (1989) in the Tamar estuary over one tidal cycle at an anchor station in the upper reaches of the estuary. Median diameters were seen to increase by greater than a factor of 4 between conditions of low salinity (0‰) and high salinity at high water (12‰). Increased particle sizes also coincide with low current velocities and low suspended solids concentrations, presumably during a period of low collision breakage. Although, at low water (salinity = 0‰ and current velocity <0.3ms^{-1}) median size values rise only marginally above those at higher current velocities (current velocity = 0.75ms^{-1}, when SPM = 0.75-1.25gl^{-1} and salinity = 0‰). Current velocities remained below 0.75ms^{-1} during the sampling period, hence the Kolmogorov microscale (l_0) was >400 μm at 1m from the bed (Nakagawa & Nezu, 1975). The size of the smallest turbulent eddies means that, turbulent shear cannot account for the finer particle size distribution on the ebb and flood. Mobilisation of fine bed sediment under higher flow velocities, so diluting the volume contribution of large flocs to the bulk SPM, will also lead to a fining of the particle size distribution, coincidental with zero salinity.

The lack of significant particle growth in Bale et al's (1989) samples during low water, either, signifies the importance of salinity in determining the particle size distribution, or may be explained by the marginally higher SPM concentration (creating increased collision/breakage size limitation). Alternatively the inability of flocs to grow in the time interval between a low enough SPM concentration and the increase in current velocities (1-2 hours) may account for smaller particles. Salinity may therefore; not significantly determine the absolute floc size, but greatly affect the rate of flocculation (Burban, 1989), when suitable conditions prevail.

Following work in the Gironde estuary, Gibbs (1989) argued for the existence of four distinct regions:

[1] A riverine zone at 0-0.1‰ salinity

[2] A coagulation zone from0.1-1‰ salinity and two zones landward

[3] A zone landward of the null point at 1-5‰ salinity

[4] A zone seaward of the null point at >5‰ salinity

In the first two zones, Gibbs (1989) argues that the particle size distribution is controlled by the salinity gradient, whilst in the latter zones it is the hydrodynamic situation which determines the particle size distribution. After zone [2], flocculation is assumed to be complete and the particle size distribution changes only according to the process of estuarial circulation. As flocs travelling seaward in the fresh waters of the upper water column, they settle out into the landward flowing saline waters and are transported back to the fresh/saline interface. At the null point, the opposition of fresh and saline flow traps them; this then creates a region of heightened SPM concentration, otherwise known as the Turbidity Maximum (TM). As this is a region of upwelling, flocs may be transported, up into the seaward flowing waters, only to settle out once more. A circulation pattern is set up, whereby large flocs are concentrated in the bottom layers, with a turbidity maximum situated at the null point, in this case at 5‰ (Figure 1.3). The surface layer particle size distribution remains constant beyond the coagulation zone, except for one region where flocs are re-circulated from the null point into the seaward flowing water creating a size and concentration maximum, some 30km downstream from the null point.

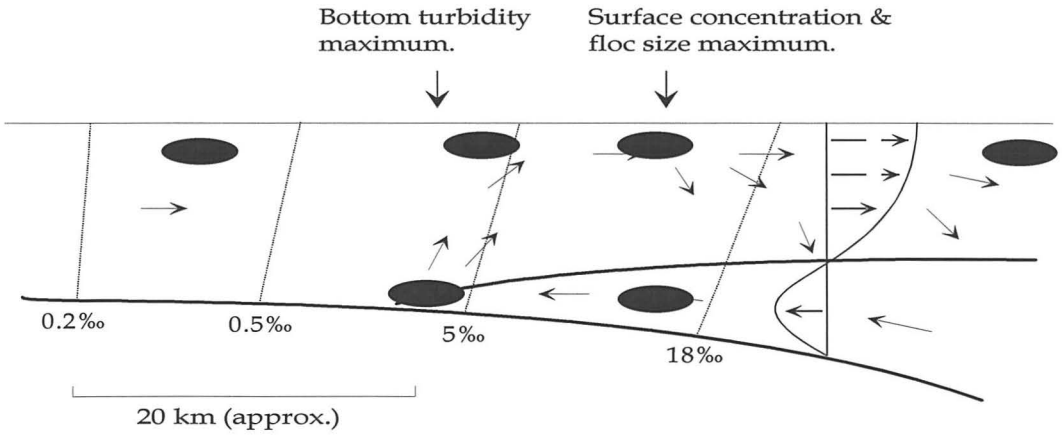

Figure 1.3. Salinity and current profiles, transport pathways and surface/bottom turbidity maxima locations for the Gironde estuary, adapted from Gibbs et al, 1989.

Particle sizes within the turbidity maximum (TM) may be derived from three areas; 1) mobilised bed sediment, 2) circulation/settling of particles into the TM, or 3) the evolution of permanently suspended indigenous particles. The significance of each of these sources remains unclear. Schubel & Kana (1972) and Bale et al (1984) observed the dominance of fine cohesive particles in the TM's of Chesapeake bay and Tamar estuary, respectively, Bale's results (for the surface TM) showing a mode at around 20-25 μm with a broad spread. Later *in-situ* results for the lower TM (Bale et al, 1989) displayed median values of 20-80 μm, which correlated well with concurrent discrete samples. Gibbs (1989) observed a poorly sorted particle size distribution containing relatively large particles. Although median diameters in the lower and surface TM were around 20 μm, larger particle size distributions existed seaward of the lower TM. Hence, maximum floc size and turbidity maxima were not coincident.

Observations by McCabe et al (1992) in the Tamar estuary during spring and neap tides, distinguishes the presence of two particle populations, with modes present at < 5.8 μm and > 100 μm. Their relative dominance was seen to change according to the spring-neap cycle on the flood tide. Small flocs were dominant upon the spring flood as opposed to a large poorly sorted population upon the neap flood. This suggests, either the resuspension of fine material, induced floc breakage or combination of both, during the higher current velocities of spring flood. The particle size distribution within the TM upon the ebb was found to be similar for both spring and neap tides, with a predominance of 30-200 μm flocs. Between late flood and the denudation of the fresh/salt water interface on the ebb, large flocs were abundant at the seaward end of the TM, with sorting taking place prior to the emergence of brackish water, whereupon sizes abruptly diminished.

As a mechanism for the generation of the TM, Gibbs (1989) favours the settling/circulation of large flocs in creating and maintaining the high particle concentrations. Bale & Morris (1987) propose the existence of a small almost

permanently suspended population with periodic input of material from resuspended sediments, resulting in the active selection of particles. The observations and conclusions of McCabe et al (1992) appear to combine both mechanisms. Faster settling flocs with settling velocities (w_S) in excess of the denudation rate of the salt-water interface (D_r), typically 1.5mhr^{-1}, resulting in high concentrations in the lower layers of the water column at the null point. Whilst slower settling flocs, where $w_S < D_r$, are transported into the surface waters by upwelling fresh water. This results in similar features to those seen in the Gironde (Gibbs, 1989). Modal peaks at < 10 μm are the result of the resuspension of fine grained material and are predominant during the high current velocities of spring flood.

The main controlling factor upon the distribution of SPM in estuaries appears to be the hydrodynamic regime, which combines estuarine circulation, the extent of differential settling and the degree of resuspension. The effect of salinity is still open to question with some authors arguing for it's importance in particle size generation (Gibbs et al, 1989; Bale & Morris, 1987) and others arguing against it's significance (Eisma et al, 1991b). Turbulent eddies appear to have no effect upon particle size distribution, sometimes being significantly larger than the suspended particles, it appears that they envelop rather than disrupt flocs.

1.5 Aims and Objectives

This study considers the natural environment extending from riverine systems, through the interface between fresh and seawater to the shallow sea environment. The most complicated and intriguing area for research within coastal ecology lies at the estuarine fresh/sea-mixing zone. In this region, where fresh and seawater meet, chemical

and physical processes give rise to changes in the nature of the sediment. The processes involved in the mixing of fresh and saline water masses have important consequences for the exchange of solids and chemicals between fresh water run-off and sea.

The aim of this work is the development of improved instrumentation for the purpose of characterising estuarine and coastal suspended particulate matter in terms of particle size. In order to achieve this there were several clear objectives. Firstly the development of an instrument capable of measuring particle size in-situ. This took the form of extensive laboratory testing of an instrument thought to have the development potential. Following satisfactory evaluation results the instrument was to be converted for in-situ use. The second objective was the deployment of this instrument in the natural environment. In order to demonstrate it's viability as a monitoring package, two case studies were undertaken involving a comprehensive study of the size characteristics of SPM in a macro tidal, highly turbid estuarine system. Measurements of size characteristics were to be acquired over a range of tidal and seasonal conditions for the entire fresh water - coastal environment.

Through the deployment of this instrument, it was also the aim to improve the understanding of suspended sediment dynamics in a turbid estuarine environment. The objective was to relate suspended particulate sizes to variations in both the dynamic regime and water quality.

In-situ Particle Sizing Using an Adapted Laser System: Evaluation and Development.

2.1 Introduction

The fundamental need for in-situ particle size measurements avoiding disruption to fragile flocs has been firmly established in the previous Chapter. Owing to the lack of commercially available instrumentation, funding for the evaluation, adaptation and subsequent field testing of an instrument thought to be capable of fulfilling these requirements, was derived from special topic initiative, GST/02/665. This formed part of SIDAL, Systems Instrumentation Development for AUTOSUB (Autonomous Submersible) and LOIS (Land Ocean Interaction Study). The objective of this study was to provide an autonomous in-situ particle size analyser where none was currently commercially available. In choosing a suitable method of size analysis several criteria were considered:

- The analytical range, in particular whether the size range would be suitable for the size of particles previously seen in estuaries (Table 2.1).
- The facility to provide reliable size information over a wide range of particle concentrations, preferably extending from coastal waters (0.5 to 100 mg l^{-1}) to estuarine turbidity maxima (10s g $^{l-1}$).
- The avoidance, or at least minimisation of floc disruption.
- The ease with which the instrument could be adapted to allow in-situ measurements.

It was with these points in mind that a technique employing focused beam reflectance (Laser Technology Inc. (Lasentec), Redmond, Seattle, WA, USA) was chosen. Commercially available Lasentec laser systems have found wide application in the process control industries as on-line particle size analysers. This has brought about their use in demanding situations involving very high particle concentrations or slurries, both wet and dry. The Par-tec series of particle size analysers from Lasentec are chiefly used in the monitoring of the size distributions in order to provide data for the optimisation of industrial and chemical process parameters. As such, absolute accuracy is not always a prerequisite, as the instrument is commonly calibrated to a particular material type and only reports on variations from a given value. It has also been used in research concerning the mechanisms controlling industrial floc breakage and aggregation (Williams, 1991), although here again the size was reported relative to a particular value.

2.2 The Par-tec100 : Method of operation

Focused Beam Reflectance Measurement (FBRM) utilises a technique whereby particles are sized according to the duration of the interaction between an individual particle and a focused laser beam. This has the advantage of basing the size distribution upon the measurement of individual particles. Also, the technique is purported to be independent of particle composition and is effective at a very wide range of particle concentrations.

The basis for the commercially available version of the Lasentec Par-tec100 is a computer controlled non-submersible probe. The probe is connected to a 'base unit', which contains much of the circuitry involved in signal editing and counting via a 32 core cable. In turn the 'base unit' is connected to a PC (IBM compatible with RS 232 serial data link). The system is flexible in that it may be used in the laboratory for the testing of discrete samples, but may also be inserted into pipelines, reaction vessels etc. via a 1" seal. Despite its use as a laboratory instrument the Par-tec100 was chosen owing to the perceived ease with which the 32 core umbilical could be extended from the standard 3m length to 100m, a necessity for estuarine and coastal work.

The Par-tec100 produces a finely focused beam of laser light, which is focused beyond the probe's cylindrical tip, i.e. within the suspending medium (Figure 2.1). The light source is a semi-conductor laser diode emitting radiation at 778 nm ± 0.5 nm. By focusing the beam to just 0.8 μm by 2 μm, some 2 x 10^{10} Wm^{-2} is provided at the focal point. A scanning focal point is produced, by mounting the focusing lens off centre within a rotating disc. This causes the focused beam to describe a circle, the diameter of which is 8.4 mm. The rotation of the disc, approximately 8400 rpm, is accurately controlled by

Hall effect motors, these ensure that the focal point's velocity remains fixed at 2.0 ms^{-1} (Figure 2.1).

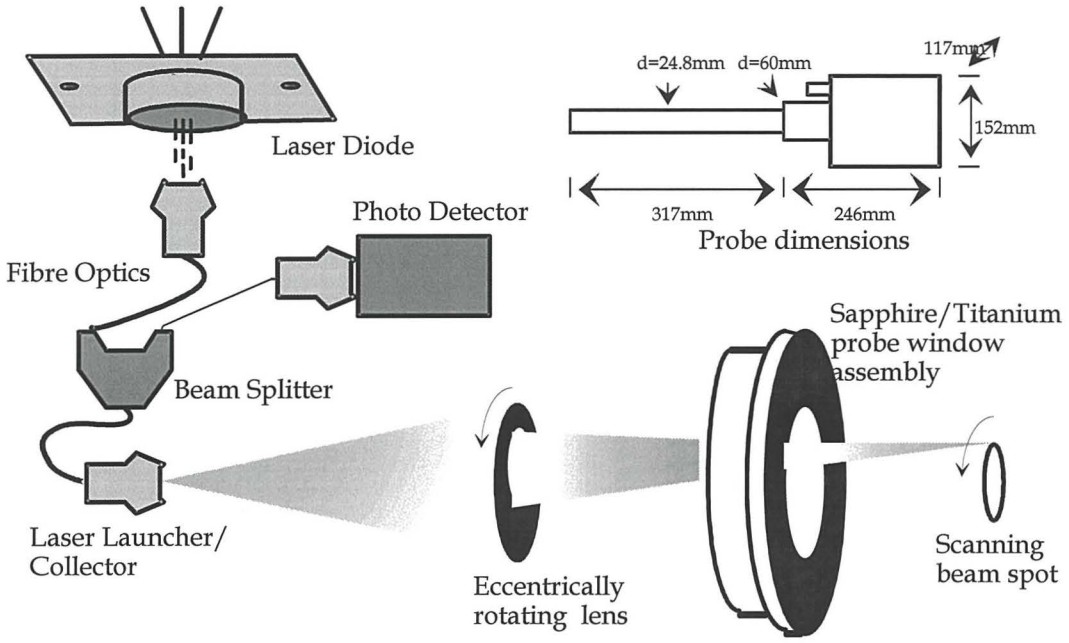

Figure 2.1 Par-tec100 probe geometry, with schematic representation of probe prior to marinisation.

As the focal point is assumed to be smaller than the particles under analysis and moving with a greater velocity, the size distribution of particles is derived from the interception of individual particles and not the pattern or signal produced by a number of particles, as in LALS. The length of time that the focused beam interacts with a particle is dependent upon the velocity of the beam and the size of the particle, or rather the chord that the beam describes as it cuts across the particle (Figure 2.2). By measuring the length of time the beam spends upon the particle and knowing the velocity of that beam, the size of the particle chord may be calculated simply from;

$$d = v * t \qquad [2.1]$$

Where v is the velocity of the beam, t is the time taken for the beam to cross the particle and d the chord length. The duration of the reflected light pulse generated by the beam as it crosses a particle surface defines t. The same optical arrangement that produces the incident beam also receives the reflected light, until a beam splitter directs the reflected light to the photodetector (Figure 2.1).

The interaction of particle and laser beam is a random process, particle diameters are not measured directly, rather it is the random chord of a particle that is measured (Figure 2.2). This is handled using a random chord algorithm within the data processing software, which assumes that all particles are spheres and produces a particle size distribution based upon spherical equivalent diameters.

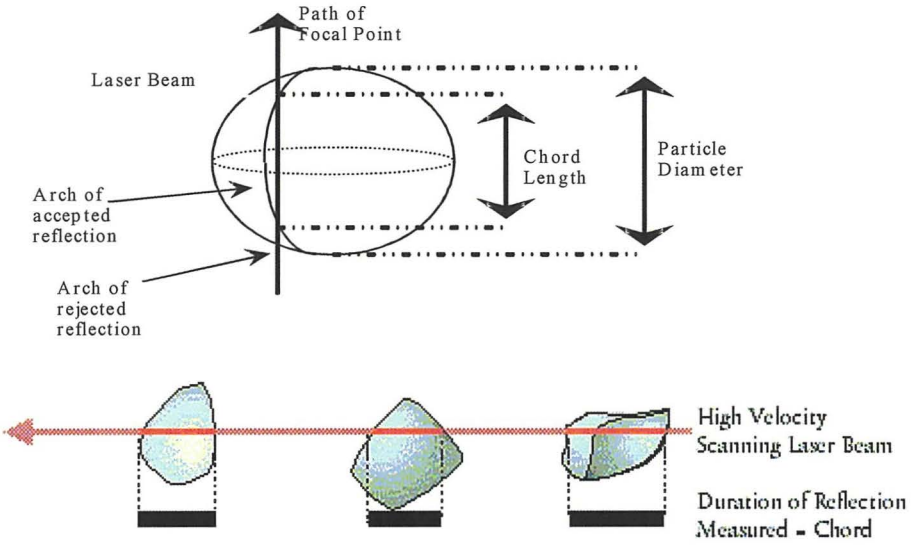

Figure 2.2 Basis of Par-tec100 measurement. Illustrating (top) the relationship between the measured chord and the actual particle diameter (adapted from Hobbel et al, 1992) and the resulting duration of the FBRM pulse (by kind permission of Lasentec WA, USA).

The measuring range of the Par-tec100 extends from 1.9 to 1000μm with 38 logarithmically spaced sizing channels. Particles outside of this range are accounted for by the first and last channels, which are <1.9 μm and >1000 μm, respectively. The sizing hardware consists of eight, 16-bit counters, which accumulate the reflected pulse duration within distinct size ranges over a precise time interval (MCD, measuring cycle duration). The measuring duration is set by the operator at a value between 0.2 and 3.2 seconds, which will depend upon the number of particles encountered, i.e. the lower the particle concentration the longer the required analysis time to achieve statistical representation of the size population. The total analysis time is given by; 8xMCD plus some computational time and hence, extends from approximately 2 to 24 seconds.

After processing, the reflected signals are sorted into the 38 sizing channels to provide a particle chord distribution. The system then allows a choice of four size distribution types, represented as a function of the total number or total volume of particles present:

- Scanned Count (ScCo) - being the uncorrected chord distribution.
- Spherical Equivalent (SpEq) - where particles are assumed to be spherical through the application of a chord correction algorithm.
- Volumetric based upon ScCo data (VDi(ScCo)) - where ScCo data are converted directly to a volumetric distribution without applying the chord correction.
- Volumetric based upon SpEq data (VDi(SpEq)) - where SpEq data are converted to a volumetric distribution.

Volume distributions (VDi) are calculated from the ScCo and SpEq number distributions by;

$$[((L_1 * L_2)^{-½} * p * P_c) / 6] \qquad [2.2]$$

Where L1 & L2 are the upper and lower limits of a channel and P_c the percentage therein. Normalisation produces a particle size distribution based upon the total particulate volume, VDi(SpEq) or VDi(ScCo), depending upon whether SpEq or ScCo distributions are used in the calculation.

The measuring zone of the Par-tec100 is confined to a small volume around the focal point. This is due to a discriminatory procedure whereby particles intercepted by the more diffuse beam away from the focal point are ignored. The criteria for rejecting reflected signals lie in the rise and decay times of an observed pulse. Particles intercepted by a diffuse beam will generate a reflected light signal that rises slowly from the background signal. Thus, by calculating the rate of change of light intensity and applying a particular threshold value, signals generated by the beam away from the focal point may

be discarded (Figure 2.3). This discrimination procedure allows the Par-tec100 to operate in conditions of very high particle concentrations, suspended solids volumes up to and beyond 10%, approximately 100 gl^{-1} for natural estuarine particles, although care may be needed in the interpretation of results. By basing the system upon the rate of change in the reflected signal and not the absolute amplitude of the pulse, the system's dependence upon particle nature is lessened. The high intensity of the beam is also designed to alleviate problems concerned with high particle concentrations and variations in particle nature, by overcoming the characteristically low reflectance efficiencies (< 5%).

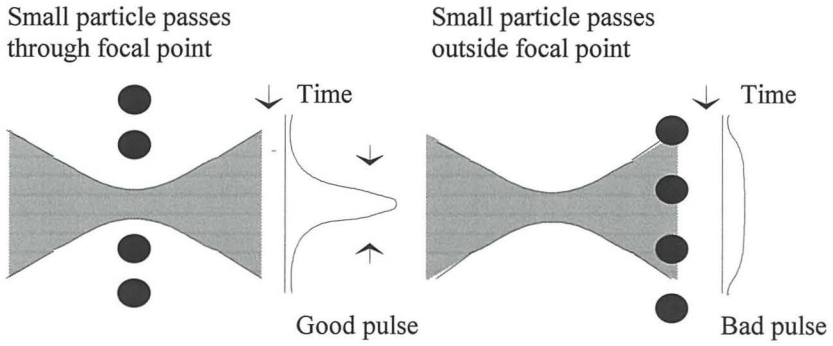

Figure 2.3 The principle of the Par-tec100's particle discrimination around the focal point.

2.3 Evaluation of the Par-tec100 performance

2.3.1 Introduction

The Par-tec100 is an 'on-line' particle size analyser which has been used for the control of industrial processes, such as; mixing, grinding, crystallisation, precipitation, etc (Lasentec Test Reports C-99-0005, 0002, A-01-0009) and has thus found applications in the sugar, aluminium and paper industries. It has also been recently evaluated for the monitoring of floc breakage and growth kinetics (Williams, 1991) within industrial reaction vessels. In industrial applications, the instrument is typically faced with a uniform, well-defined material, but in natural water SPM may be comprised of a range of component materials. Materials such as, diatom fragments, algal cells, bacteria, faecal pellets, mucal webs, sand sized mineral grains, silt and clay particles. The physical characteristics of such a collection vary greatly, more so in their size, rather than their density, opacity and shape. An evaluation of the Par-tec100's response to naturally occurring particles was therefore a pre-requisite to its application in-situ.

The operator is given control over several parameters, which govern the collection and presentation of particle sizing data, including the duration of measurements and the position of the focal point. During laboratory use of the instrument, these parameters are changed in order to optimise the response of the system to the nature and concentration of particles being analysed. The changing nature of the natural hydrodynamic system and the particles therein, may make it necessary to alter these parameters in-situ. It was, therefore, vital to understand the effect that changes to the instrument control parameters may have upon the interpretation of the particle size distribution. The instrument's effectiveness in

dealing with rapidly changing turbidity and particle velocities determine its potential flexibility in-situ, and was also in need of elucidation.

2.3.2 Initial comparison with alternative techniques

In order to evaluate the Par-tec100, calibration trials were carried out with a number of different, commercially available calibration standards and direct comparison with other techniques used for sediment particle sizing. Standard instrumentation calibration materials are generally small in size (<100μm) and so represent only a small portion of the total Par-tec100 working range. In order to extend this range it was necessary to compare the Par-tec100 against existing well established particle sizing techniques. A Malvern 2200 LALS particle size analyser was used for initial comparative tests. It was particularly suited to this task owing to its accuracy over a relatively large working range, 1.9 to 188μm or 5.8 to 564μm, dependant upon lens configuration. Also, a similar model had been converted for in-situ estuarine particle size analysis, which would allow direct in-situ comparison. Optical microscopy was also used, principally in the characterisation of particles with sizes beyond the scope of the Malvern, i.e. > 600 μm. An Electro-resistive particle sizer, the Coulter Counter Multisizer II, was also used for finer materials.

2.3.2.1 Materials and Method

Commercially available calibration particles (Duke Scientific, CA, USA) were analysed using the Par-tec100, whilst held in suspension in a glass beaker. Particles used in the evaluation included pollen (mean diameters: 7.4, 29.7 and 78 μm), latex (19 μm) and glass (nominal diameters: 8.0 ±0.8, 31.5 ±2.2 and 85.7 ±4.3 μm) so allowing the effect of various material types to be examined. A number of secondary standards (mean diameters: 6.5, 23.6, 39.5, 89.4 and 171.7 μm) were produced by fractionating ashed

sediment using settling time criteria (Appendix 1). Samples of larger particles were obtained by sieving sand to produce various fractions providing mean diameters of: 21.5, 133.6, 228.3, 403.5, 447.6, 624.4 and 766.1 μm. The size distributions of the secondary standards were determined using the Coulter Counter for the finer material with Malvern LALS system and optical microscopy characterising the larger sand grains and sediments.

2.3.2.2 Results

The validity of size measurements using the Par-tec100 were determined by comparing results with existing laboratory techniques, using a number of calibration standards and well defined natural particle populations (from Coulter Counter, Malvern Laser Diffraction & Optical Microscopy). The volumetric mean particle size of each population was used as a primary indication of the relative similarity between the Par-tec and other methods. This was felt to be a valid means of comparison given the high degree of sorting of the particle populations, achieved through successive sieving or settling for the natural particles and via the manufacturing process for the standards. The comparison indicated a clear but consistent discrepancy in the Par-tec's measurement of particle size. Results show that the Par-tec100 tends to progressively oversize fine material less than 125 μm, whilst undersizing material greater than medium sand sized, 250 μm (Figure 2.4). For example, a natural ashed sediment of 23.6μm nominal mean diameter was sized at 69.4μm, whilst a sand sample of 447.6μm nominal mean diameter was sized at 310.4μm, an error of 194% and 31% respectively. However, a clear trend was observed as seen in Figure 2.4, the errors encountered were wholly reproducible and were consistent for a variety of materials, including algae. Glass and latex proved to be exceptions, as these were oversized to a greater extent than natural materials.

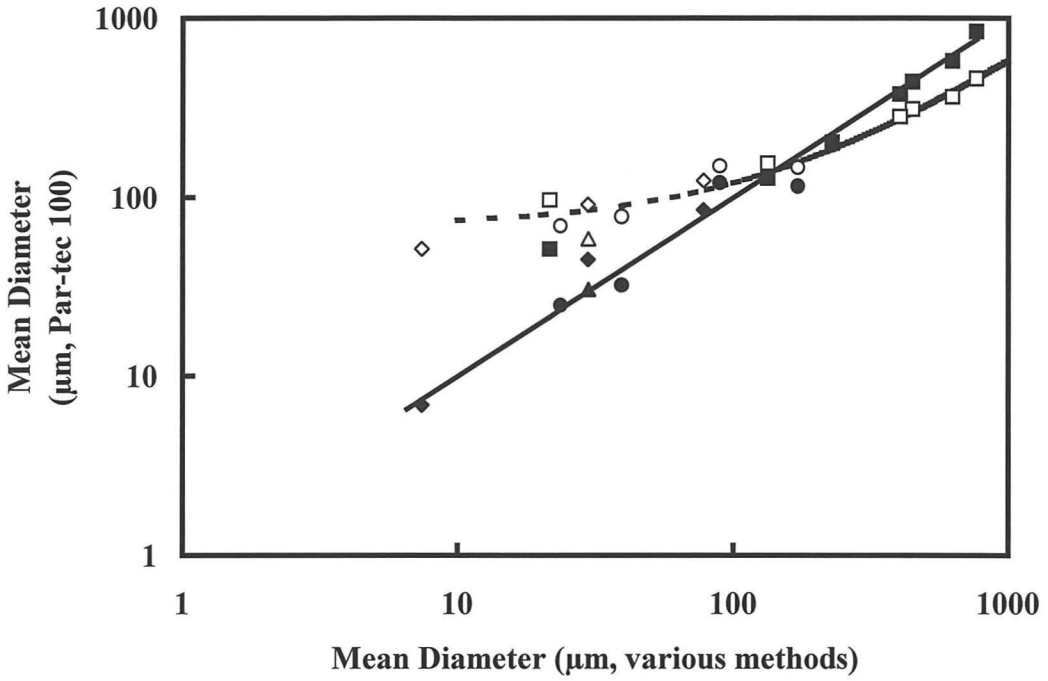

Figure 2.4 Comparison of mean particle sizes derived from the Par-tec100 with other optical techniques for a range of standard materials: pollens (diamonds), ashed sediments (circles), sands (squares) and algal cells (triangles). Open symbols represent the pre-calibration Par-tec100 mean size, solid symbols denote the calibrated value. The dashed line is the best fit to pre-calibrated data and the solid line is the 1:1 relationship

2.3.2.3 Calibration

The general form of particle size distributions obtained with the Par-tec100 correlated well with those of other techniques, for a variety of material types and sizes (Figure 2.5). However, the mean size values exhibited significant deviation from the 1:1 relationship (Figure 2.4).

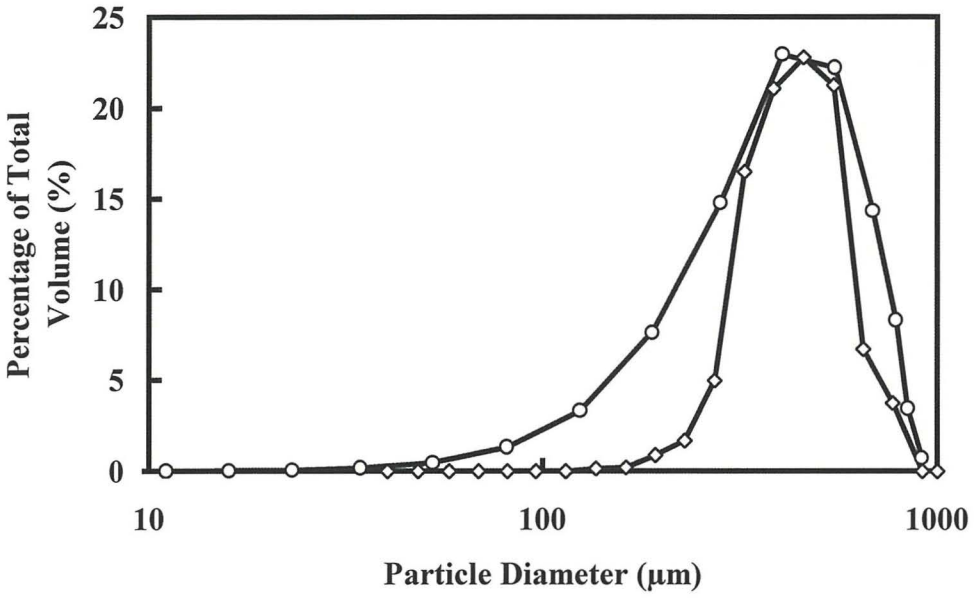

Figure 2.5 Comparison of the volumetric size distributions for 447.6 μm (mean diameter) sand as measured by the Par-tec100 (open circles) and by optical microscopy (open diamonds). Channels below 10 μm have been excluded from this figure owing to their possessing zero particle counts.

As the size spectra generated by the Par-tec100 were consistent with those of the Malvern Instruments laser diffraction instrument, a calibration technique, which re-scaled the limits of the Par-tec100 size intervals, was developed. This involved factoring the limits of each size channel with a value (S_f) derived from the ratio of the actual mean diameter (M_a) to the measured mean diameter (M_o). Thus, a sample with a mean diameter of 20 μm which might be measured as 30 μm by the Par-tec100, if scaled by a factor of 20/30 would reduce the size interval limits by 1/3 and result in a new measured mean of 20 μm. However, the scaling factor also needed to vary with mean particle diameter. This was achieved from the plot of Par-tec100 mean diameter values against that of other techniques and by determining a line of best fit to the data. The degree of offset between the Par-tec100 and the 1:1 relationship allowed the calculation of scaling factors needed to correct data that are at any point over the size range of the instrument. Equation 2.3

defines the scaling factor needed to 'calibrate' a size spectrum from measured mean diameter.

$$Sf = (4.97\ M_0^{0.32}) - (5.287\ M_0^{0.30}) \qquad [2.3]$$

This method applies to all estuarine particles at all particle concentrations. Once the channel limits had been re-scaled, the statistical characteristics, such as mean, standard deviation and coefficient of variance for individual spectra could be re-calculated. Particle size spectra are still relevant and may be displayed after the application of the calibration factor to the channel limits. The details of pre and post calibration differences are seen in Table 2.1.

Sample	Mean dia.(μm) (Various Methods)	Par-Tec Mean (μm) (Pre-calibration)	Par-Tec Mean (μm) (Calibrated)
AS 5-10μm	6.52	29.09	3.83
P 5.8-9μm	7.40	51.48	11.33
Sa <63μm	21.54	96.67	49.07
AS 10-30μm	23.62	69.40	23.93
P 24.8-34.6μm	29.70	90.93	38.83
AS 30-63μm	39.50	77.89	29.80
P 69-87μm	78.00	124.75	72.33
AS 63-125μm	89.41	150.17	130.17
Sa 63-125μm	133.60	154.85	132.19
AS 125-250μm	171.66	146.60	129.25
Sa 125-250μm	228.28	199.37	224.12
Sa 250-500μm	403.52	282.79	412.37
Sa 250-500μm	447.58	310.36	478.64
Sa >500μm	624.39	363.63	582.00
Sa 500-1000μm	766.06	460.11	794.81

Sa = Sand, AS = Ashed sediment, P = Pollen,

Table 2.1 Results from pre and post calibration size determination of calibration and laboratory standards.

2.3.3 Replicability Tests

Particle size distributions are collected by the Par-tec100 over a set measuring cycle, termed Measuring Cycle Duration (MCD). For each MCD one analysis is undertaken and the resulting distribution recorded, the operator may set the duration of the MCD. When there are sufficient particles in suspension, a reliable size distribution may be observed within this short space of time. According to the manufacturer's instructions, the minimum number required is 1000 particle counts. However, when particle concentrations are low these targets may not be achievable, in this case it may become necessary to average over successive size distributions in order to build up an effective particle count. With the Par-tec100 it is possible to average up to 50 measuring cycles, the number of which is termed the 'Cycles to Average' (CtA). In a closed system with a stable population of particles, this allows greater statistical accuracy. However, in a dynamic system, where particle aggregation, disaggregation, resuspension or deposition will take place, excessive averaging will provide data that is misrepresentative of the true particle size distribution at any given moment. In conditions of low particle concentrations, less than 100 mgl^{-1}, it may be necessary to record with 10 cycles to average (approximately every 5 minutes) in order to achieve sufficient particle counts, although a single cycle may be desirable. As the number of counts decreases, at some point the counts will become too low to provide statistically reliable results and the observed particle size distribution of a population may not be wholly representative. This has important ramifications for the minimum suspended particulate matter concentration that may be reliably analysed (Section 2.3.5).

2.3.3.1 Materials and Methods

In order to test repeatability and the possible existence of a minimum count limit, calibration standards of differing size were analysed at one suspended solids concentration. Adjusting the MCD and CtA values, reducing these values to simulate low particle concentrations through counting fewer particles mimicked changes in particle concentration.

2.3.3.2 Results

It is reasonable to assume that the accuracy in determining the size distribution of populations of particles is proportional to the number of particles counted. When the system was configured with the maximum MCD (3.2 seconds) and CtA (for this experiment 30 cycles) the greatest number of particles were counted (Figure 2.6). This therefore represents the most statistically valid determination of size. The variation in the MCD value does not appear to greatly affect the accuracy of the instrument, unless it falls below 0.5 to 0.7 seconds. Irrespective of the MCD value, if the measurement is averaged over fewer cycles then the greater will be the subsequent oversizing of the population, although the error is small, + 1 - 2 μm, where the MCD is sufficiently large. Comparison of measured mean size with the total analysis time shows clearly the dependence of the system upon registering sufficient particle counts (Figure 2.7).

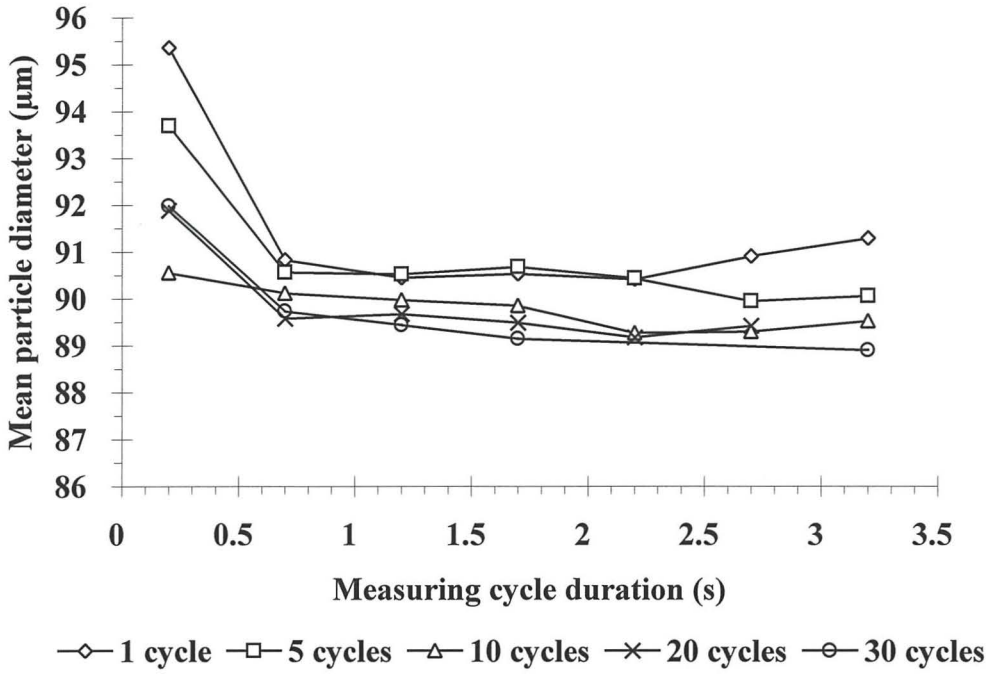

Figure 2.6 Relative accuracy of the Par-tec100 in relation to measuring cycle duration and averaging.

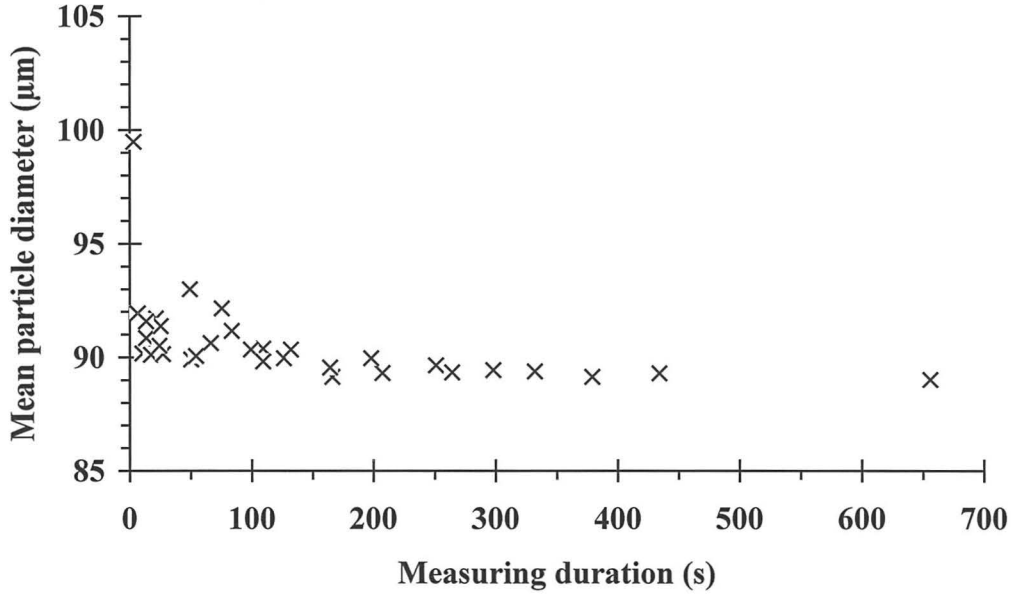

Figure 2.7 Relative accuracy of the Par-tec100 in relation to analysis time.

2.3.4 The Effect of Varying the Focal Point Position

Although the Par-Tec employs a laser providing over 2 x 10^{10} W m^{-2} at the focal point, the depth of its intrusion into the suspending medium is reputed to affect the observed size distribution. In a field situation, with rapid changes in particle concentration and perhaps particle size, this would necessitate a movement of the focal point in order to achieve the optimum distance from the window. For a remotely operated instrument this would mean either; a remote means of focal adjustment, or an autonomous feedback device. Experiments were carried out in order to determine the exact nature of the focal positioning dependence and also to elucidate the possibility of using a fixed focal position.

2.3.4.1 Materials and Methods

Suspensions from unimodal samples of corn pollen (69-87μm) and two ashed sediments (5-10μm) & (10-30μm), were produced with particle concentrations of 1000, 100 & 10 mg l^{-1}. The size distribution of each suspension was measured with the focal point set at a range of distances (0.05 to 4mm) from the window. In order to alleviate the potential effects of particle concentration changes, mean particle size is reported relative to the size measured when focusing procedures, as recommended by the manufacturer, were employed. This requires that the positioning of the focal point be such that the maximum reflected light intensity is achieved. The distance from the window is then referred to as the optimum position.

2.3.4.2 Results

The mean particle size for each sample is presented as a function of particle concentration and focal position (Figures 2.8a to 2.8c). Focal distance is seen to have a dramatic effect upon the observed size distribution, although within 0.9 mm the mean size remains reasonably constant, whilst errors are seen to increase with focal distance when beyond this value.

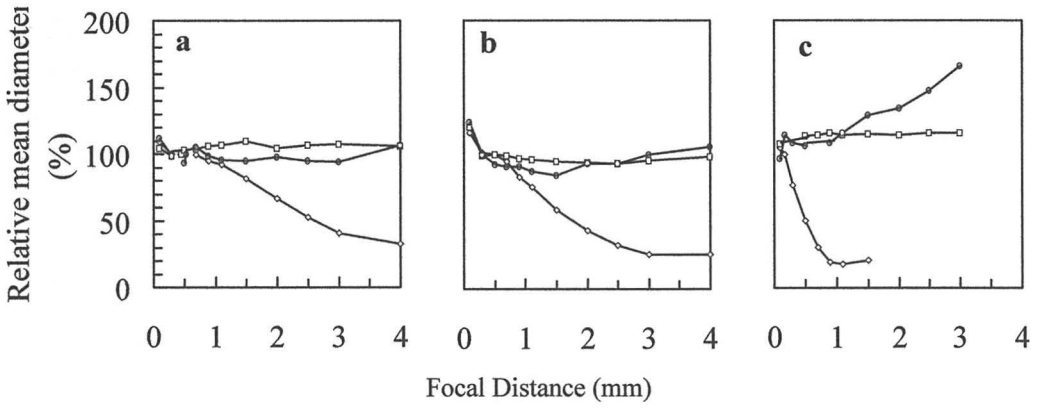

Figure 2.8 Mean particle diameter (as a percentage of the true mean) plotted against focal distance for three samples with different mean diameters (a - 78 μm, b - 23.6 μm and c - 7.4 μm) at three particle concentrations: 10 mg l-1 (circles), 100 mg l-1 (squares) and 1000 mg l-1 (diamonds).

At high suspended particle concentrations (1000 mg l^{-1}), the mean particle size of the finest particles was noticeably under-estimated when the focal point was located beyond 0.2 mm from the window surface. Measurements of the two larger samples indicate that the analysis was unaffected at distances out to 0.8mm. For concentrations below 100 mg l^{-1}, the focal distance was generally not critical for all three sizes, although the smallest particles were oversized at focal distances beyond 1mm. On the basis of these experiments, estuarine particles above 20 μm can be measured with some confidence using

using a fixed focal distance of 0.8 mm. Only if the sample consisted primarily of particles smaller than 20 μm,r would a focal distance setting nearer 0.2mm be required.

2.3.5 Response to Variations in Particle Concentration

The Par-tec100's primary application is in the analysis of slurries, with particle concentrations measured in excess of several 10s g l^{-1}. In the natural waters of Northern Europe and North America, suspended particulate matter concentrations can be found ranging from < 1 mg l^{-1} to >100 g l^{-1}. In particular, within a single estuarine system the variation over a tidal cycle may cover several orders of magnitude. Natural processes such as extreme river runoff, the generation and movement of fluid mud layers or the presence of a Turbidity Maximum, are capable of generating very high SPM concentrations. Such processes can then provide a mechanism for the rapid, large-scale movement of sediment within an estuary. Given their importance in sediment transportation it would be highly beneficial if a greater understanding of particle behaviour in such turbid conditions could be gathered from in-situ measurements. However, the high concentrations generated by these events are normally beyond the scope of existing in-situ size analysis instrumentation.

2.3.5.1 Materials and Methods

In order to determine the accuracy of the Par-tec100 over a wide range of particle concentrations, several of the calibration and secondary materials mentioned above (section 2.3.2.2) were analysed at concentrations ranging from 10 mg l^{-1} to 50,000 mg l^{-1}. Particles were kept in suspension using a four bladed impeller within a glass beaker.

2.3.5.2 Results

The particle size distributions at a number of particle concentrations indicate that the particle size spectra, based upon the mode and standard deviation, are relatively constant (± 3% modal variation) over suspended concentrations that range from 10 to 50,000 mg l^{-1} (Table 2.2). The median size is also seen to vary by only a small amount (± 5%). However, another size distribution descriptor, the mean size is seen to vary by up to 14%. This trend toward larger mean sizes with increasing concentration is attributed to particle co-incidence, where small increases in the number of apparently larger particles at high concentrations produce a disproportionate effect on the mean size. This is due to the inability of the instrument to resolve separate particles at very high particle concentrations. This provides a clear indication that in the case of the Par-tec100 the use of mean size alone is a poor indicator of the character of a non-normal distribution. The adoption of the median size in providing a descriptor for particle size variations in the following field deployments is valid, owing to the relatively small error caused by concentration variations in relation to the expected natural particle processes.

Concentration ($mg\ l^{-1}$)	Mean diameter (µm)	Std. dev. in mean(µm)	Median diameter (µm)	Std. dev. in median(µm)	Modal diameter (µm)	Std. dev. in mode(µm)
50,000	104.77	0.88	126.86	1.64	142.72	1.51
25,000	105.01	1.04	130.18	1.26	145.20	2.07
12,500	106.03	0.62	127.79	1.06	146.40	2.32
6,250	99.60	1.79	122.40	2.36	144.38	3.23
5,000	80.96	1.45	118.03	1.03	139.40	3.35
2,500	97.96	0.83	123.19	0.75	146.64	3.56
1,250	90.35	1.05	114.96	1.29	137.76	4.39
625	86.28	1.05	117.00	0.77	140.05	4.44
500	84.21	1.15	113.34	1.37	136.52	5.40
250	88.44	1.73	117.01	1.43	139.55	5.89
125	75.73	1.99	112.63	4.17	136.80	12.71
63	75.99	3.10	111.16	7.21	133.74	15.12
Coeff. of Var.	12		5		3	

Table 2.2 Results of particle size determination at varying levels of particle concentration up to 50 gl^{-1}.

2.3.6 Response to Variations in Particle Velocities

The Par-tec100's premise of accurate particle sizing is based upon the supposition that the scanning velocity of the focused laser beam is significantly greater than the particle velocity, i.e. as if the particle were stationary relative to the focal point. The Par-tec100 scans at approximately $2ms^{-1}$, whilst particles are generally subject to lower current velocities, such large currents are not uncommon.

2.3.6.1 Materials and Method

A simulation of a range of particle velocities was undertaken in order to clarify the importance of particle velocity in the Par-tec100's interpretation of particle size spectra. This was conducted by adjusting the speed of an impeller mixing device in order to simulate differing current velocities. The particle size spectra of a sample of deflocculated bed sediment from the Tamar estuary was recorded at three impeller speeds of; 1500 rpm, 1000 rpm and 500 rpm. Speeds less than or in excess of this range resulted in either, settling of material from suspension, or excessive vortexing, resulting in the entrainment of air bubbles.

2.3.6.2 Results

The mode and standard deviation in the distribution of particle sizes was used to characterise each analysis at differing impeller velocities. Thus, any changes brought about by increased particle motion would be seen either in the appearance of larger or smaller particles. From this test, it was seen that the Par-tec100 appears unaffected by large particle velocities, with little variation seen in either the mode or standard deviation (Table 2.2). With particles, travelling in excess of 2 ms^{-1} , directed at the Par-tec100 window, i.e. travelling at 90° to the scanning motion of the beam, it is the relative sizes of

the particle and the depth of the focal point / measuring volume which become important. From this experiment, it would appear that the measuring volume, which may change according to particle type, is sufficiently large to allow measurement of particles travelling at speed, prior to their exiting the focal point.

	Volume distribution		*Number distribution*	
Impeller speed (rpm)	**Mean diameter (μm)**	**Std. deviation (μm)**	**Mean diameter(μm)**	**Std. deviation (μm)**
500	305.6	182.2	27.5	24.6
750	303.6	171.2	26.8	24.7
1000	305.8	168.2	26.4	25.0

Table 2.3 Results of partice size determination at varying impeller speeds in a reaction vessel, simulating increased particle velocity relative to the focused beam.

2.4 Marinisation of the Par-tec100

The Par-tec100 is principally a laboratory-based instrument meant for use in reaction vessels and pipelines. Apart from the probe tip, the instrument is not designed for marine use. Other instruments in the Partec range, namely the 200 & 300 series, possess a submersible probe connected to a base unit via an optical cable. Unfortunately, restrictions on the cost and length of the cable preclude its use in estuaries and coastal waters. Despite this the Partec200 has been successfully used in Riverine systems (Phillips & Walling, 1999).

In order to facilitate in-situ measurements in water depths of up to 100 m, modifications to the original design were necessary. This involved mounting the probe unit in a watertight cylinder machined from PVC plastic. Access to the probe was made possible by fitting the end caps with piston-mode O-ring seals (Fig. 2.9). Communications between the standard probe and control unit were originally via a 2 m length of 32 core cable. For the submersible instrument this cable was replaced by a 100 m length of marine

grade cable with 12 conductors. The reduction in conducting core numbers was achieved by moving the pulse counting, power supply and scanning motor control circuitry from the control unit to the probe housing cylinder. In this way, the new cable carried only 24 V and 12 V supplies and the RS-232 serial link to a PC located with the surface control unit. This enabled a considerable cost saving in cable as well a reduction in both the weight of the cable and the drag imposed by flowing water when deployed. For in-situ deployments the submersible section was housed in either a lightweight cradle (Photo 1) or a heavyweight tripod (Photo 2). Depending upon the type of frame used, the Par-tec100 could be deployed either as a bottom lander or more usually as a vertical profiler.

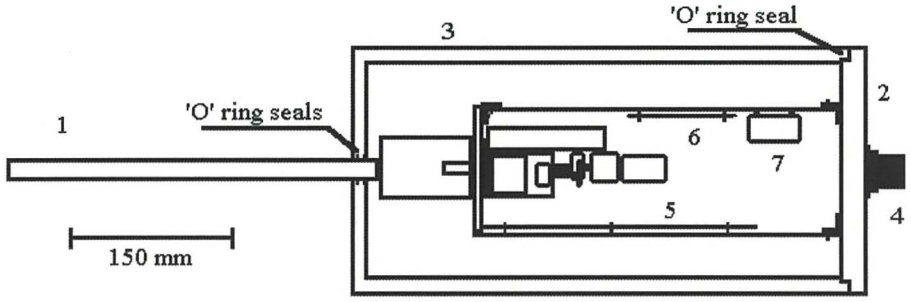

Figure 2.9. Schematic representation of the adapted Par-tec100 probe unit showing the light guide, scanning mechanism and focusing lens(1), the PVC cylinder (2 & 3), watertight cable termination (4) and electronic circuitry and power supplies (5,6 & 7).

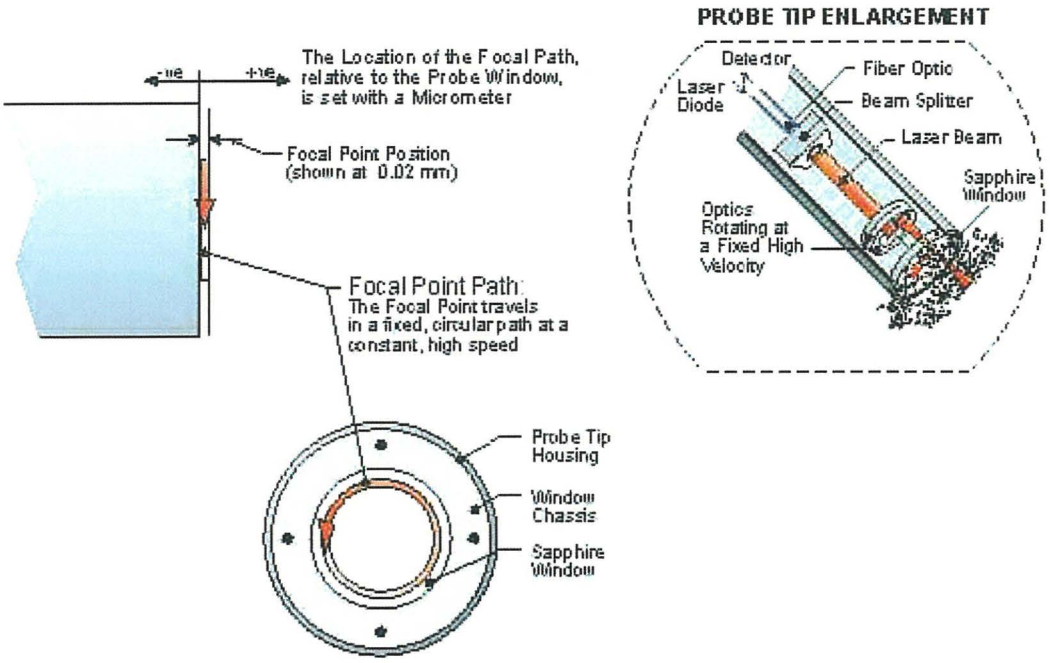

Figure 2.10. Schematics of the probe tip, which remains unchanged from the original instrument (by kind permission of Lasentec WA, USA).

2.5 Discussion

The Par-tec100 is primarily a laboratory based instrument and so, the purpose of this evaluation was to determine whether the instrument possessed the potential to collect representative particle size distributions in-situ. In-situ sizing of natural suspended particlulates, in any environment, presents many difficulties, not least of which is the nature of the particles themselves. In evaluating the instrument, it has been necessary to take account of the instrument's absolute accuracy in determining particle size, the influence of particle concentration, of particle velocity and variations in the systems parameters. From this evaluation, it has been found that the instrument could provide a significant step forward in in-situ particle size characterisation.

Comparisons with other techniques have shown the instrument to produce erroneous results at the coarse and fine end of its working range (Section 2.3.2). This has

also been proven to be the case with the Partec200 (Phillips & Walling, 1998). Whilst this appears consistent for the range of natural materials used, along with certain calibration materials, the case of glass and latex differs somewhat. Glass and latex are oversized to a degree far in excess of other materials. However, the reproducible nature of the error concerning natural particles, has allowed the formulation of a calibration procedure. In this case glass and latex have been ignored, based upon the evidence that the error is not related to the reflection coefficient of the particles. This is seen in the similarity of the offset for algal cells and the rest of the natural particles. Thus, natural organic materials such as, cells, exudates, etc., which possess a low index of refraction are characterised by an offset of the same degree as clays, silts, sands, pollens. In this way the calibration procedure will be valid for all estuarine and near coastal suspended particulates, irrespective of their aggregate components.

Particle geometry is a possible source for size interpretation error and will depend largely upon the surface angle that a particle presents to the incident beam and surface roughness. For a perfect sphere a small percentage of the reflected signal equating to the particle's leading and trailing edge may be discounted (Figure 2.2), depending upon the threshold levels of the discriminating software (Hobbel et al, 1992). Non-spherical particles are characterised in the same manner as spheres, by the application of the chord correction algorithm. For highly non-spherical particles, such as cylinders this has the effect of producing a volumetric size distribution exhibiting three to four distinct peaks, the largest contributor being the cylindrical long axis. Care must be exercised in the application of the chord correction and also in the interpretation, particularly where multiple populations appear to occur.

The instrument's performance over such a wide range of particle concentrations is consistent, with only a 3% variance in the mode. The susceptibility of the median and

particularly the mean to small changes in the coarse fraction of the distribution can be seen in the slightly larger variances (5 and 12% respectively). These errors are induced by particle masking effects and the failure of the system to differentiate between separate particles. The number distributions of these analyses exhibit low variance, indicating that the actual number of mis-sized particles due to masking is relatively low. The system is capable of operating above 50 g l^{-1}, whilst analysis in concentrations below 100 mg l^{-1} is possible providing time is available for averaging successive cycles. The size of the particle population and the dynamic situation will determine the absolute lower limit of the system, although, as a guide, a count of 1000 is a desirable confidence level, whether achieved through one cycle or averaging over several.

In order to achieve high spatial and temporal resolution, it is necessary to keep analysis times to an absolute minimum. The data acquisition aspect of the Par-tec lends itself well to rapid analyses, with as little as 2 seconds being possible. The need for focusing prior to each run, slows the process considerably and is also greatly hampered by rapid fluctuations in particle concentration and perhaps sizes. The results from section 2.3.4 identify a region within which the focal point may be set for the duration of measuring. This region lies between the optimum position and the window of the probe and so keeps particle masking effects to a minimum. Below 1 g l^{-1} this may be within 0.8 mm from the window. The use of a fixed position, without the need for focusing procedures, will greatly improve instrument efficiency, in terms of spatial coverage and temporal resolution. Such a procedure was used in subsequent field deployments.

The Par-tec100 has the potential to provide size information in conditions that will easily negate the use of other techniques and should add to the scientific knowledge concerning particle behaviour in dynamic tidal systems. However, the need for calibration whilst not being of great detraction, does bring into question the instrument's efficiency in

dealing with fine material. The development of later electronics packages for the 100 series may overcome this shortfall, but financial restrictions preclude its part in this study. The calibration procedure itself does provide an accurate means of accounting for the instrument's offset whilst retaining sufficient detail. In the worst case, the instrument is still capable of detecting rapid changes to the particle population, which will shed light upon the processes affecting natural aggregates in estuaries and coastal waters.

The Characteristics of Suspended Particles in the Ouse and Humber Estuary of Eastern England

3.1. Estuarine Sediment Transport Processes

Estuaries in Northern Europe have historically been areas of intense industrialisation and conurbation, as gateways for the river borne transport of minerals and metals from mining areas. Commercial and military ports have flourished at estuary mouths, fuelling urban, thence industrial expansion. This has provided estuaries with material, in addition to natural terrigenous sediments, ranging from PCB's (Polychlorinated Biphenyl), radionuclides to phosphates and nitrates from increased agriculture. Although the balance between sediment input and output remains unclear, estuarine hydrodynamic processes and indigenous fauna have the potential to effect the retention of natural particles. This may lead to a build up of pollutants associated with either suspended or deposited sediments within the system. The clarification of the processes enacted within estuaries and the response of SPM to such events, is therefore vital to the successful management and conservation of estuarine systems.

3.1.1. The Classification of Estuaries

Estuaries represent the interface between precipitation controlled fresh water run-off and tidal sea waters. An estuary may be defined as (Barretta-Bekker et al., 1992):

"...a semi-enclosed body of water that has a free connection with the open sea and within which seawater is mixed with fresh water from land.....The landward limit has been defined at 0.01‰ chlorinity."

In a classic stratified estuary, the tidal incursion of denser saline waters will form a salt wedge underlying the low salinity out-flowing waters of the river. Such a structure will migrate up estuary on the tidal wave till high water. Stratified estuaries may be characterised by poor vertical mixing, a sharp salinity contrast and a generally small tidal range (microtidal). The result of tidal dominance is strong vertical mixing and a significant incursion of the tidal wave into the estuary, whereas partially mixed estuaries are intermediate with poor distinction between bottom and surface waters.

A precise classification of estuaries was devised by Hansen & Rattray (1966) and covers well-mixed to stratified estuaries, with a tentative extension to fjords. However, its basis upon the mean tidal cycle properties of salinity and flow velocity led Jay & Smith (1988) to propose a new two parameter classification of shallow stratified estuaries. As a basis two Froude numbers describing barotropic (F_t) and baroclinic (F_b) non-linearity (density variations) are used:

$$F_t = z / H \qquad [3.1]$$

$$F_b = (Dr_H / Dr_V)^{1/2} \qquad [3.2]$$

Where : z = mean tidal amplitude over the basin, H = mean depth over the basin, de_V = vertical salinity difference in mid-estuary and Dr_H = horizontal density difference

between the two ends of the estuary. An estuary is termed highly stratified if $F_b < 1$ and weakly stratified or partially mixed if $F_b > 1$ (Figure 3.1). The difference between the latter two estuary types depending upon the value of F_t. Spatial/temporal tidal and river flow variations, mean that a plot of estuarine data (F_t against F_b) for a particular estuary will describe an envelope, which may transgress the models internal boundaries. Hence estuaries may be mixed or stratified depending upon the observers location and the state of the tide.

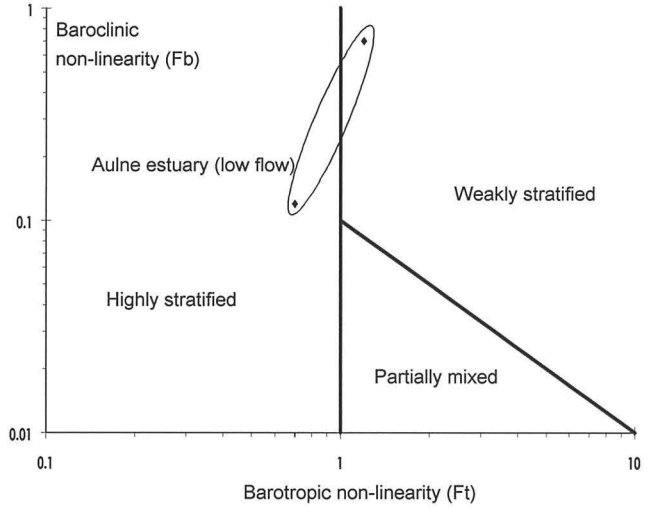

Figure 3.1 : Classification of estuaries. Aulne estuary data source : Allen et al., 1980.. Adapted from Jay & Smith, 1988.

3.1.2. The Characteristics of Estuarine Turbidity Maxima

The Turbidity Maximum, a region of maximum SPM concentration, has long been established as a significant feature of estuarine sediment dynamics. It is situated at the head of the saline intrusion, the null point (1‰ to 5‰), where the convergence of seaward (fresh) and landward (saline) flowing waters create a two layer flow (Dyer, 1988; Gibbs et al, 1989). The generation of SPM concentration maxima is still not fully understood, Officer (1981) supposed that no single cause was responsible, rather that it is generated by

the combined effects of sediment erosion and deposition, tidal dynamics and the residual estuarine circulation. However two mechanisms have been proposed as the principle cause, these are, gravitational circulation (Gibbs et al, 1989) and tidal pumping (Allen, 1980).

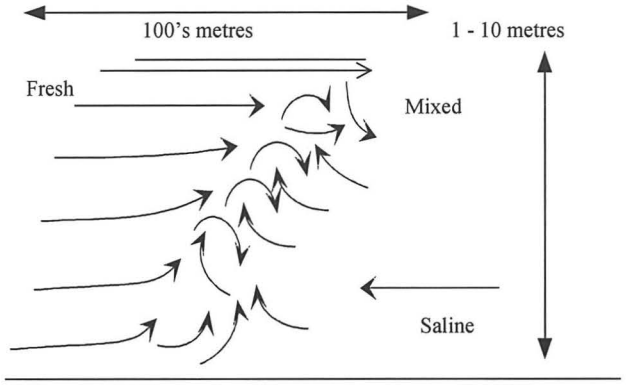

Figure 3.2. Upwelling and circulation patterns at the salt/fresh water interface, (Winant & Bratkovich, 1977), adapted from Gibbs et al, 1989.

Gravitational circulation is the process by which particles are transported around the salt/fresh water interface according to their inherent settling velocities and the turbulent characteristics of the tidal flow. Essentially particles are transported landward by the inflowing saline water until the turbidity maximum region is reached, whereupon, upwelling waters at the nose of the intrusion transport the material into the outflowing fresh water. Settling of material from the fresh surface waters into the saline waters occurs under favourable conditions at slack water or if the particles possess sufficiently large settling velocities. An illustration of gravitational circulation in the Gironde estuary is shown in Figure 1.3. Tidal pumping is the result of an imbalance between the duration of the flood and ebb tides, caused by friction as the tidal wave travels through the estuary. Up-estuary on the flood a sharp rise in water level is produced as the tidal wave over comes friction and the volume of water is constrained by the narrowing channel, in some

cases resulting in a distinct tidal bore. On the ebb the same volume of water passes through the estuary mouth but over a considerably longer period, hence current velocities are generally less than on the flood. Over-tides, particularly M_4 (quarter diurnal) in relation to M_2 (semi-diurnal), also affect the passage of the tidal wave and tidal asymmetry.

The inequality in current velocities creates greater sediment scour on the flood than ebb, leading to net sediment transport landward of the estuary mouth after sediment has settled to the bed during slack high water. Sediment may only reach as far inland as the salt wedge intrudes, therefore tidal asymmetry leading to tidal pumping provides a mechanism for the delivery of material to the null point and its subsequent entrapment and contribution to a bottom turbidity maximum. Bottom and surface TM's may not necessarily coincide spatially. Surface TM's may be generated by upwelling fresh water (Figure 3.2) transporting bottom TM material seaward along the fresh/saline interface into surface waters as the fresh layer thins, gravitational circulation may then allow the return of the material and aid in sustaining the bottom TM (Gibbs et al, 1989).

In calculating sediment fluxes over tidal cycles, Dyer (1975) demonstrated that for the Gironde, the flux due to residual flow was dominant over tidal pumping in contributing to the mean sediment flux, whereas for the Thames, the reverse was true. In the Tamar the controlling factor was seen to vary according to tidal range (Uncles, 1985), with tidal pumping predominant during spring tides and advection during neap tides (Dyer, 1988). In these three cases vertical gravitational circulation is seen as unimportant, although in the Chang Jiang estuary, China it is seen as dominant over tidal pumping (Jilan & Kangshan, 1986).

Clearly the dominant mechanism in generating and sustaining the TM may vary from that of tidal pumping, however in the majority of estuaries studied it is of primary importance, not only in TM generation but also location. The TM location at the head of the saline wedge is thus a function of the tidal wave incursion as demonstrated by Dobereiner & McManus (1983), who also found it to be dependent upon the spring/neap tidal cycle and river run-off.

3.1.3. Turbulent Characteristics of Open Channel Flow and their Effect upon SPM ParticleSizes

In conditions of turbulent flow, a wide range of velocity fluctuations and eddies exist. Such eddies vary from those of large scale low frequency (length L) to small scale high frequency (length l), beyond which energy is dissipated into heat by viscous forces. Smaller eddies are dependent upon the local energy dissipation rate and viscosity, they are assumed to be isotropic and independent of the mass flow (Kolmogorov, 1941). Below a particular size of eddy (l) motional energy is dissipated directly to heat, hence viscous forces dominate, this is termed the viscous sub-range. The size of l is dependent upon the properties of the fluid and energy spectra, defined by the Kolmogorov microscale (Equation 3.3). Above l, inertial forces dominate and energy is transferred to smaller eddies in an energy cascade without dissipation (inertial sub-range), (Harnby, 1982). The critical eddy size is given on the Kolmogorov microscale as:

$$l_0 = (v^3/E)^{1/4} \qquad [3.3]$$

Where, v = kinematic viscosity and E = energy dissipation. (van Leussen, 1988; Nienow, 1982). For particles of $d \gg l_0$, rupture will occur when the turbulent energy fluctuations exceed the strength of the floc. Breakage may also occur due to the pressure

differences upon opposite sides of the floc, such that bulgy deformation and fracture occur (van Leussen, 1988; Ani et.al., 1991). Although Parker (1972) suggested that stripping of primary particles from the floc surface was the principle contributor to floc breakage, when $d \sim l_0$. Collision induced breakage is another mechanism involved in disaggregation (Burban et al, 1989). Envelopment, within eddies, of particles in the viscous sub-range will avoid disruption (Eisma, 1986). Alternatively, the inherent low energies of viscous sub-range eddies may be too weak to overcome the stronger binding strength of small flocs.

In open channel flow 80% of the total turbulent energy is generated in just 10-20% of the total water depth, i.e. the bottom boundary layer (van Leussen, 1988). Energy dissipation increases almost exponentially towards the bottom, hence for mean flow velocities of 1.5 ms^{-1} and 0.5 ms^{-1} (in a 10m channel) the smallest turbulent eddies will rise from 50 to 200μm at the bottom to 600 to 1200μm at the surface, respectively (Nakagawa & Nezu, 1975). Such a distribution of eddy sizes might be thought to result in finer particles occurring nearer the bed after the breakup of large flocs settling out from surface waters. Increasing current velocities at the bed (on the flood or ebb) would re-suspend the resultant fragments for re-aggregation in the surface waters, setting up a cyclical process (van Leussen, 1988). However, from *in-situ* studies (Eisma, 1991; Gibbs et al, 1983b), the largest flocs are to be found near the bed (with the exception of the Scheldt (Eisma et al, 1991b)), where upon settling they are enveloped within an eddy, which at 1m from the bed will be 200 to 600μm (1.5 ms^{-1} to 0.5 ms^{-1}, respectively).

3.1.4. Factors Influencing the Size of Particles in Natural Waters

The factors controlling the spatial and temporal evolution of particle size spectra in natural systems are understood to be:

- Salinity.
- Organic matter (present as surfacial coatings or framework).
- The frequency of particle collisions (dependent upon mechanism).
- The probability of particle-particle adherence upon collision.
- The probability of disaggregation upon collision.
- Turbulent shear resulting in disaggregation.
- pH.
- Temperature.

There exists a network of relationships between each of these factors. The probability of particle-particle adherence upon collision is related to Organic matter content, dependent upon the extent to which a particle is coated and possibly the nature of the coating. The probability of disaggregation upon collision is also related to Organic matter content by the strength of inter-particle bonds. Collision frequency is dependent upon the particle concentration (number of particles for a given volume), particle size (finer particles being less prone to collision (Burban, 1989)) and the turbulent energy field. However, whilst increased turbulence raises the collision frequency, it also exerts a break-up force across the floc (depending upon the scale of turbulent eddies on the Kolmogorov microscale), which may lead to disaggregation through bursting (Ani et al , 1991) or particle stripping (Parker, 1972).

The quantitative contribution to aggregation/disaggregation of each factor has yet to be determined. Numerous workers in the waste treatment and process industries have

carried out laboratory investigations into floc behaviour and formation (Tambo & Watanabe, 1979; Tambo & Hozumi, 1979; Williams, 1992). These studies have formed the basis for much of the work on freshwater (Tsai, 1987) and estuarine flocs (Gibbs, 1985; 1989; Burban, 1989; Ani et al , 1991). Field investigations along similar lines require the use of *in-situ* instrumentation (Bale & Moris, 1987; 1989; 1991; Eisma, 1986; 1990; 1991a; Gibbs et al, 1989; Kranck, 1992; van Leussen, 1993).

3.1.4.1. Mechanisms of Particle Aggregation

Particles may be brought together through several mechanisms, for example; differential settling, Brownian motion, turbulent shear or pelletization. Upon collision though, two factors may influence their sticking efficiency; the cation concentration of the suspending medium and the extent or efficiency of the particles organic coating. In the absence of coatings, particles may flocculate in the presence of cations which suppress the particles electrical double layer, so allowing van der Waals forces to intercede. Particles in nature exist with organic or oxyhydroxide coatings, which impart a uniform negative charge (Hunter & Liss, 1982), therefore increased salinity may go some way to reducing the negative surface charge but will not neutralise it, thus differential mineral flocculation is negated by such coatings (Hunter & Liss, 1982). However, the large natural polymers (mucopolysaccharides), present in the coating, which protrude from the water mantle surrounding the particle, may become attached to another particle or polymer chain. Such binding, termed Steric Stabilisation, may have an efficiency of 10-100%, depending upon the polymer (Edzwald, 1975; Eisma, 1991a). The contribution of each binding mechanism, to the evolution of the particle size distribution in estuaries, is likely to be subject to increasing scrutiny, with the advent of realistic *in-situ* sizing methods.

3.1.4.2. The Influence of Organic Material upon Estuarine Suspended Particles

In many estuarine systems the organic content of particles accounts for some 5-15% by weight, 12-33% by volume of the total SPM concentration. However, it is of significantly greater importance in its contribution to determining the aggregation behaviour of flocs and discrete particles. It is important to understand therefore, that the organic material contained within and on suspended particles moving through the low salinity region, undergoes changes which are directly related to salinity. To use inorganic clay particles as an example, the major component of SPM in turbid estuaries prior to encountering low salinity, particles sourced from river input which have undergone little in the way of transport are relatively free from surface coatings (Neihof & Loeb, 1974; Hunter & Liss, 1982). However, Neihof & Loeb (1974) and Hunter & Liss (1982), have showed that particles become quickly coated with organic and hydroxide coatings upon contact with seawater. Indeed, it would appear that all coastal and estuarine suspended particles are associated with organic coatings. The source of these coatings is Dissolved Organic Carbon (DOC) and planktonic/benthic derived polymers (carbohydrates). Whilst in general, organic and hydroxide coatings have been recognised as fundamental to the aggregation process of fine suspended matter, particular compounds are likely to be of significantly more importance than others, such as carbohydrates and fulvic acids Eisma (1986).

Size analysis of discrete samples using the methods of Coulter Counting and Pippetting, methods which may disrupt fragile aggregates, when compared with carbohydrate analysis and in-situ size measurements, (floc camera), allowed the fragility of flocs through the low salinity region to be investigated (Eisma, 1991). As a result, finer

particles were seen using the discrete methods in the low salinity region than in the remainder of the estuary. Although there was no discernible change in the *in-situ* floc size (Eisma, 1991). Observations in the low salinity region of several Northern European estuaries have shown that the flocs are more fragile than at higher salinities and that it is associated with a peak in dissolved carbohydrates (Eisma, 1986). Although, such a peak may be masked during periods of increased uptake by plankton (spring and summer). The suggestion is that the mobilisation/dissolution of particle associated carbohydrates, most likely polysaccharides, at low salinities induces a weakening of the floc structure (Eisma, 1986; 1991a). This then causes the appearance of finer particle size distributions, when employing discrete methods of analysis. Eisma et al (1991b) proposes that, although weakened by carbohydrate mobilisation this does not affect the *in-situ* floc size, although this is contrary to the evidence of Bale et al (1989), where *in-situ* observations of the Turbidity Maximum in the Tamar estuary reveal the presence of a fine suspended population. Whilst this may be caused by the mobilisation of fine bed sediment (Bale et al, 1989), it is also associated with low organic matter content, as a result of the lower productivity levels encountered in a turbidity maximum environment. The total carbohydrate component of suspended particles in the turbidity maximum is therefore accepted as being low. This suggests that flocs in this region will be relatively weak, in which case the cause of fine particle size distributions is likely to be the increased collision frequency function resulting from the high particle concentrations within the turbidity maximum. The significance of this function will depend upon the actual particle concentration and floc strength in the collisions.

3.2. Particle Size Characterisation in the Humber Estuary

The Humber estuary and its tributaries drain a large portion of the English landmass, approximately 20 %, which is comparable to the Severn watershed. The land is drained from the north by the Ouse, Aire, Derwent and Hull, whilst from the south, it is the Trent, Don, Idle and Eau. The confluence of the Ouse and Trent is situated at Trent Falls some 60 km from the mouth of the estuary at Spurn Point. The limit of the saline influence within the Ouse is defined by the weir at Naburn, situated 62 km further up estuary from Trent falls. With an estimated 3 x 10^6 tonnes of sediment in suspension between Trent Falls and Spurn Point (Jackson & Norman, 1970) an understanding of sediment transport processes is important for the management of such a busy waterway. Due to its economic importance in the region, several sedimentological surveys of the Humber estuary have been carried out in the past. The accurate determination of the channel course particularly in the upper estuary is allied to the regions industrial legacy in places such as Selby. Multidisciplinary studies have gone some way to interpreting the geological history of the estuary and provide good sources of information regarding the estuarine bed sediments and underlying strata. Bed sediments are found to vary considerably along the estuarine axis, but without any obvious pattern. Particularly in the lower stretches, patches of gravels, sands and muds lie in close proximity. However in the upper reaches much of the bed is composed of fine sand or compacted muds (Uncles & Stephens, 1996).

Much of the work concerning suspended particulate material has focused upon its transport and the very large variations in SPM concentration experienced spatially and seasonally within the estuary. In analysing ten years of suspended sediment data,

Gameson (1977) highlighted the extremes of SPM concentration that can occur at any point along the estuary over a tidal cycle. The mean suspended sediment concentrations for particular stations, for example Blacktoft and Whitton, were observed to be lowest at (Blacktoft) or after (Whitton) high water slack, with a sharp rise on the ebb tide concentrations maximised prior to low water slack. Mean concentration values quoted by Gameson (1977), extend from 600 to 4000 mg l^{-1} for Blacktoft and 100 to 2000 mg l^{-1} for Whitton, with extreme values in the Ouse reaching just under 10,000 mg l^{-1}. Spatially, concentrations along the Ouse - Humber axis were found to increase from Naburn (10 mg l^{-1}) to the confluence at Trent Falls (2000 mg l^{-1}), whereupon they decreased seaward along the estuary (100 mg l^{-1} at 20 km from Trent Falls). A high degree of seasonality was also observed in the mean SPM concentrations of the respective systems components (Humber, Ouse, Trent). Whereas, elevated solids concetrations were to be found in the Ouse during the months of August to November (500 mg l^{-1}), in the Humber it is during December to January (300 to 400 mg l^{-1}) that suspended particulate material is highest, with July characterised by lower concentrations (150 mg l^{-1}). These variations differ significantly in their pattern, with the Ouse varying in a square waveform whilst in the Humber the variation is sinusoidal.

A more recent survey by Uncles & Stephens (1996) concentrated upon sediment transport along the Humber - Ouse, paying particular attention to the role of the turbidity maximum. The variation in SPM concentrations over tidal cycles during Uncles & Stephen's (1996) surveys were greater than those observed by Gameson (1977), particularly in relation to the appearance of fluid mud layers and strong lutoclines (Figure 3.3). Uncles & Stephens (1996) report the sizes of suspended material after analysis in the laboratory as comprising of small microflocs, the bulk of material (97 to 100 %) being less than 63 μm with a small fraction (4 to 6 %) less than 2 μm. After chemical disaggregation

the bias shifted in favour of discrete primary particles (80% < 8 μm and 30% of clay sized material). Until 1995 no in-situ observations of particle size were available for the Humber estuary.

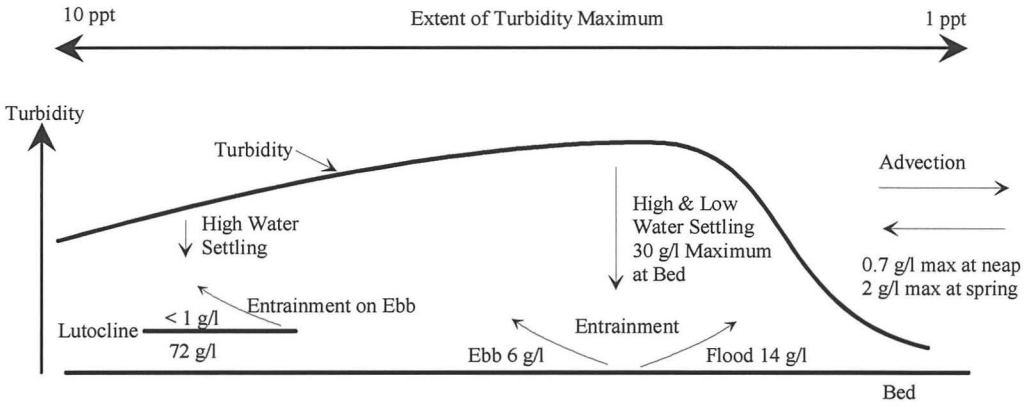

Figure 3.3 Summary of sediment transport observations made by Uncles & Stephens (1996) in the Humber - Ouse turbidity maximum region, March 1994.

3.3. Survey Sites, Instrumentation and Sampling Rationale

During 1995, it proved possible to collaborate with workers involved in the LOIS RACS (C) program. This meant that particle size measurements using the Par-tec100 could be allied to sediment transport studies carried out in the Humber Estuary and the Holderness Coast (Figure 3.4). This provides a suitable framework for the interpretation of the processes affecting SPM flocculation, deflocculation and transport in environments ranging from very high to low SPM concentrations. Collaboration with R. Uncles and J. Stephens allowed a detailed survey of the Humber estuary to be carried out. Sites were sampled extending along the Ouse & Humber estuary from the weir at Naburn to Hull. Inclusion within the LOIS RACS (C) cruises aboard RS Challenger allowed surveys in the

lower estuary and Humber plume region to be undertaken. The objective of these surveys was to characterise the physical and seasonal attributes, primarily concerning the in-situ particle size of suspended particulate matter along the axis of the estuary. Particular attention was paid to the turbidity maximum and the plume regions. Anchor stations of 13 hours duration were carried out (Table 3.1) with measurements taking place through the water column at regular intervals. Particle size measurements were carried out at the same time as water quality and current velocity measurements (R. Uncles & J Stephens, Plymouth Marine Laboratory). This provided the high degree of temporal and spatial resolution in terms of both the SPM characteristics and current velocity. This would aid in characterising rapid changes in the SPM size distribution brought about by equally rapid changes in the hydrodynamic regime, such as at times of resuspension or in the initial stages of SPM settling.

Station	Date	Tide	Range
Selby	24th August 1995	Neap + 3 days	6.7m
Selby	28th September 1995	Spring + 1 day	7.5m
Blacktoft	21st August 1995	Neap	5.7m
Blacktoft	26th September 1995	Spring - 1 day	7.5m
Whitton channel	18th July 1995	Spring + 4 days	6.9m
Whitton channel	17th March 1995	Spring	7.1m
Humber bridge	16th March 1995	Spring - 1 day	6.9m
SG23	8th June 1995	Neap	3.2m
SG10	7th June 1995	Neap - 1 day	3.4m
SG13	3rd June 1995	Spring + 3 days	4.5m
SG24	4th June 1995	Spring + 4 days	4.3m
HW5	4th November 1994	Spring	6.7m
HW5	22nd January 1995	Spring + 3 days	5.0m
HW7	7th November 1994	Spring + 3 days	6.0m

Table 3.1 Sampling stations and dates of the Humber - Ouse survey 1994-1995.

In order to attempt the distinction of a seasonal variation in the size characteristics of suspended particulates, sites along the Humber - Ouse were sampled at different times

of the year, between November 1994 and September 1995. In effect two surveys were carried out, one from the RS Challenger, for the purpose of covering the Humber plume region and eastern coastal zone and the second from the RV Seavigil, for the purpose of covering the upper estuary, in particular the turbidity maximum region.

In the upper estuary four sites were successfully surveyed, three of which were repeated. An axial run consisting of five point stations was also carried out. Further axial profiles and anchor stations were planned, however on several occasions instrument failure curtailed these activities. In the Humber plume region seventeen, 25 or 13 hour anchor stations were carried out during five separate cruises, excluding repetitions, there were 12 unique sites.

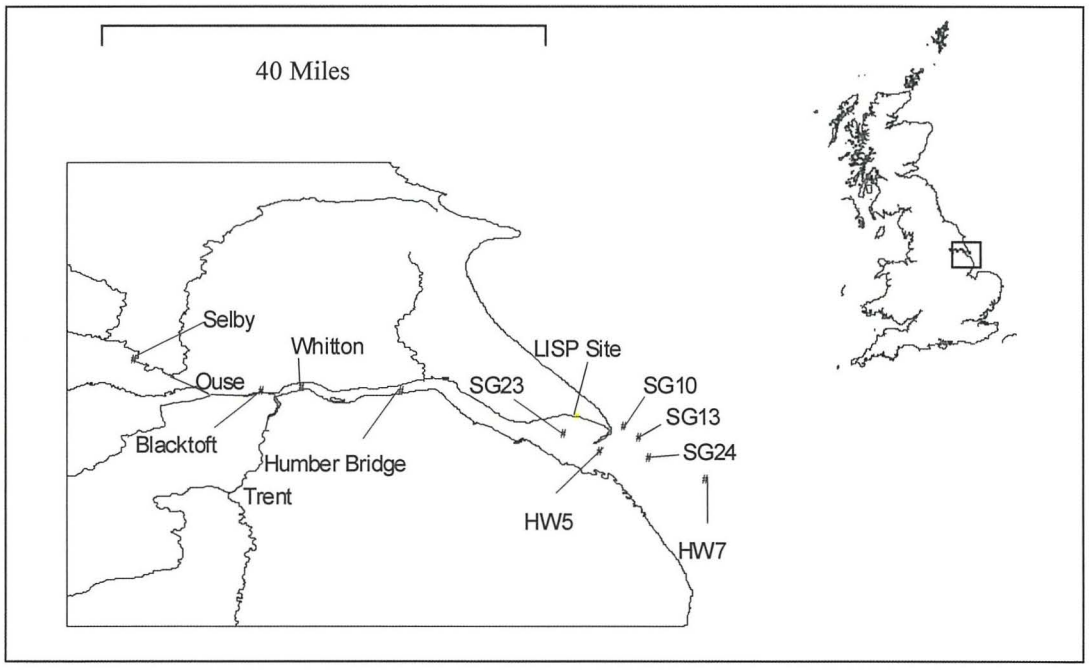

Figure 3.4 Location of survey stations along the Humber estuary and extending out to the Humber plume, carried out between November 1994 and September 1995.

Instruments were deployed from the RV Seavigil (National Rivers Authority), with the exception of Blacktoft, whilst the vessel was anchored at station for the entire semi-diurnal tidal cycle. Two separate rigs were used, one comprised the Par-tec100, depth

gauge, with occasional turbidity sensors, salinometer and current meter. The second rig was made up of OBS and transmissometer sensors, salinometer and NBA rotary vane current meter, which provided pH and temperature as well as current speed and direction (R. Uncles & J Stephens, Plymouth Marine Laboratory). This second package provided the majority of the master variable data, salinity, current speed and turbidity. A pump was also connected to either of the rigs in order to provide bottled samples at depth for gravimetry, particularly when high turbidity swamped the sensors. Both rigs were raised from the bed at approximately the same times using a HIAB crane, with measurements taken at 0.5 to 1m intervals, dependent upon water depth. Profiles were measured every 20 to 30 minutes. At Blacktoft, a hand driven crane was used to raise and lower both rigs, like wise for RV Seavigil deployments both rigs were never displaced more than 2 to 3m from each other. The high turbidity encountered ensured that analysis times for the Par-tec100 could be kept to a minimum. Unless the turbidity fell significantly, a measuring cycle duration of 3.2 seconds and 2 cycle average was used, allowing rapid, high resolution profiling. The focal position was set at a value conducive to allow measurements at the highest turbidity expected to be encountered, 0.8 mm, or 0.2 mm when close to the turbidity maximum.

From RS Challenger the manner of deployment was similar, excepting that the time constraints brought about through operating the Par-tec100 at low particle concentrations limited the profiles to a surface and bottom measurement. With the exception of cruise CH119A, master variable data was gathered from a vertical profiling CTD package and an ADCP located in the ships hull operating on ten minute averages. The Par-tec100 was lowered in a heavy cradle without periphary equipment (Photograph 2).

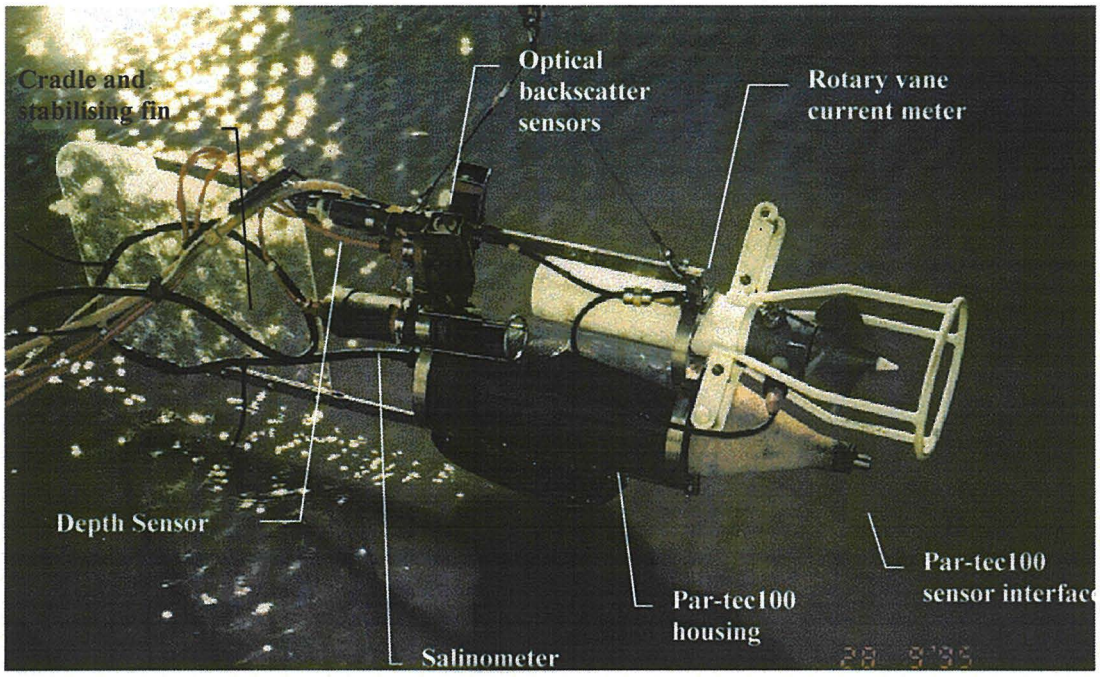

Photograph 1 The instrumentation used in the survey of Humber - Ouse stations, showing the Par-tec100 in-situ particle sizer situated in a lightweight cradle with stabilising fin. The attached peripheral equipment was used in the measurement of current velocities, salinity and SPM concentrations. Optical backscatter sensors were in the range 0-100 and 0-1000 mg l-1.

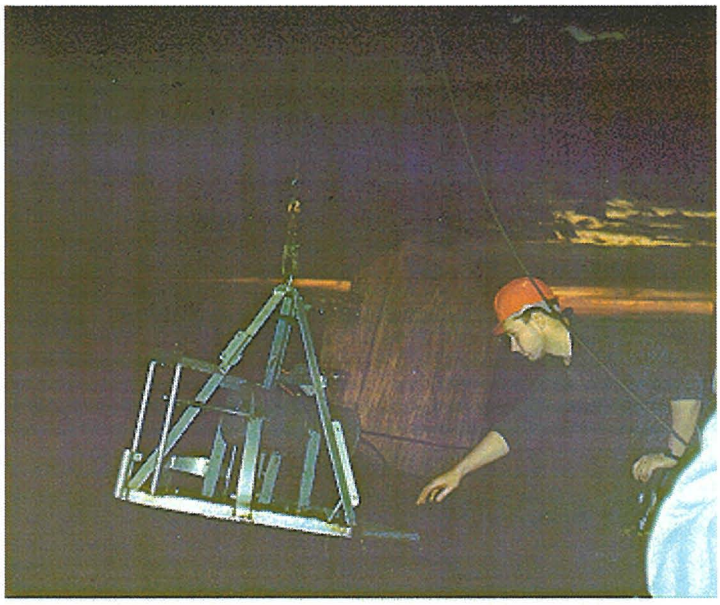

Photograph 2 Instrumentation used in the survey of offshore sites in the Humber estuary and along the East coast. Showing the Par-tec100 mounted in a heavy duty tripod with stabilising fin.

3.4. Results

3.4.1. Detail of Tidal Cycle Variations at Unique Stations

3.4.1.1. Selby - 24th August 1995

Selby, in the upper reaches of the Ouse, is characterised by a prolonged ebb and rapid flood resulting in a pronounced bore. Salinity varied between 0 ppt (LW, 16:00 hrs) and 1 ppt (HW, 20:30 hrs, Figure 3.5b) with SPM levels (Figure 3.5d) between < 1000 and < 75000 mg l^{-1}, at low and high water, respectively. Current velocities (Figure 3.5c) slackened significantly over high water only (<0.2 m s^{-1}) and maximised during the flood tide (1.4 m s^{-1}), at other times velocities ranged from, 0.2 m s^{-1} (at the bed) to 1 m s^{-1} (at the surface). Shear (Figure 3.5e) was strongest during the passing of the bore (up to 7 s^{-1}) and relatively high when the water depth fell below 2 m. Over high water, particulate concentrations exhibited a strong vertical gradient with a thin surface layer of relatively low concentration (< 10 g l^{-1}), at the bed particulate concentrations were up to 60 g l^{-1}. Median particle sizes over high water (Figure 3.5a) appear homogenous throughout the water column (< 300 μm) with the exception of 0.4 to 0.8 m above the bed (< 400 μm). Near bed concentrations maximise (< 75 g l^{-1}) upon the early ebb, coincident with a deepening of the low turbidity layer at the surface. This is brought about by the settling out of large particles (< 400 μm) forming at the surface and in mid water to leave particles of 80-90 μm diameter. From 3.8 m to 3.1 m above the bed there is a shift in the mode to over 200 μm, with the median increasing to 255 μm (Figure 3.6). Below this depth the particle size distribution is multimodal, with the possibility of two distinct particle populations with modal values of 120 and 430 μm. With the increase in particulate matter

concentrations from an elevation of 1.6 m to 0.3 m, a decrease of 311 μm to 266 μm, in the median particle size was observed (Figure 3.5d).

The early ebb currents show no vertical stratification, particularly in the surface waters, resulting in the low shear values observed. Entrainment of material from the mid to bottom of the water column is brought about by stratification of the ebb currents and increased near bed shear ($< 2\ s^{-1}$). The existence of a mid depth size minima (< 300 μm) may be attributed to entrainment and breakage of material from the lower water column, whilst in the surface particles remain relatively large owing to the lack of shear and low concentrations. The ten fold decrease in turbidity towards low water ($10\ g\ l^{-1}$ at 15:00 hrs and $1\ g\ l^{-1}$ at 16:00 hrs) suggests that the up estuary nose of the turbidity maximum is to be found between the 0.4 and 0.6 iso-haline. During this period an inverse relationship exists between particles sizes and shear. This produces an inverse vertical size gradient, with the low shear surface layer containing large particles thinning as low water approaches and shear increases up the water column. Strong current velocities over low water ($< 1\ m\ s^{-1}$ at the surface) combined with the shallow water depth to generate high levels of shear (< 6 to $7\ s^{-1}$). Despite this, the bed sediment, consisting of compacted clays, resisted resuspension. Upon the flood a very strong shear gradient is observed in the lower water column, the upper column experiencing little or no shear until the arrival of the tidal bore (18:30 hrs). The increase and vertical homogeneity of particle sizes and particulate concentrations as high water approaches, indicate the arrival of the turbidity maximum.

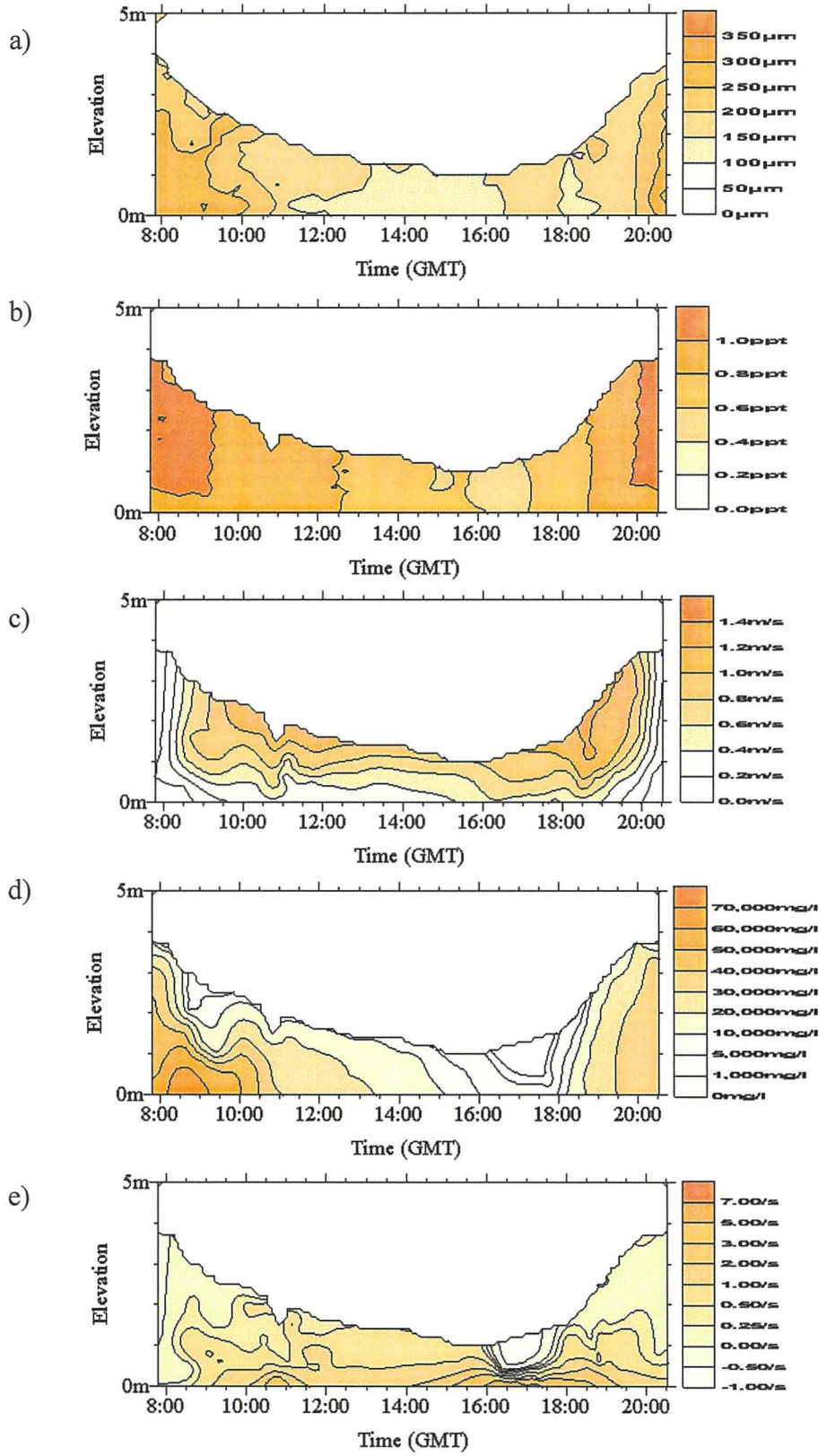

Figure 3.5 Time and spatial series of contoured data from Selby, August 1995. Data comprises, a) particle size, b) salinity, c) current velocity, d) SPM concentration and e) shear.

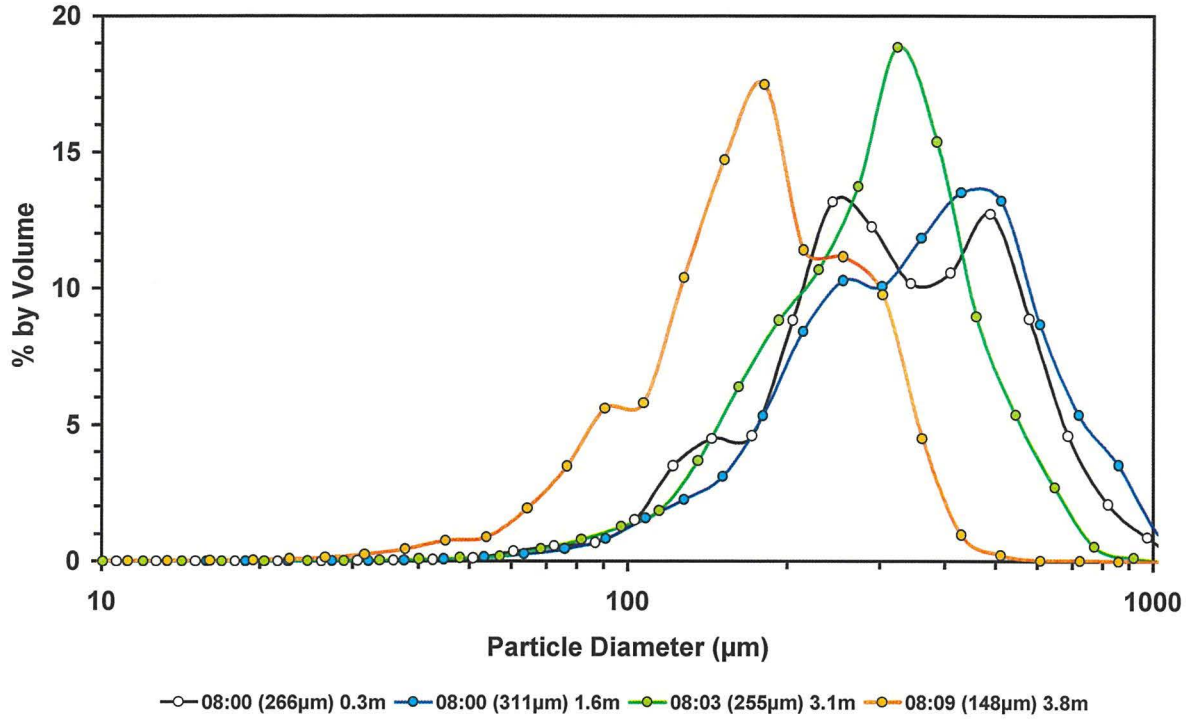

Figure 3.6 Particle size spectra from Selby, August 1995 at High water (08:00 hrs), through the water column. Legend refers to time of sample, median particle diameter (µm) and elevation above the bed (m).

3.4.1.2. Selby - 28th September 1995

There is a good deal of similarity between the tidal profiles for the 28/09/95 and 24/08/95, although the near spring tide (28/09/95) generated slightly higher current velocities (1.6 m s^{-1}) upon the flood tide (Figure 3.7c). Despite high current velocities, lower SPM levels were observed (generally < 10 g l^{-1}, Figure 3.7b) suggesting that the turbidity maximum was located further down estuary at > 0.7 ppt (Figure 3.7a). The highest particle concentrations coincided with high water slack (11:00 hrs) and the movement of large particles (< 500 μm) down the water column. As on the 24/08/95, high water slack sees floc growth and settling out (Figures 3.6b & e, 10:30 to 11:30 hrs), producing pronounced minima and maxima in both particle concentration and size, respectively. Settling also appears to continue well into the development of strong ebb currents, once again the current lacks vertical stratification and therefore low shear was observed (Figure 3.7d). The development of higher shear near to the bed (11:30 hrs) and then extending up the water column, brings about re-entrainment of settling flocs from the middle to lower water column. (Figures 3.7b & e). The size of particles close to the bed (< 0.4 m elevation) remains small (< 100 μm, Figure 3.9) throughout high water and the early ebb, the majority of this period coinciding with increased shear and high particle concentrations at the bed. Entrainment of particles into the upper column sees a change from a normal particle size distribution (Figure 3.9, 10:25), to one that is distinctly multimodal (Figure 3.9, 11:24). As the ebb progresses, the distribution of particle sizes returns to a normal distribution but with a shift in size from a mode of 423 μm to 570 μm (Figure 3.9, 11:56).

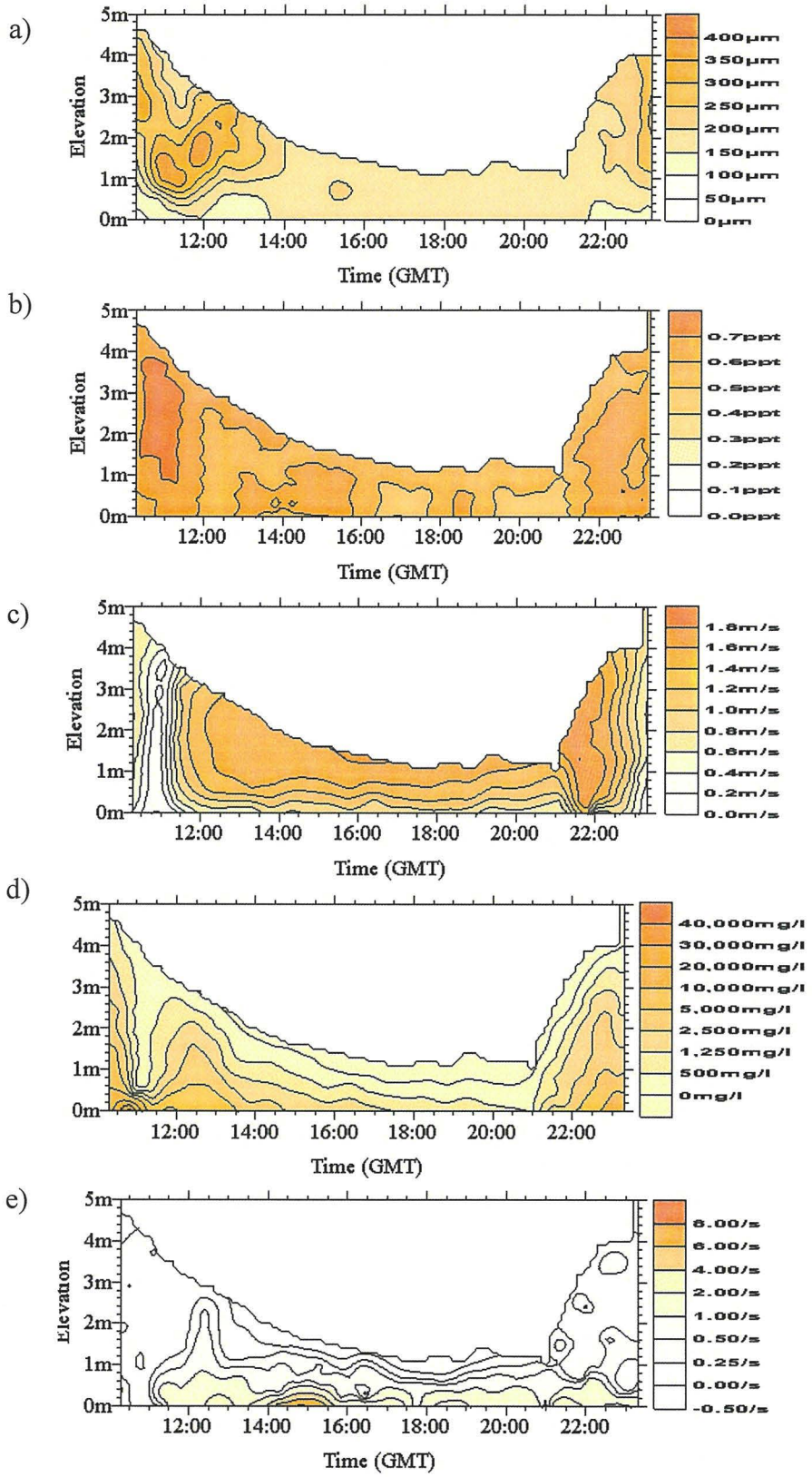

Figure 3.7 Time and spatial series of contoured data from Selby, September 1995. Data comprises, a) particle size, b) salinity, c) current velocity, d) SPM concentration and e) shear.

The size of particles throughout the rest of the tidal cycle, until high water slack (23:30 hrs), remains unchanged (< 150 μm) being purely advective in its behaviour (Figure 3.10), despite high near bed shear (< 8 s^{-1}, between 14:30 to 15:30 hrs). The evening high water sees the return of higher particle concentrations, indicating the up estuary nose of the turbidity maximum. Once again settling takes place as shear and current velocities decrease, with floc growth in the upper water column. Close to the bed particle size decreases to < 100 μm. A settling velocity distribution of (Figure 3.8) in the range 150 to 300 μm (Appendix 1) was obtained for the high water slack period during which clearing of the water column was seen to be taking place. Average calculated values range from 0.06 mm s^{-1} for 150 μm diameter particles to 0.4 mm s^{-1} for 300 μm diameter particles. Particles above 225 μm exhibit little variation in settling velocity, whilst below this value, settling velocities decrease rapidly for finer particles.

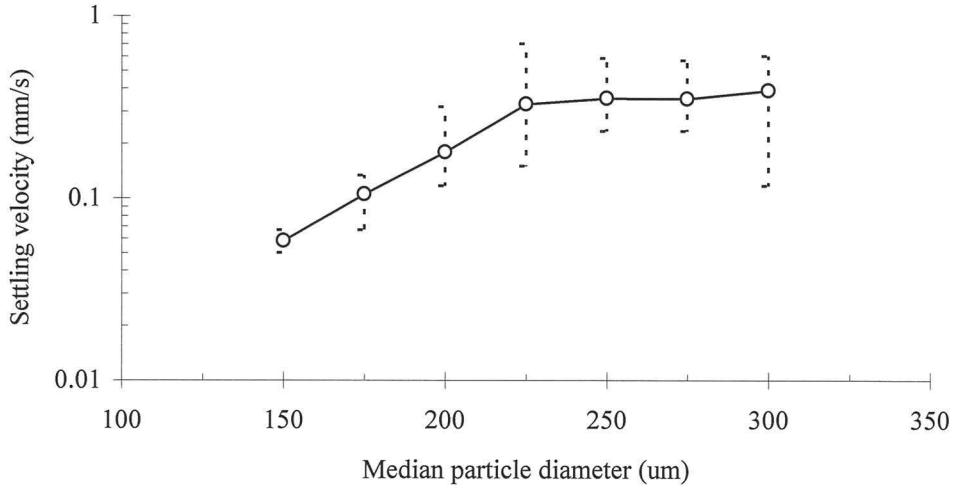

Figure 3.8 Settling velocity distribution of suspended particulates around high water (10:00 hrs) at Selby on the 28th September 1995.

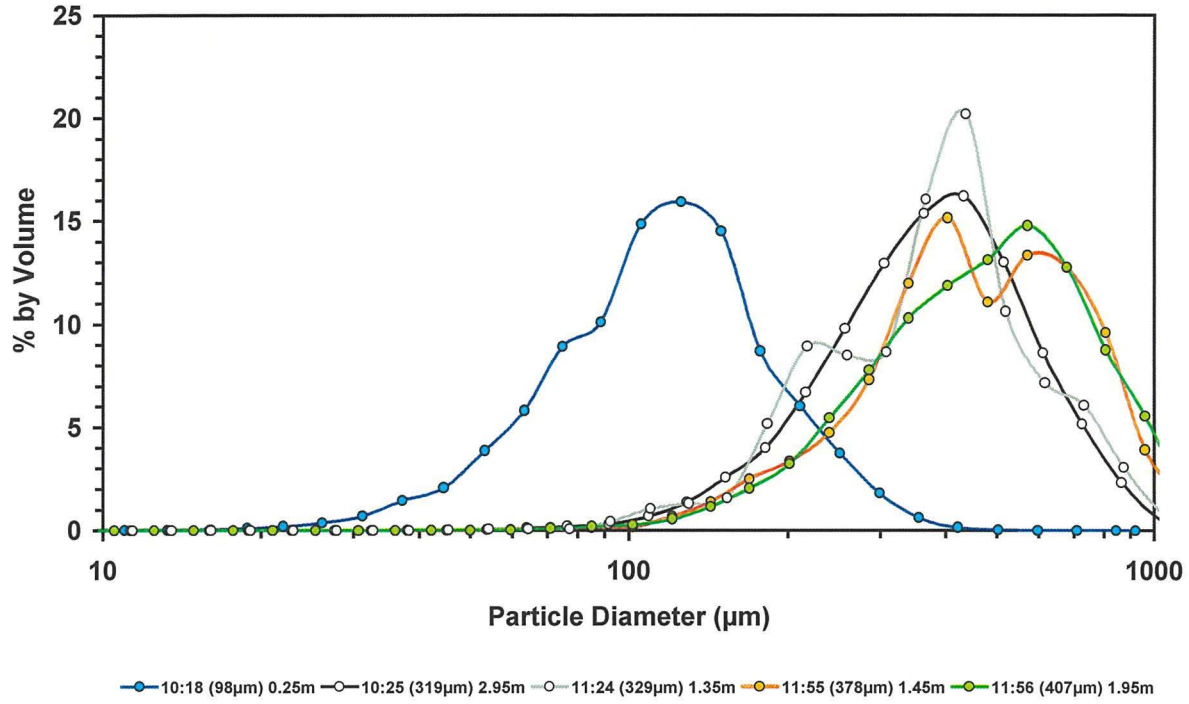

Figure 3.9 Particle size spectra from Selby, September 1995 at High water slack (10:00 hrs), through to the on set of the ebb tide (12:00 hrs). Legend refers to time of sample, median particle diameter (µm) and elevation above the bed (m).

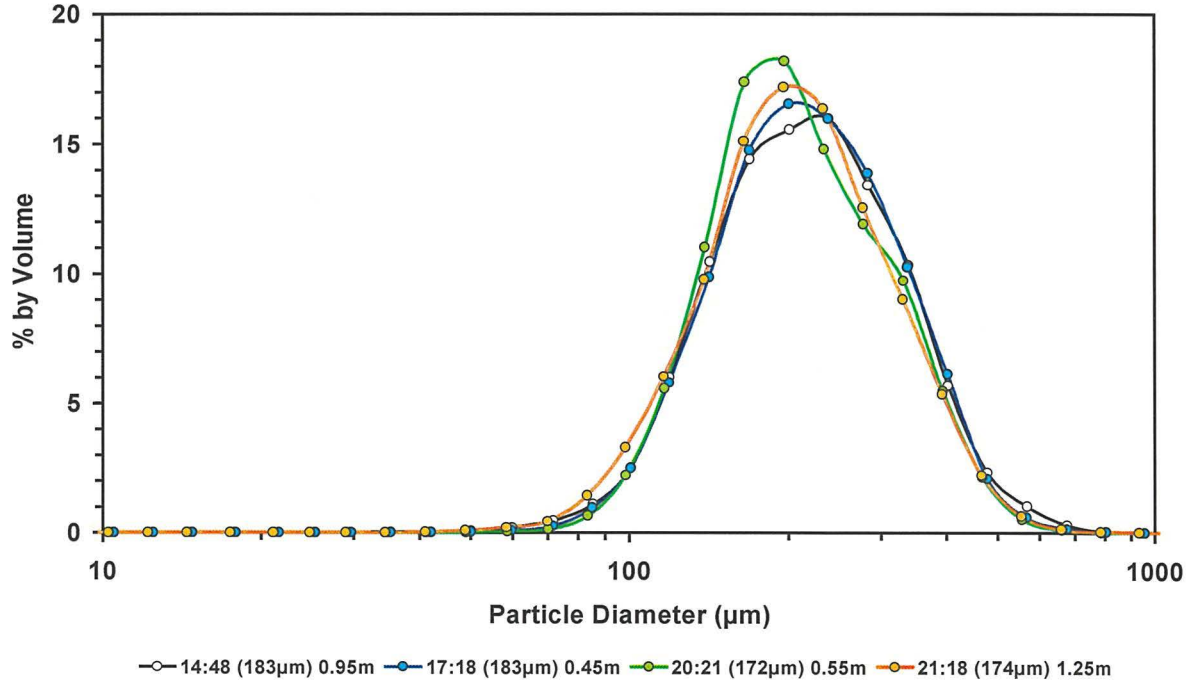

Figure 3.10 Particle size spectra from Selby, September 1995 during the ebb tide until Low water slack (21:00 hrs). Legend refers to time of sample, median particle diameter (µm) and elevation above the bed (m).

3.4.1.3. Blacktoft - 21st August 1995

Owing to the neap tide, current velocities at Blacktoft were considerably lower than Selby, at less than 1.2 m s^{-1} on the flood tide and less than 1 m s^{-1} on the ebb (Figure 3.7b). Particulate concentrations remained high throughout the tidal cycle at < 2 g l^{-1} in the upper water column, extending down to < 100 g l^{-1} near to the bed (Figure 3.11c). Such a strong gradient was brought about by the encroachment of a fluid mud layer, one hour before low water (LW, 10:00 hrs), which persisted until the following ebb tide. Particle concentrations with in the mud layer ranged from <100 g l^{-1} to 30 g l^{-1}, the lack of a distinct lutocline being due to the relatively high concentrations in the rest of the water column. The < 0.2 m s^{-1} current velocity and < 0.1 s^{-1} shear boundaries (Figure 3.11d) help define the suggested upper boundary of the mud layer. Following high near bed shear (08:00 to 09:00 hrs), particle sizes in the water column and near bed ranged from 200 μm to 1000 μm near the bed (Figure 3.11e), thereafter reducing with the appearance of the main body of the mud layer (10:00 hrs). The high concentrations give rise to turbulent damping (after 10:00 hrs) which promotes the growth of flocs, hence particle sizes within this body are large (> 1000 μm). On the flood tide, the mud layer is seen to thin as higher current velocities (< 0.8 m s^{-1}) near the bed, along with an increase in water column concentrations this suggests entrainment from the mud layer surface. Further flocculation and settling at high water (16:00 hrs) leads to a thickening of the layer. Upon the ebb tide drastic thinning of the layer occurs, the lower current velocities in comparison to the flood and the apparent lack of resuspension suggest movement of the layer down estuary. Throughout the tidal cycle, large shear exists directly above the layer, in some cases (13:00 to 15:00 hrs) this is directly linked to particle size minima and therefore shear controlled floc breakage.

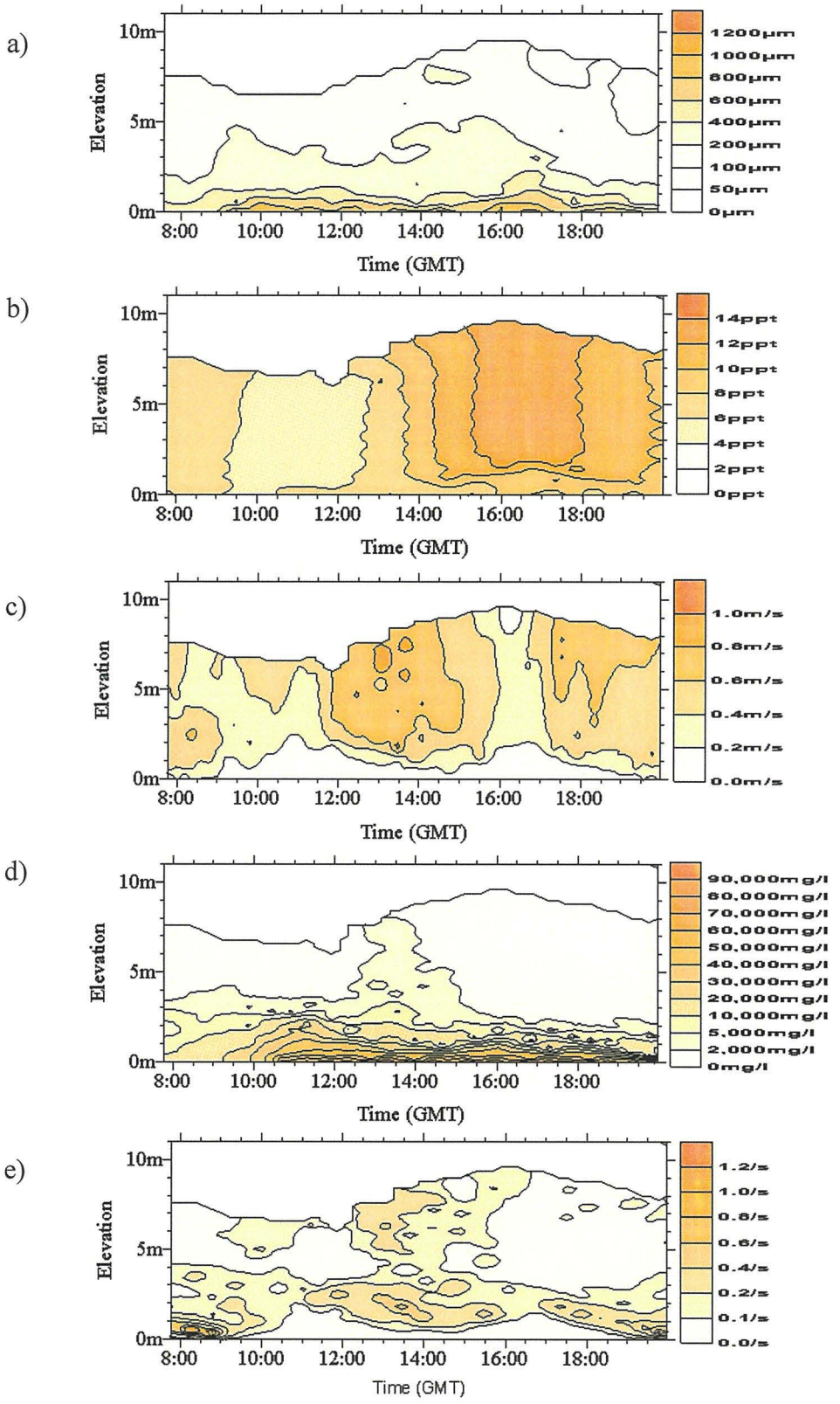

Figure 3.11 Time and spatial series of contoured data from Blacktoft, August 1995. Data comprises, a) particle size, b) salinity, c) current velocity, d) SPM concentration and e) shear.

3.4.1.4. Blacktoft - 26th September 1995

The spring tide of the 26th September contrasts greatly with the neap tide of 21st August, primarily in the behaviour of the SPM and hydrodynamics. Salinity ranged from 14 to 16 ppt at high water, to < 2 ppt at low water (Figure 3.12a), with the water column appearing well mixed. Current velocities were strongest upon the flood tide (< 1.4 m s^{-1}) with little or no vertical stratification, particularly before and after high water (Figure 3.12b). Shear remained low for the most part of the tidal cycle, with only localised high shear close to the bed during the maximum ebb and flood tides (Figure 3.12d). Particulate concentrations (Figure 3.12c) displayed little in the way of vertical structure, with the exception of the surface waters during low water when near bed concentrations maximised (< 28 g l^{-1}). Towards high water particle concentrations decreased to less than 4 g l^{-1}. Particle sizes exhibit a predominantly inverse relationship with particulate concentration, with the largest particles (< 600 μm) occurring in the middle of the water column at high water slack and the smallest (< 100 μm) during maximum flood currents. The distribution of particle sizes through the water column over high water (Figure 3.13), bears many similarities to that of Selby (Figures 3.6 & 3.9). This despite the fact that from the contour plots of concentration and size (Figures 3.12a & 3.12d) there is no obvious pattern of settling. However, at the bed and at the surface, particle diameters remain low with median values less than 200 μm (Figure 3.13). The multimodal nature of the size distributions at 4.25 m and 6.25 m elevation, shares similar modes with that of Selby, i.e. approximately 200-250 μm, 400-500 μm and 700-800 μm (Figures 3.9 & 3.13).

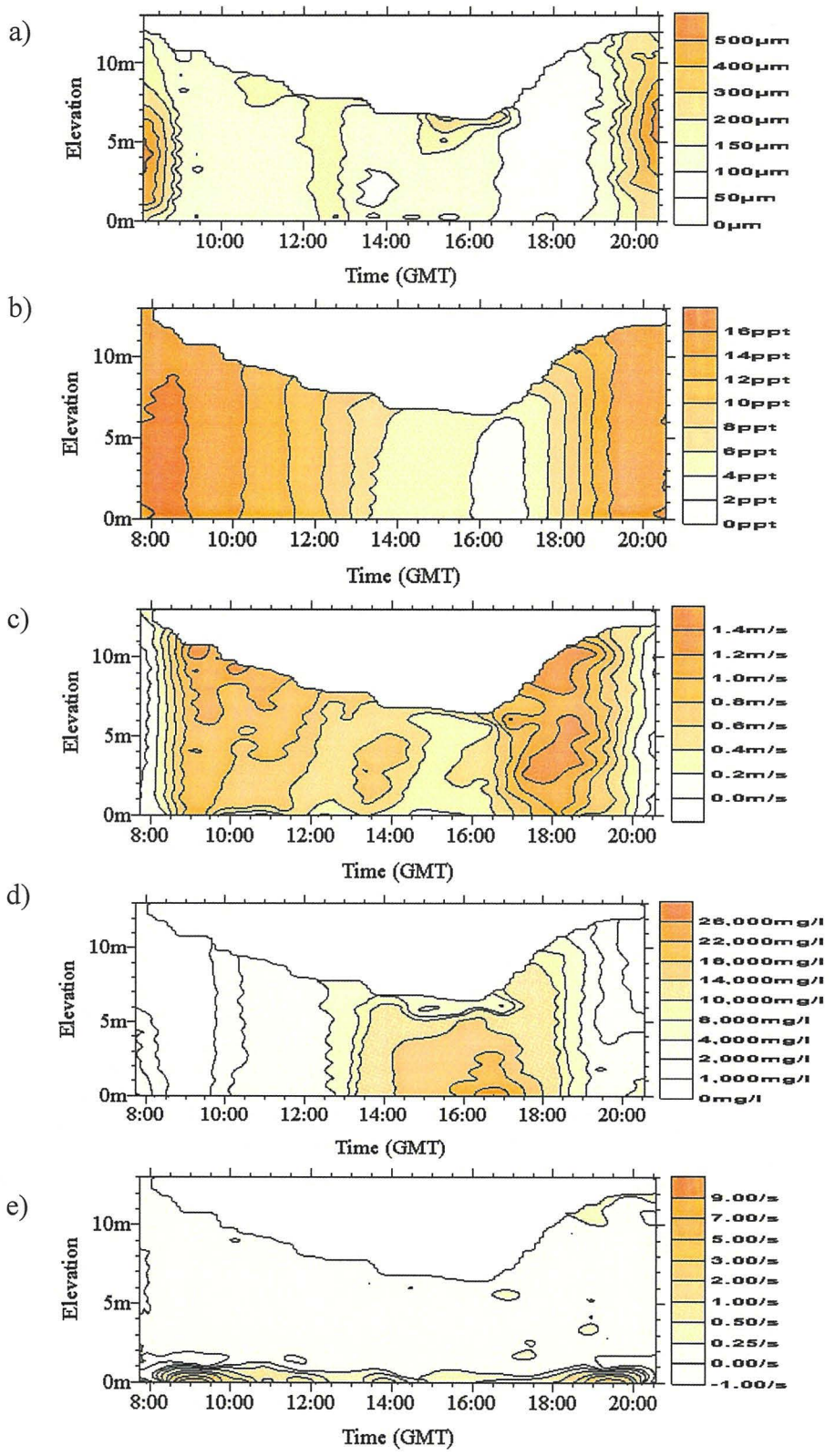

Figure 3.12 Time and spatial series of contoured data from Blacktoft, September 1995. Data comprises, a) particle size, b) salinity, c) current velocity, d) SPM concentration and e) shear.

The behaviour of suspended material was purely advective with no sign of resuspension and despite the possibility of floc growth at high water slack, little in the way of particle settling. One feature in common with the neap tide of the 21/08 was the presence of large flocs at the surface during low water (median diameter, both regions possessing low SPM concentrations and low shear. Unlike Blacktoft on 21/08, the high particle concentrations present near to the bed at low water are characterised by normal distributions of small particles, median diameter approximately 90 μm (Figure 3.14).

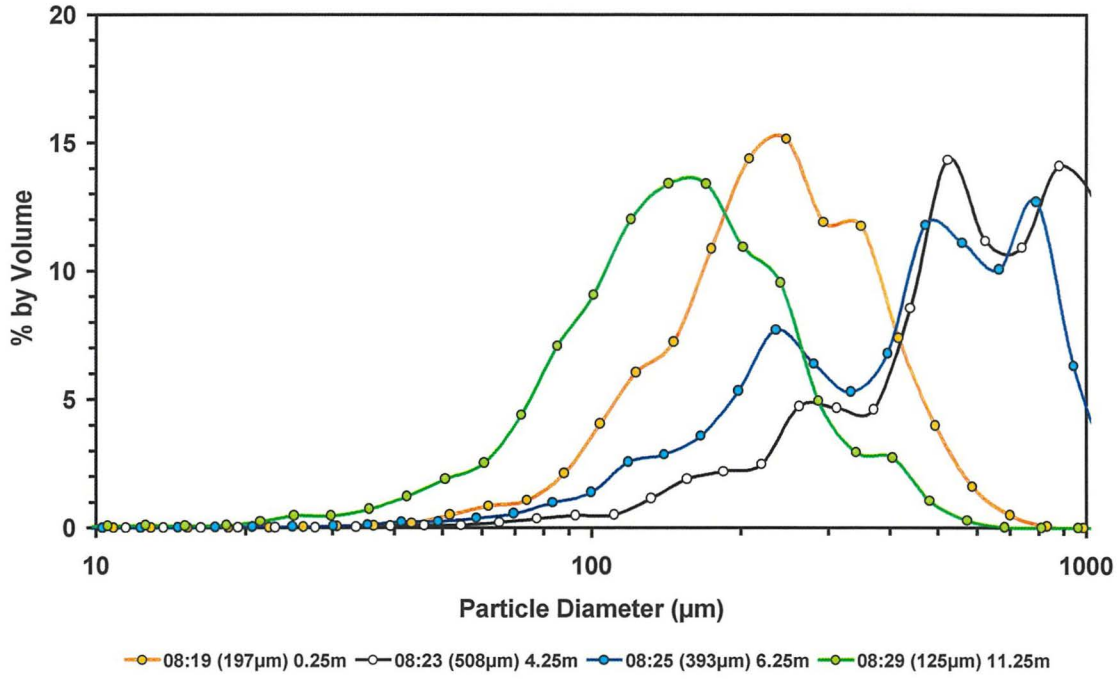

Figure 3.13 Particle size spectra from Blacktoft, September 1995 at High water (08:00 hrs), through the water column. Legend refers to time of sample, median particle diameter (μm) and elevation above the bed (m).

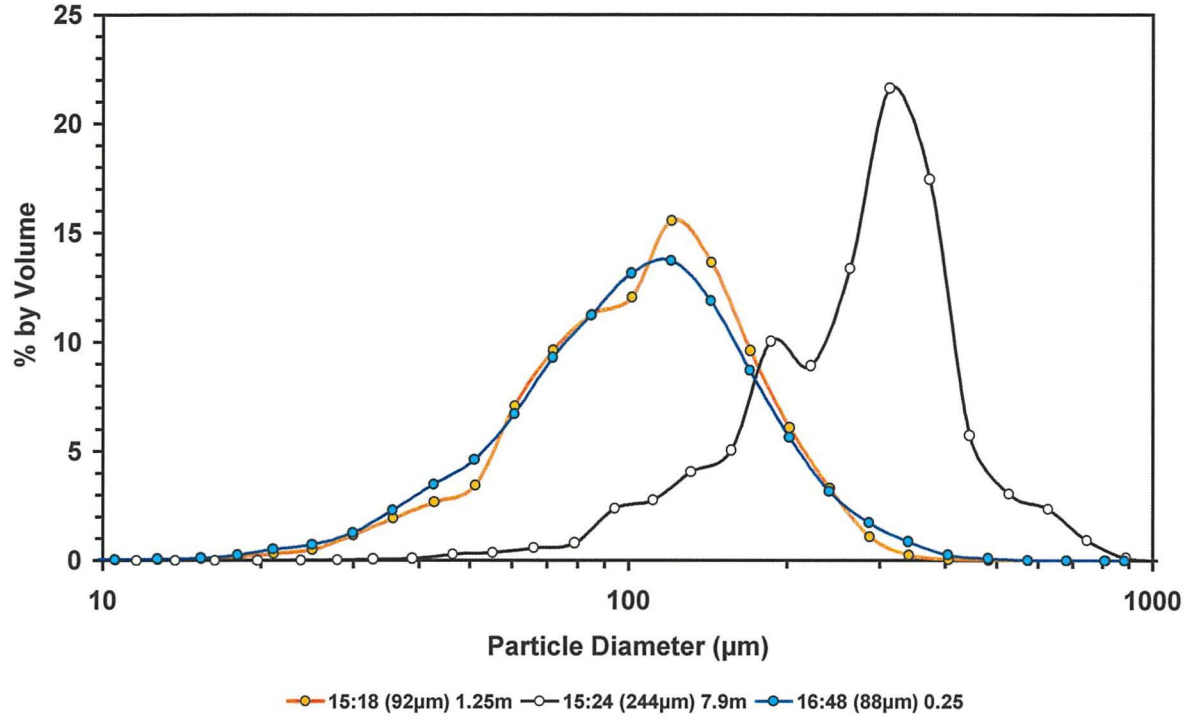

Figure 3.14 Particle size spectra from Blacktoft, September 1995 on the ebb approaching Low water (18:15), at surface and near bottom. Legend refers to time of sample, median particle diameter (µm) and elevation above the bed (m).

3.4.1.5. Whitton channel - 18th July 1995

Whitton channel is situated seaward of the confluence at Trent Falls. During the anchor station a wide range of salinities, from 4 ppt at low water to 20 ppt over high water were observed (Figure 3.15a). In common with Selby, a distinct tidal bore (up to 10 cm wave height) was seen upon the flood tide. SPM concentrations (Figure 3.15c) were lowest during high water slack at < 0.5 g l^{-1} and remained relatively low throughout the tidal cycle at < 4 g l^{-1}, with the exception of low water where concentrations exceeded 10 g l^{-1} marking the extent of the turbidity maximum. On the ebb tide a strong vertical gradient in current velocity (Figure 3.15b, 1.4 m s^{-1} at the surface, 0.6 to 0.4 m s^{-1} at the bed) occurred giving rise to strong near bed shear (Figure 3.15d, < 1.2 s^{-1}). The largest

particles, 500 μm median diameter, were observed at high water around mid high water slack in the lower water column (Figures 3.15e & 3.17). Particle size distributions at this time indicate the probability of floc growth in the upper to mid water column, with particle sizes increasing closer to the bed, i.e. from 586 μm at 2.6 m elevation to 722 μm at 1.6 m elevation (Figure 3.17). At the bed, the particle size distribution is well sorted with a well defined mode of 423 μm. Such a profile allied to the variations in SPM concentration suggest a clearing of the water column to leave fine particles of < 100 μm (Figure 3.18) with settling velocities too small to allow their deposition. After 12:00 hrs, when the ebb currents are approaching maximum, both SPM concentration and their size are seen to increase as material is entrained from the bed. Whilst the size of material during entrainment is smaller (< 300 μm) than during the settling phase, the particulate concentrations are similar. This suggests that much if not all of the material deposited over high water is subsequently resuspended. The discrepancy in the size of particles during settling and resuspension appears related to the significantly higher near bed shear during the ebb tide causing the disruption of large flocs as they are entrained. As low water approaches, particulate concentrations increase with the emergence of the turbidity maximum, whereas particle sizes are seen to decrease, picking up again upon the flood tide and maximising in mid water as high water slack approaches. A settling velocity distribution (Figure 3.16) was calculated for particles in the range 150 to 400 μm (Appendix 1). Unlike Selby (28/09/95), settling velocities are consistent throughout the range, at approximately 0.1 mm s^{-1}, with the exception of the larger particles which fall to 0.04 mm s^{-1}. This may be explained in part by the low number of samples for these particles.

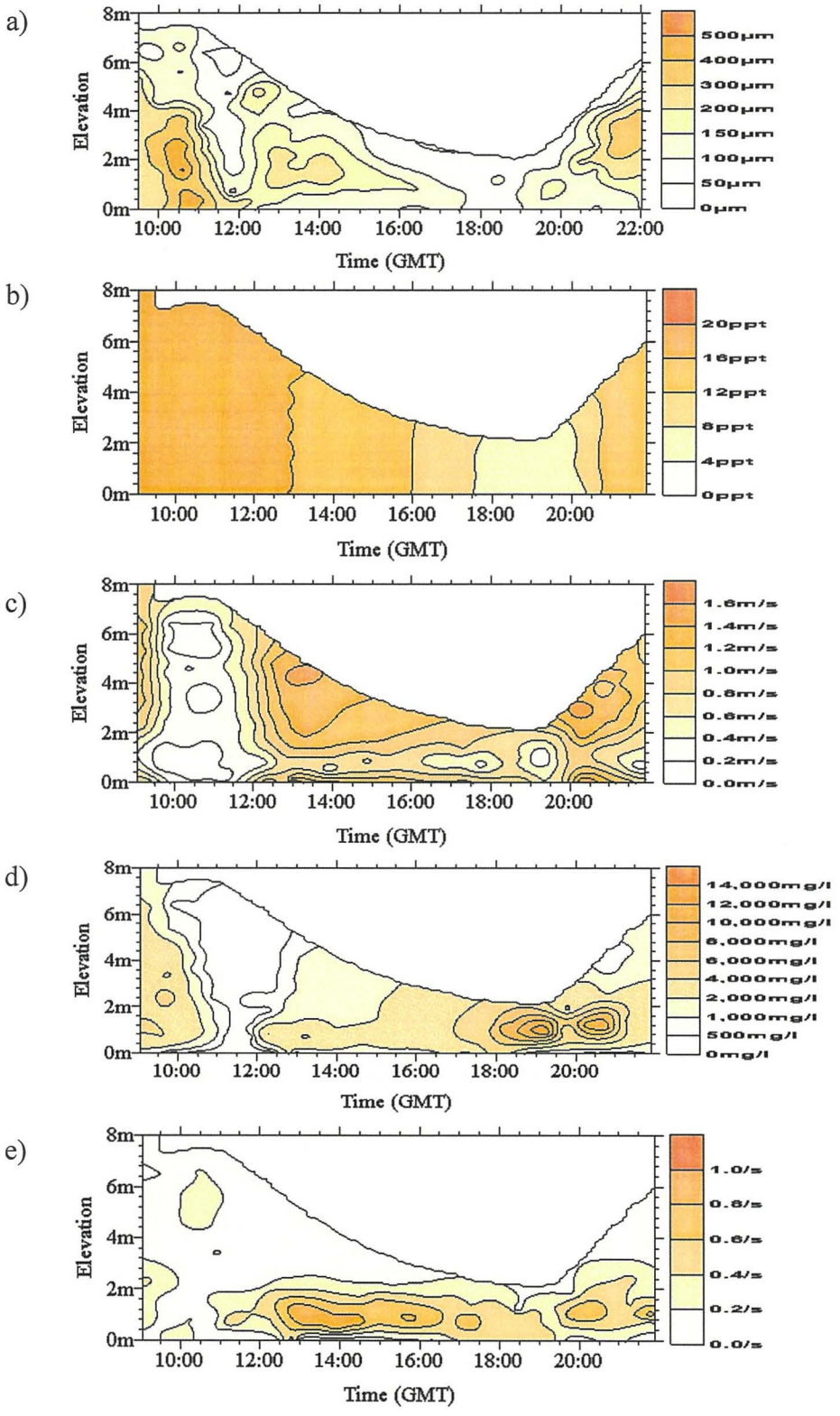

Figure 3.15 Time and spatial series of contoured data from Whitton Channel, July 1995. Data comprises, a) particle size, b) salinity, c) current velocity, d) SPM concentration and e) shear.

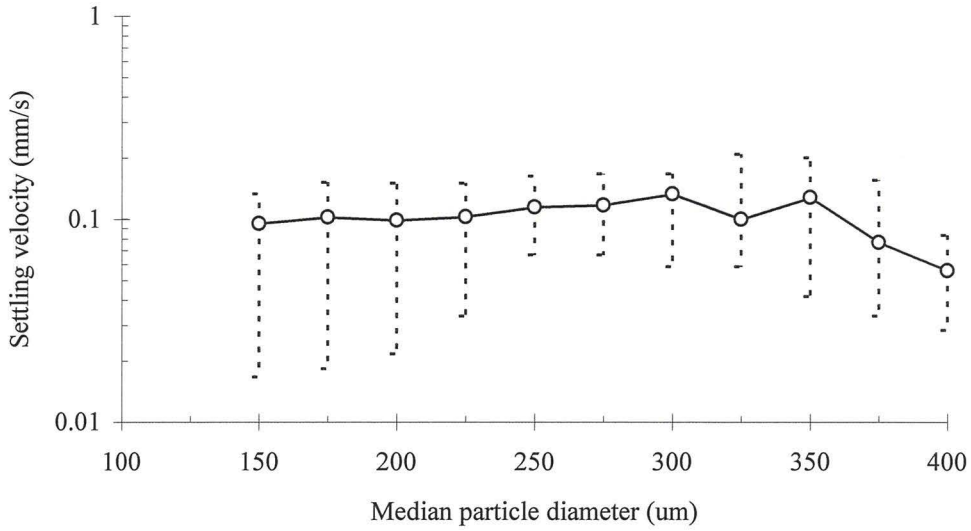

Figure 3.16 Settling velocity distribution of suspended particulates around high water (10:00 hrs) at Whitton channel on the 18th July 1995.

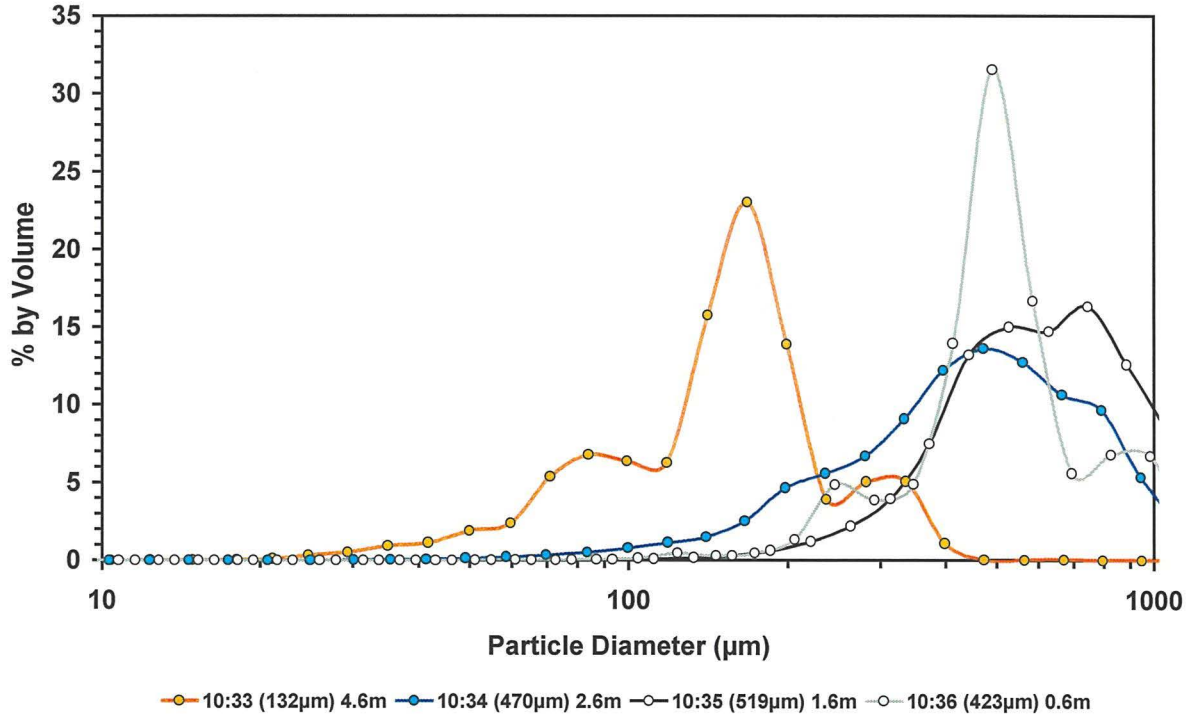

Figure 3.17 Particle size spectra from Whitton Channel, July 1995 during High water slack (10:15), through the water column. Legend refers to time of sample, median particle diameter (µm) and elevation above the bed (m).

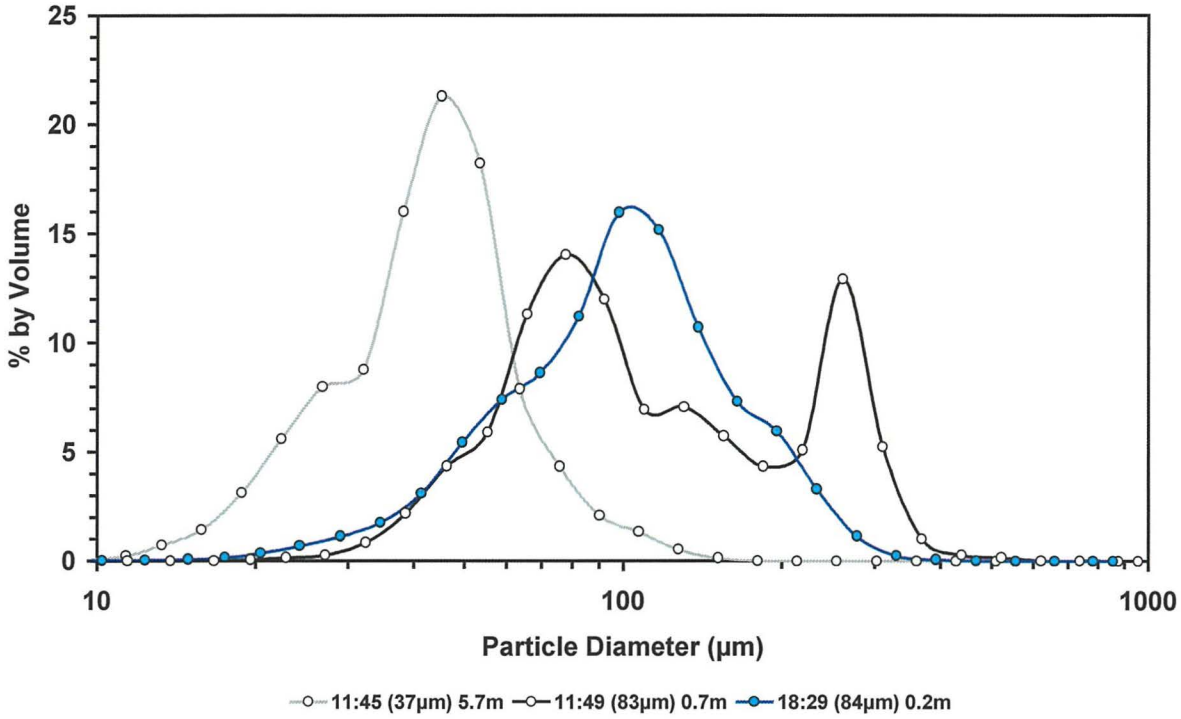

Figure 3.18 Particle size spectra from Whitton Channel, July 1995 at the onset of the ebb tide (11:45), at surface near bottom. Size spectra at low water slack (18:30) also included. Legend refers to time of sample, median particle diameter (µm) and elevation above the bed (m).

3.4.1.6. Whitton channel - 17th March 1995

Par-tec100 deployments during this anchor station were curtailed after low water owing to storm conditions. In comparison with the mid tide of July, salinity during this spring tide ranged from 1 ppt to 6 ppt (Figure 3.19a), whereas current velocity (Figure 3.19b), SPM concentration (Figure 3.19c) and shear (Figure 3.19d) were all greater than in July. The highest particle concentrations occurred at the bed during the maximum current velocities of the ebb (1.6 m s^{-1}, 10 g l^{-1} at 09:30 hrs) and flood (1.4 m s^{-1}, 16 g l^{-1} at 17:30 hrs), whilst during the rest of the tide concentrations remained below 4 g l^{-1}. Shear velocities are consistently high throughout the tide close to the bed, with the greatest shear coinciding with the high particle concentrations of the flood tide. Owing to the strong

wind, considerable shear was evident at the surface. Particle sizes exhibit the same overall behaviour during high water slack as seen during the mid tide of July. Settling of large particles (up to 500 μm) to leave a much finer population (< 100 μm) is followed by entrainment, once again the entrained particles being finer (< 300 μm) than the original source material. The particle size gradient over high water slack is considerably more enhanced than at all other sites exhibiting similar settling behaviour. Between the elevations of 6.2 m and 0.5 m (Figure 3.20, 08:00 hrs) the gradation results in a change from a median particle size of 44 μm to 475 μm, an order of magnitude. Evidence of particle settling is seen in the similarity between the size distributions at 08:02, 6.2 m and 08:30, 4.4 m, in comparison to the wider, increasingly multimodal distribution of 08:28, 3.5 m. An inverse gradient is found on the ebb tide from 10:00 hrs, with a median diameter of 129 μm at the bed and 221 μm at surface (Figure 3.21), coincident with increased near bed shear. The size distributions throughout the ebb and over low water slack were characterised by a normal distribution, unlike the multimodal forms of high water slack.

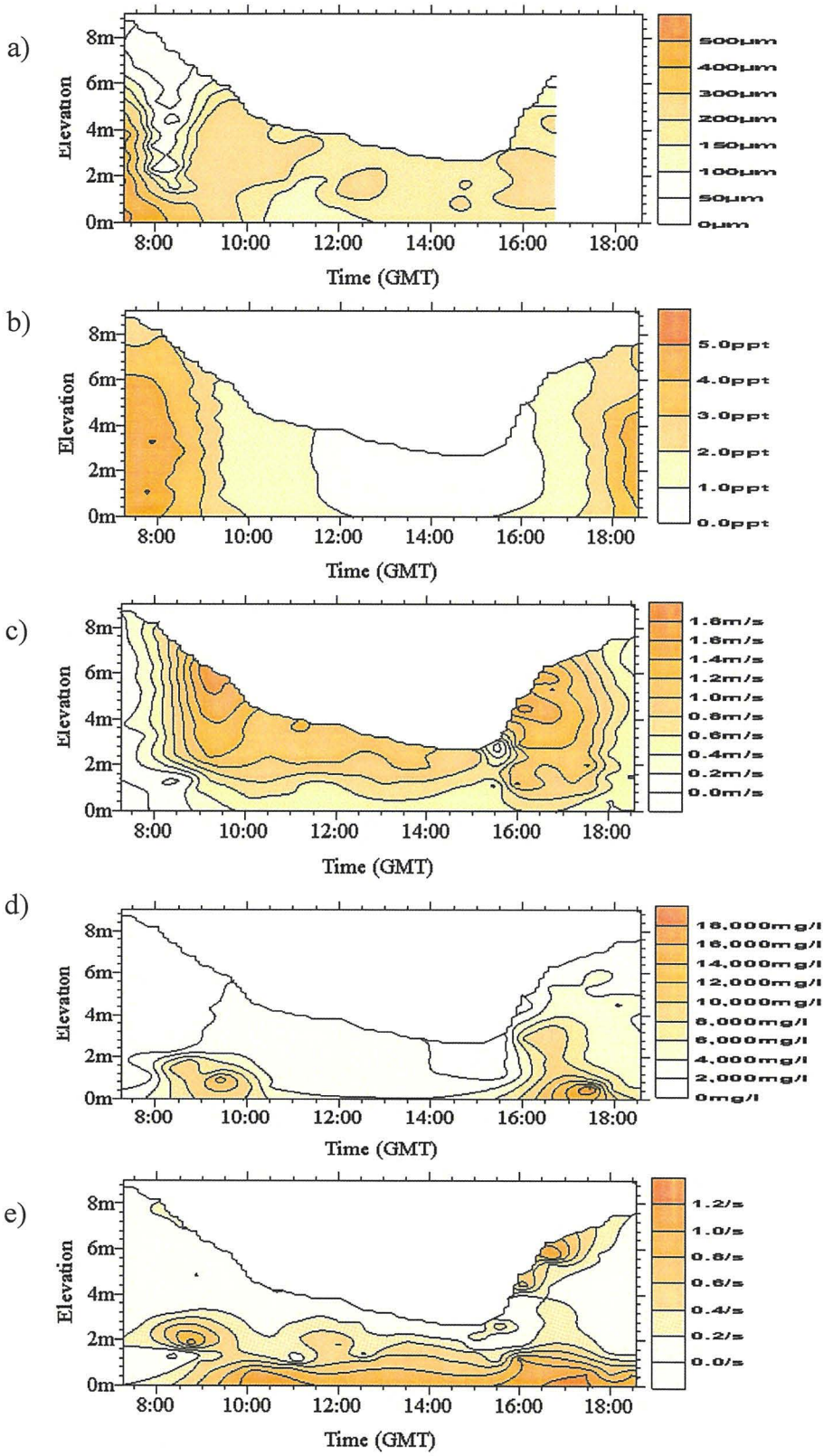

Figure 3.19 Time and spatial series of contoured data from Whitton Channel, March 1995. Data comprises, a) particle size, b) salinity, c) current velocity, d) SPM concentration and e) shear.

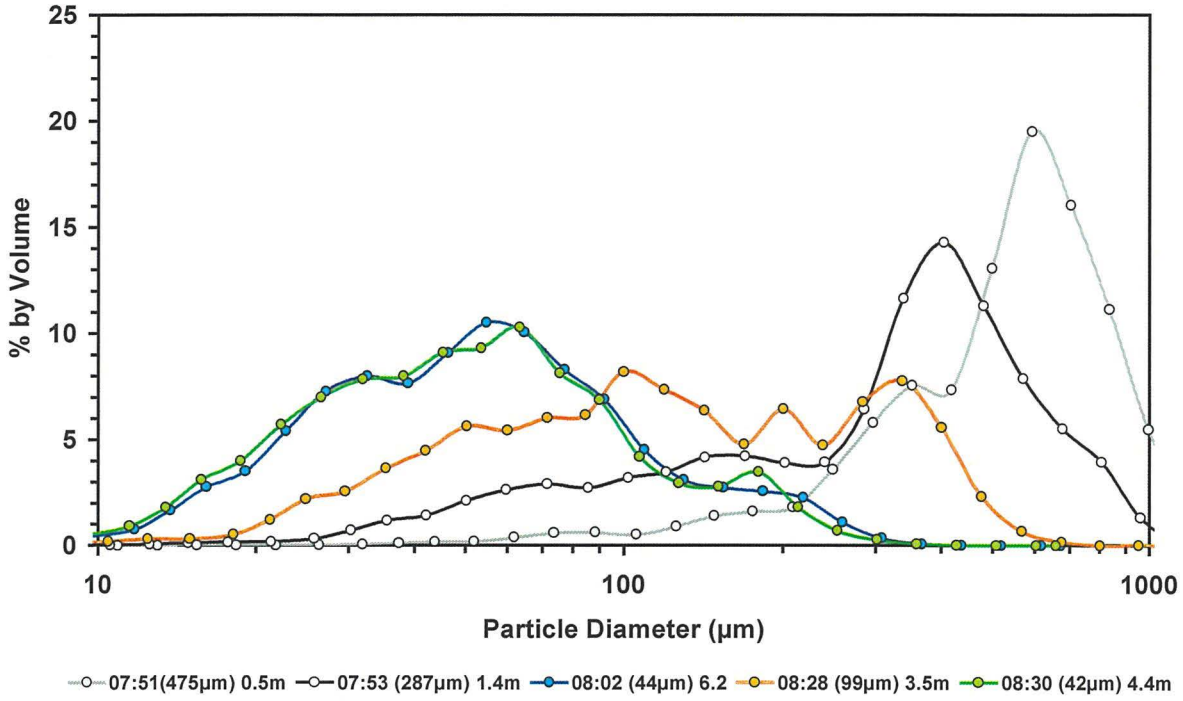

Figure 3.20 Particle size spectra from Whitton Channel, March 1995 during High water slack (07:45) and at the onset of the ebb tide (08:15). Legend refers to time of sample, median particle diameter (µm) and elevation above the bed (m).

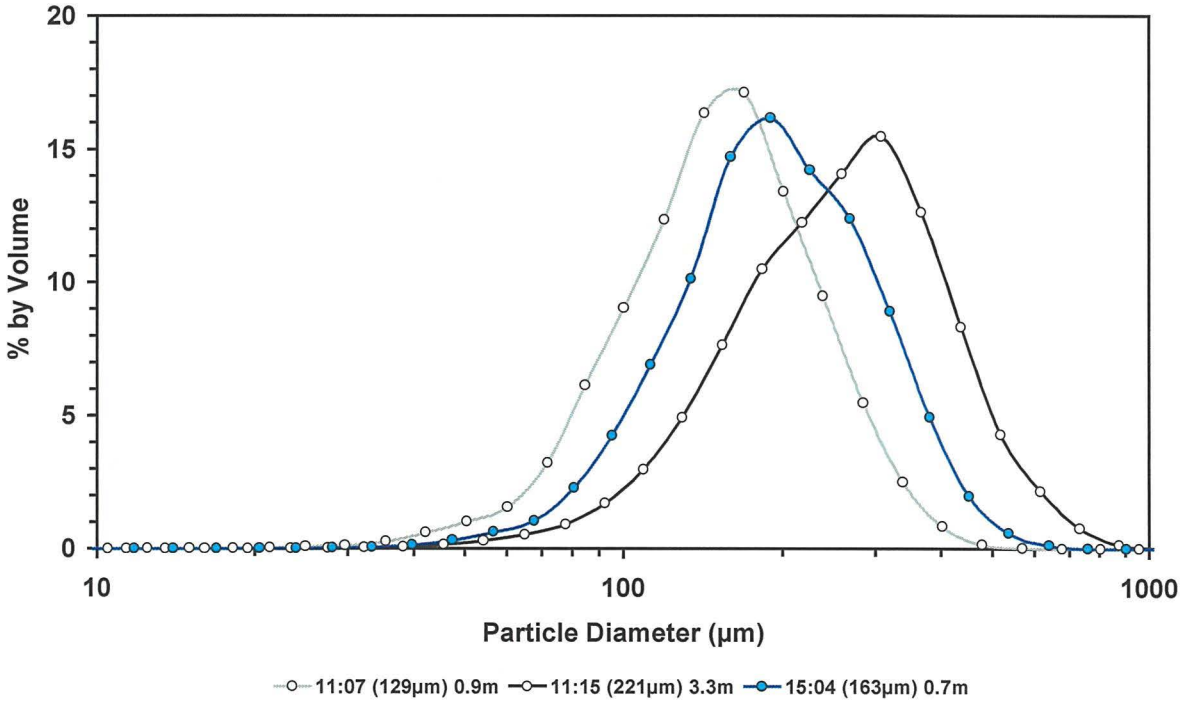

Figure 3.21 Particle size spectra from Whitton Channel, March 1995 during the ebb tide and at low water slack (15:15). Legend refers to time of sample, median particle diameter (µm) and elevation above the bed (m).

3.4.1.7. Humber bridge - 16th March 1995

At this station salinity was vertically well mixed although SPM concentration and current speed showed some vertical structure at certain stages of the tide. Salinity ranged from 2 ppt at low water to 15 ppt at high water (Figure 3.22a). Minimum current velocities (0.2 ms^{-1}) were measured at slack water and maximum current velocities (1.5 to 1.7 ms^{-1}) were encountered approximately two hours after high and low water (Figure 3.22b). SPM concentration varied with current speed but maximum concentrations (3 g l^{-1}) lagged behind maximum current speed (Figure 3.22c). Minimum mid-water SPM concentrations (200 mg l^{-1}) occurred at high water. Calculated shear values, expressed as the vertical rate of change in current velocity, remained relatively low (0.4 s^{-1}) over the tidal cycle except close to the bed during periods of high current velocity when values exceeded 1.0 s^{-1} (Figure 3.22d). Particle size exhibited considerable variation over the tidal cycle (Figure.3.22e). The smallest median diameters were measured in the surface waters during high water slack currents and throughout the water column just after low water (Figure 3.23). Larger particles, which were nearly an order of magnitude greater than those observed at slack water, were measured shortly after the period of maximum flood tide currents (17:00 hrs). As current velocity decreased further, median particle sizes increased with time and depth (Figure 3.24). A similar increase in median particle size was observed towards low water when the ebb tide velocities were decreasing; maximum median diameters occurred at approximately mid-depth. Intermediate size particles were measured during periods of accelerating current velocity and coincided with remobilisation of bed material as indicated by increased concentrations of SPM.

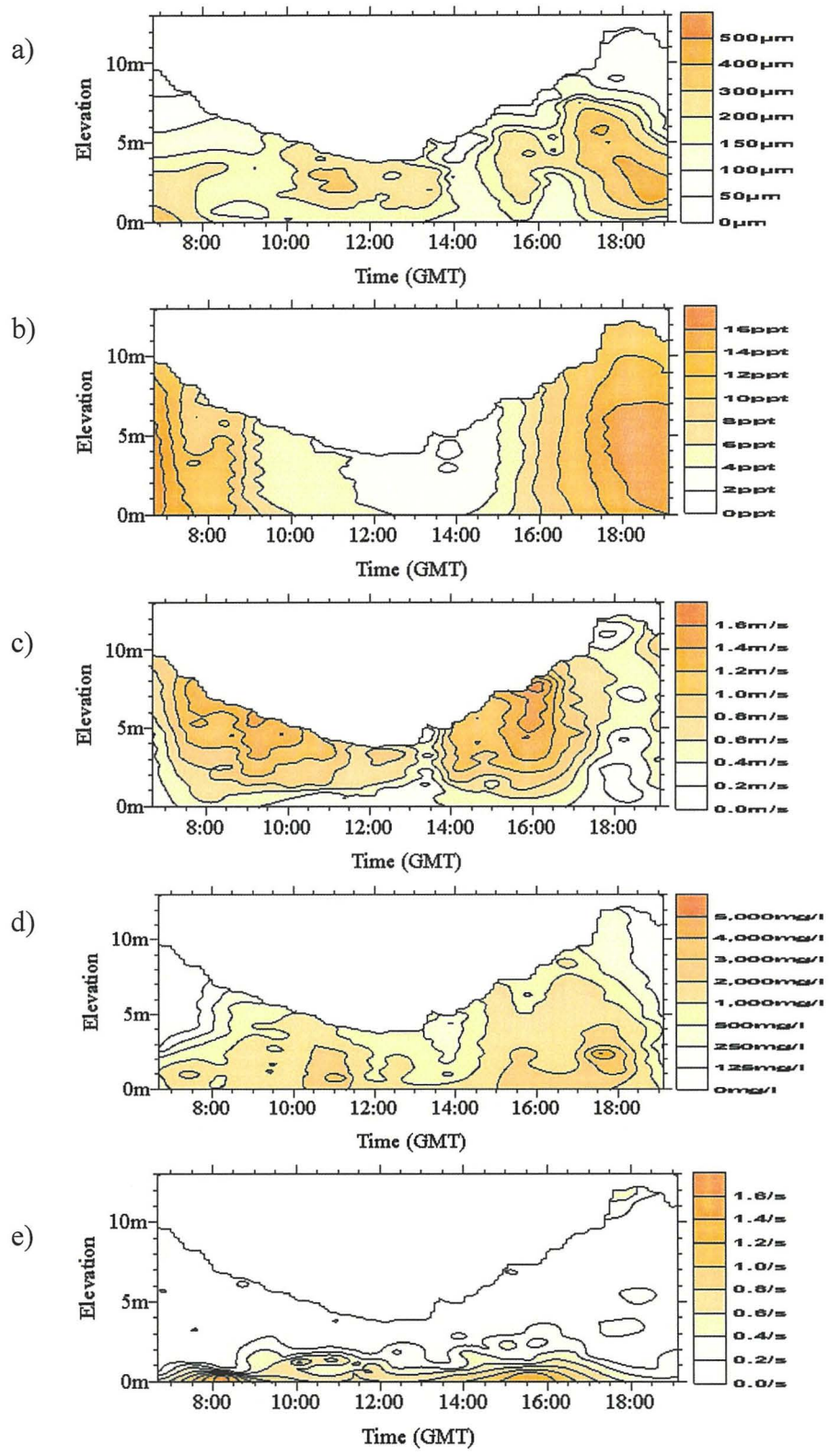

Figure 3.22 Time and spatial series of contoured data from Humber Bridge, March 1995. Data comprises, a) particle size, b) salinity, c) current velocity, d) SPM concentration and e) shear.

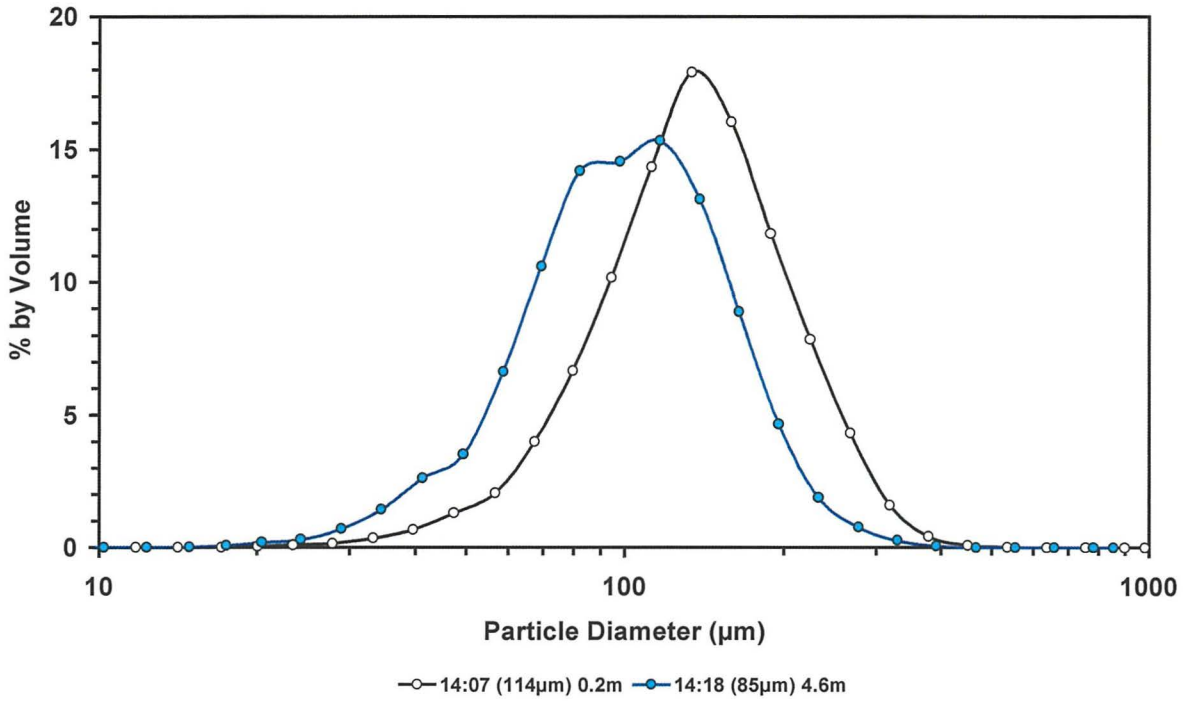

Figure 3.23 Particle size spectra at the Humber Bridge, March 1995 during the flood tide, shortly after low water slack (13:30) at surface and near bottom. Legend refers to time of sample, median particle diameter (µm) and elevation above the bed (m).

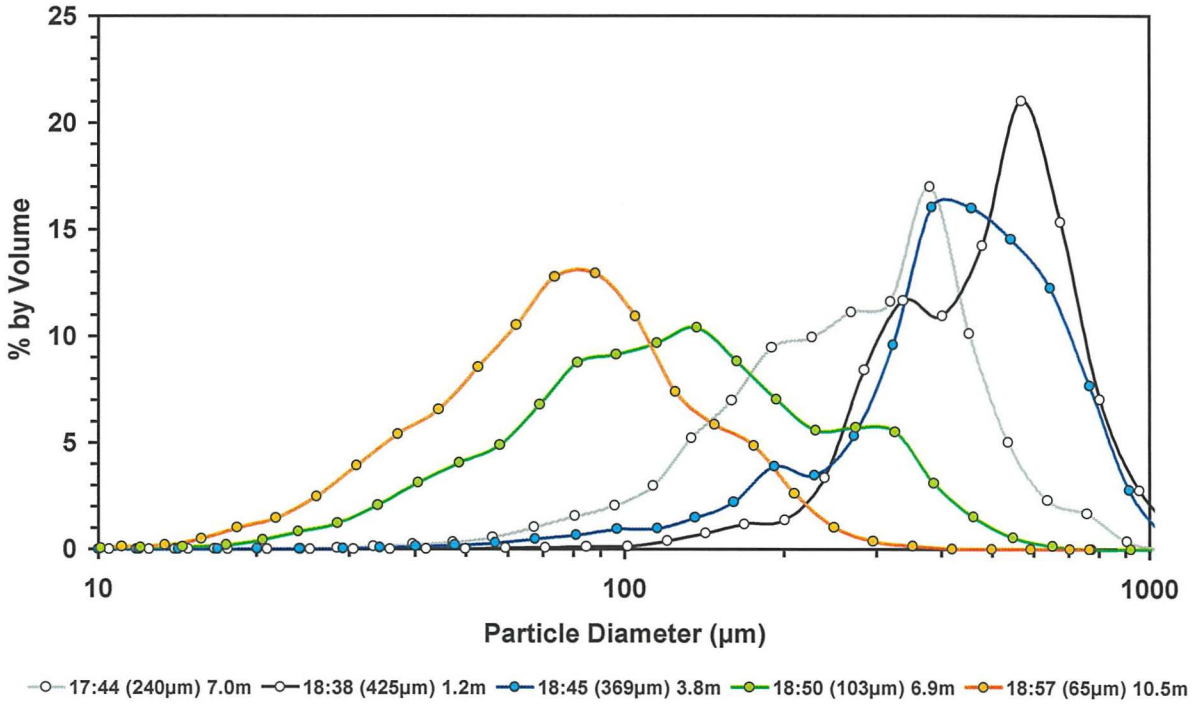

Figure 3.24 Particle size spectra at the Humber Bridge, March 1995 during High water slack (18:00 hrs), through the water column. Legend refers to time of sample, median particle diameter (µm) and elevation above the bed (m).

3.4.1.8. SG23 - 8th June 1995

Station SG23 lies in the mouth of the Humber estuary, north of the main navigation channel (Figure 3.4) and was sampled during the Challenger cruise 119A. The salinities encountered at SG23 were considerably higher than at any of the other estuarine stations. Salinity ranged from 34 ppt at high water to 29 ppt at low water (Figure 3.25a). Consequently SPM concentrations are considerably lower, maximising at 100 mg l^{-1} and falling as low as 10 to 20 mg l^{-1} (Figure 3.25c). Surface currents were strongest (1.2 m s^{-1}) prior to and after high water, but remained low in the bottom waters throughout the tidal cycle (0.2 to 0.4 m s^{-1}). Shear velocities showed little variation, being consistently below 0.1 s^{-1}, rising to only 0.2 s^{-1} on the flood and ebb tides. Median particle diameters extended from 40 to 130 μm, with the largest particles occurring over high water (Figure 3.25e). The characteristic 'v' profile observed in the median diameters at stations in the upper reaches of the estuary was also observed, which suggests that particle settling had been taking place towards the end of low water (07:00 to 08:00 hrs). Although the higher surface currents do not extend to the bed, the marginal increase appears to coincide with larger particles and higher concentrations being distributed into the upper water column (08:00 to 10:00 hrs). Over high water, the process of particle settling and re-entrainment is repeated, at least in respect of the size of particles (Figure 3.25e). There is no suggestion from the SPM concentration profile that significant amounts of material are either settling or being entrained (Figure 3.25c). With the onset of the ebb (15:00 hrs) current velocities at the bed are higher than those of the flood and particle sizes are relatively uniform throughout the water column, an indication of greater mixing between surface and bottom

waters. The approaching low water sees the return of high particle concentrations and also high particle sizes as the ebb tide slackens.

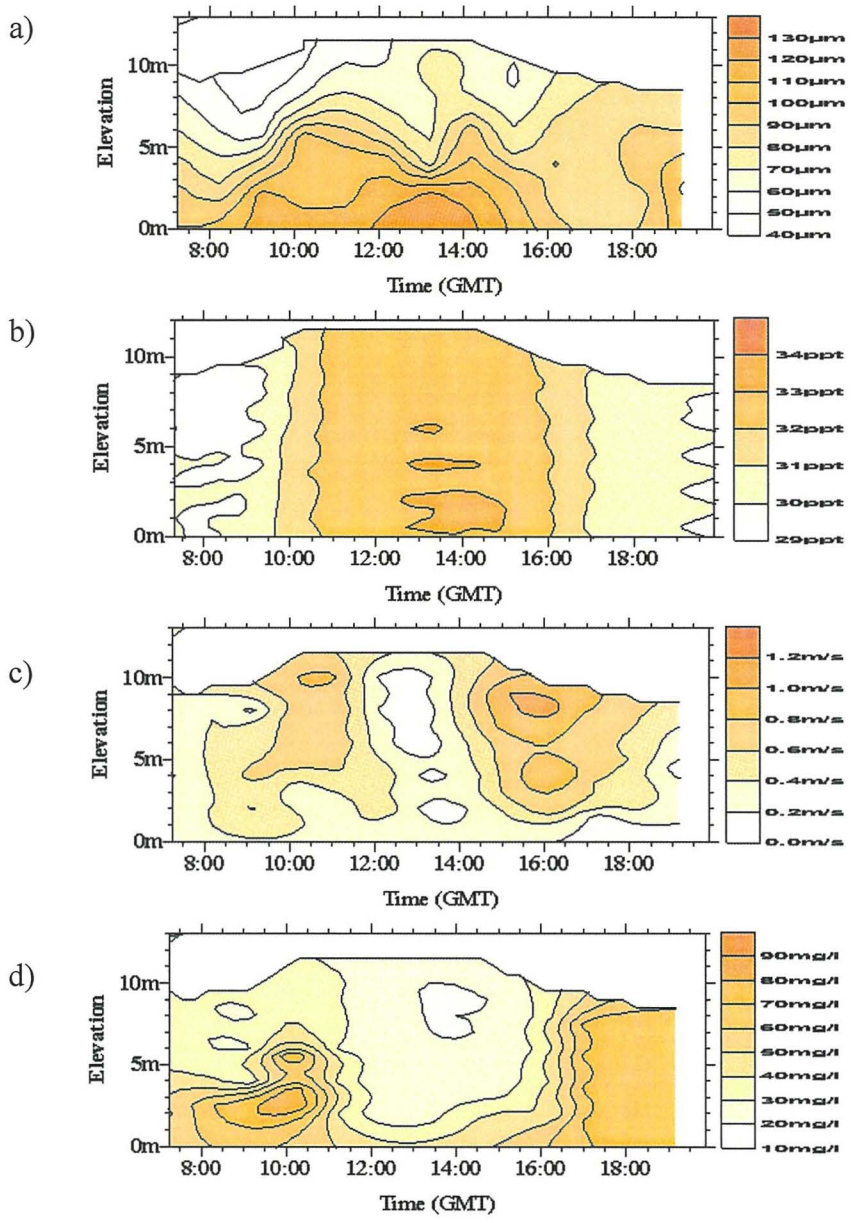

Figure 3.25 Time and spatial series of contoured data from SG23, June 1995. Data comprises, a) particle size, b) salinity, c) current velocity and d) SPM concentration.

3.4.1.9 SG10 - 7th June 1995

Station SG10 lies close to the northern extremity of the Humber Plume outside of the mouth of the Humber estuary (Figure 3.4) and was sampled during Challenger cruise CH119A. Salinities varied little between high and low water, 34 ppt and 32.5 ppt respectively (Figure 3.26b) on a near neap tide (neap -1day). SPM concentrations also showed little variation and remained low at less than 30 mg l^{-1} throughout the tidal cycle (Figure 3.26d). Current velocities in the surface waters reached a peak of 1 m s^{-1} approximately 3 hours either side of high water, at 08:00 and 16:00 hrs (Figure 3.26c). However, close to the bed they remained below 0.6 m s^{-1} on the flood and 0.4 m s^{-1} on the ebb tide. From the SPM concentration profile alone there is no clear evidence of either particle resuspension or settling. Particle sizes vary from 60 μm in the surface waters at low water to 100 μm in the bottom waters at low water (Figure 3.26a). In terms of size, at high water the distribution of particles throughout the water column appears relatively uniform. The onset of the ebb brings about an increase in particle size which gradually extends vertically through the water column (12:00 to 15:00 hrs), the reverse is true for the flood (08:00 to 10:00 hrs) (Figure 3.26a), as the marginally greater particle concentrations of the plume are advected through the site. As low water approaches on the ebb a distinct particle size gradient forms as the particles in the surface waters become smaller (16:00 to 18:00 hrs). This coincides with an increase in near bed SPM concentrations (Figure 3.26d) which suggests that particles are settling out.

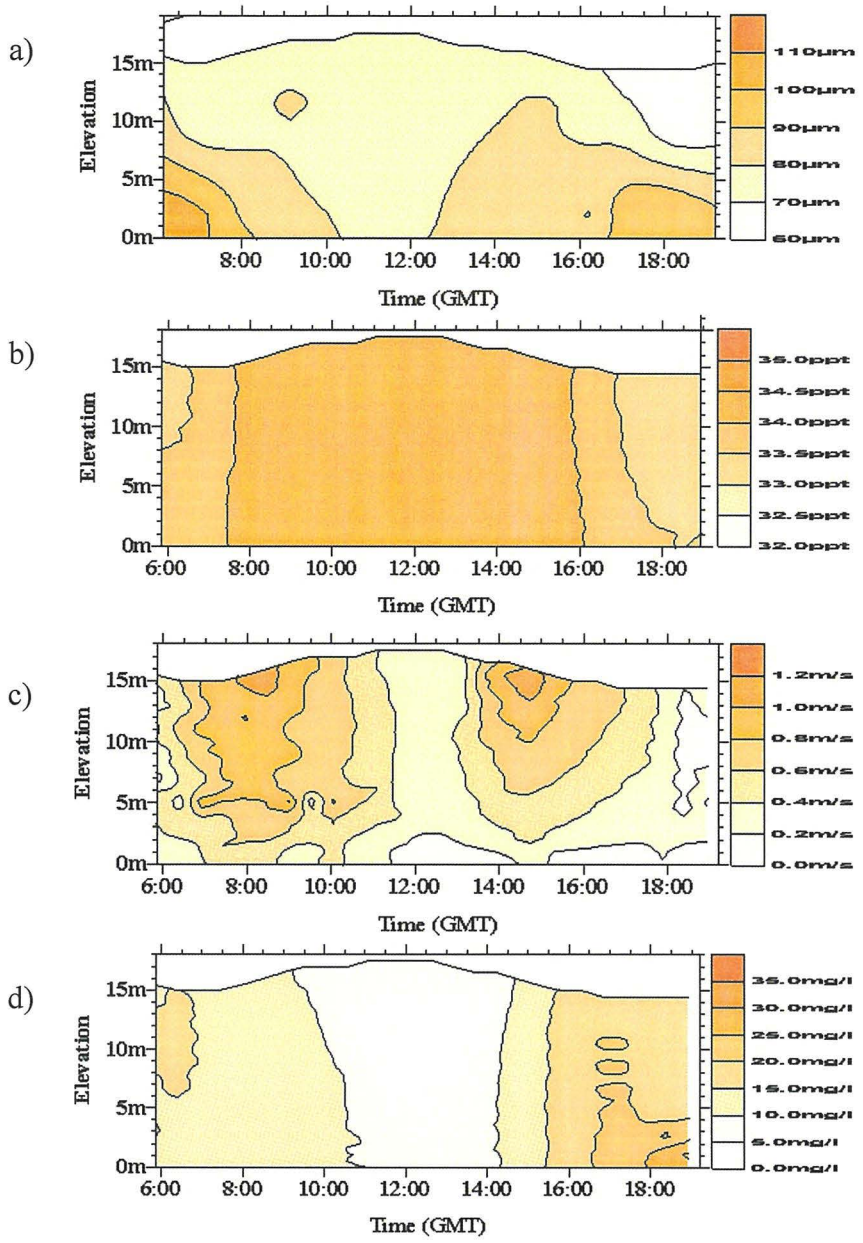

Figure 3.26 Time and spatial series of contoured data from SG10, June 1995. Data comprises, a) particle size, b) salinity, c) current velocity and d) SPM concentration.

3.4.1.10 SG13 - 3rd June 1995

Station SG13 lies on the outer northern edge of the Humber plume region outside of the mouth of the Humber estuary (Figure 3.4) and was sampled during Challenger cruise CH119A, 3 days after a spring tide. As is true for all of the outer stations within this study, the salinity varied by only 2 ppt between high and low water (Figure 3.27b). Current velocities maximised at 1.4 m s^{-1} in the surface waters, approximately 3 hours before and after high water slack. Particle sizes observed over the tidal cycle extend from 70 μm to 130 μm (Figure 3.27a). The largest median particle sizes seen coincided with the highest SPM concentrations, at low water slack (15:00 to 16:00 hrs, Figure 3.27a) and were confined to the lower water column (0 to 4 m from the bed). Measurements began just before high water slack as currents were decreasing. SPM concentrations remain low during this period (4 - 8 mg l^{-1}) although particle sizes increase near to the bed over high water slack (up to 120 μm at 10:00 hrs). Over the subsequent ebb, particle sizes continue to fall until currents slacken at 14:00 hrs. The SPM concentration at this point changes little (20 mg l^{-1}). The end of low water slack sees the largest floc sizes, with maximum particle sizes observed at 16:00 hrs, whilst the flood tide is characterised by falling SPM concentrations and particle sizes. The smallest median particle sizes were observed in the surface waters between low water slack and maximum flood current velocities (16:00 to 1700, Figure 3.27a). Shear values remain low throughout the tidal cycle, with the majority of the water column experiencing less than 0.2 s^{-1} (Figure 3.27e).

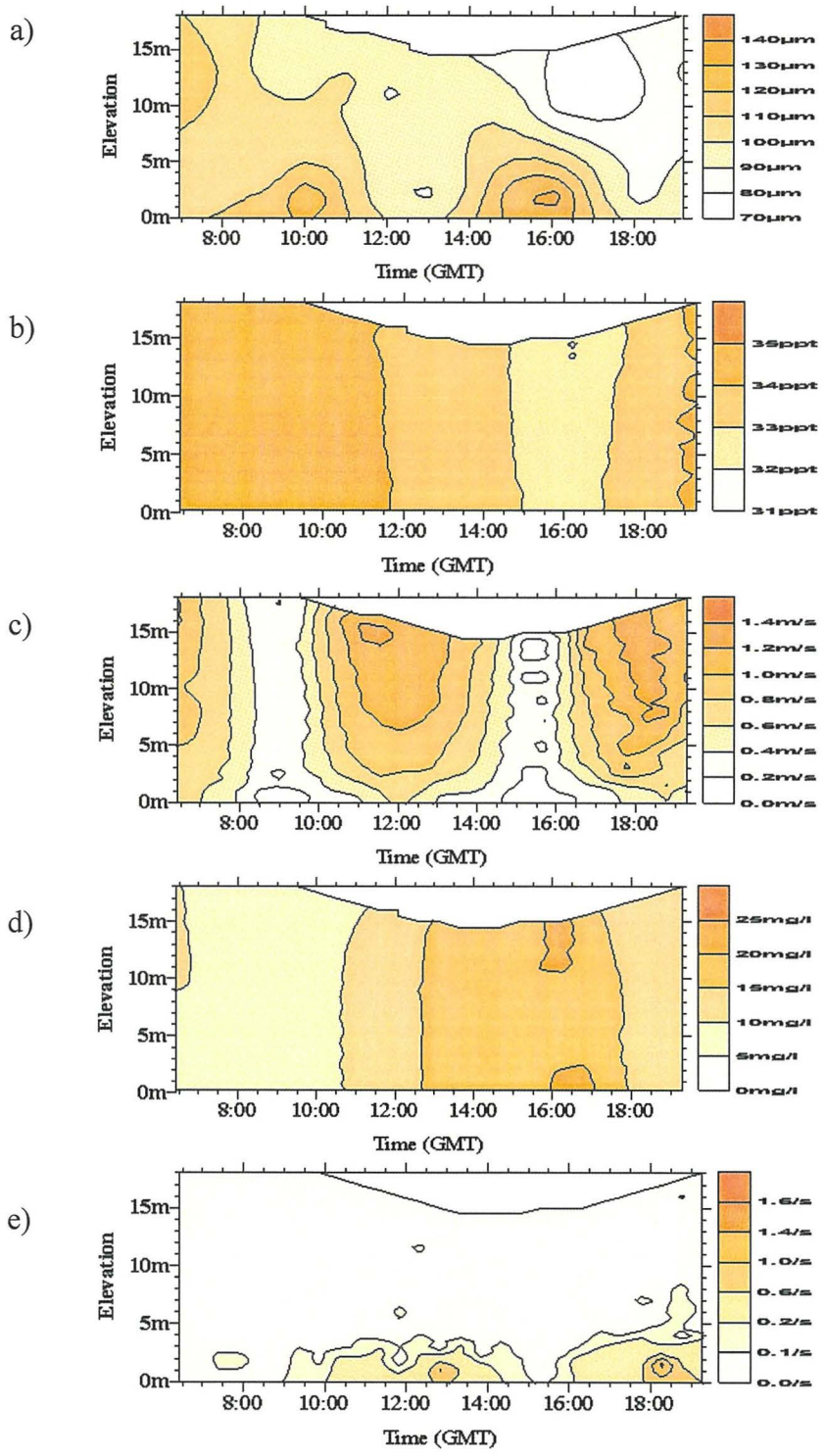

Figure 3.27 Time and spatial series of contoured data from SG13, June 1995. Data comprises, a) particle size, b) salinity, c) current velocity, d) SPM concentration and e) shear.

3.4.1.11 SG24 - 4th June 1995

Station SG24 at the mouth of the Humber estuary (Figure 3.4) was surveyed on a 4.3 m tide, four days after a spring tide. Measurements during Challenger cruise CH119A began just prior to high water slack and continued till the same point of the tide was reached on the following flood. Salinity varied by only 1 ppt, between 34.5 and 33.5 ppt (Figure 3.28b). Current velocities were strongest (0.8 to 1.0 m s^{-1}) in the surface waters 3 to 4 hours before and after high water (07:00 and 13:00 hrs, Figure 3.28c). At such times, despite a strong vertical gradient, calculated shear values remained low close to the bed (< 0.4 to 0.8 s^{-1}, Figure 3.28e). SPM concentration exhibited little vertical structure and little variation (8 to 14 mg l^{-1}) for the majority of the tidal cycle (Figure 3.28d). The largest concentration of SPM (< 15 mg l^{-1}) occurred at the onset of low water slack (15:00 hrs), the size of the material in suspension differing little from the following flood (110 μm at 15:00 hrs, 15 mg l^{-1} as opposed to 90 μm at 17:00 hrs, 9 mg l^{-1}, Figure 3.28a). The largest median particle sizes measured (150 μm), occurred around high water slack at 10:00 hrs. A small peak in SPM concentrations at 11:00 hrs, close to the bed, coincides with the later peak in particle sizes. This lack of any significant change in SPM concentration and the pattern of current velocity changes during low water slack, may indicate the settling (09:00 hrs) and resuspension (11:00 hrs) of low numbers of large flocs. The volume of such flocs proving sufficient to influence the particle size distribution but not the distribution of SPM concentration.

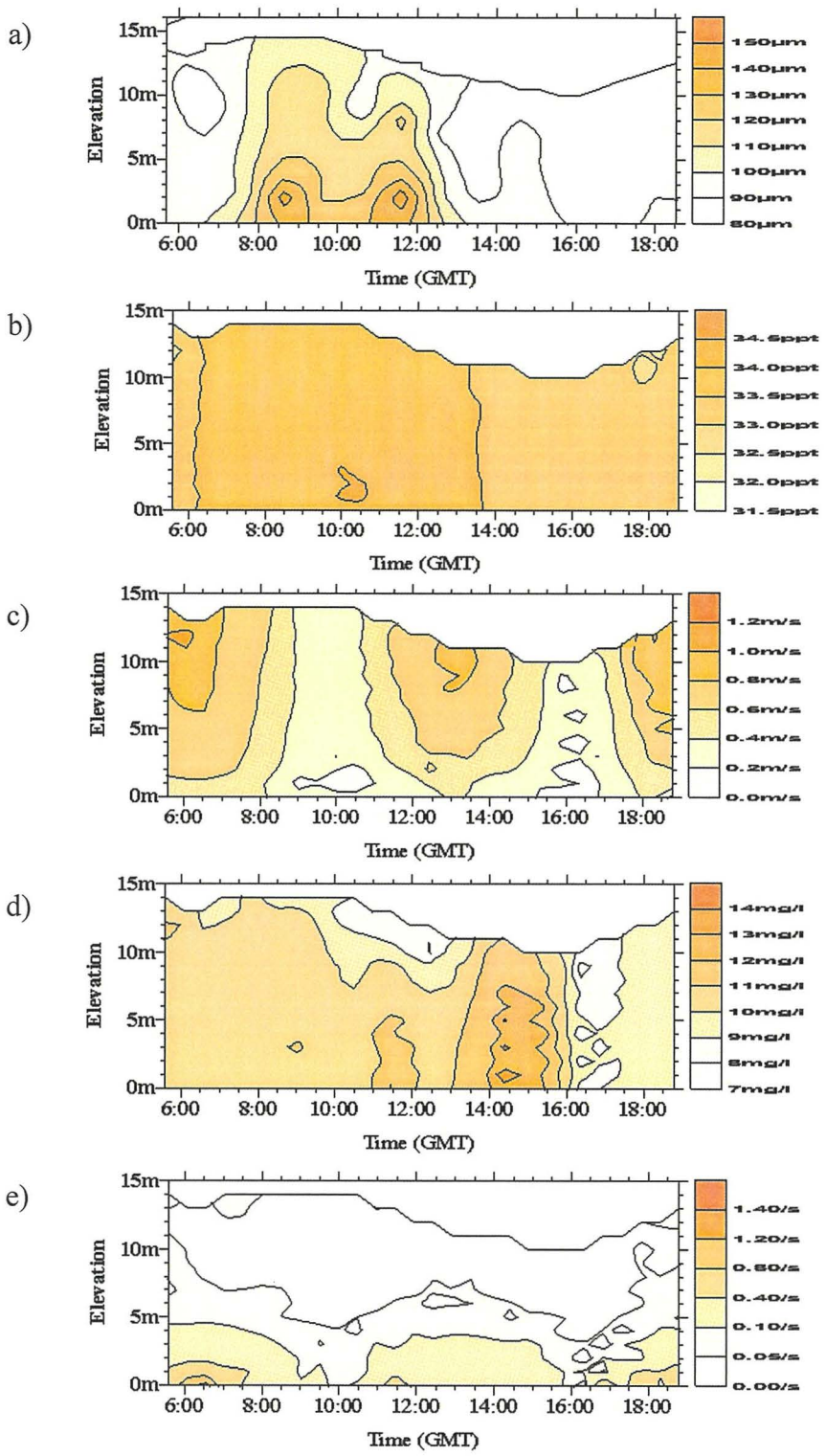

Figure 3.28 Time and spatial series of contoured data from SG24, June 1995. Data comprises, a) particle size, b) salinity, c) current velocity, d) SPM concentration and e) shear.

3.4.1.12 HW5 - 4th November 1994

Station HW5 is situated SE of Spurn Head at the entrance to the estuary and lies just off the main shipping channel. The site was surveyed for a period of 25 hours on a 6.7 m spring tide during Challenger cruise CH115C. Current velocity data is only available for the first 12 hours owing to instrument malfunction. Salinity varied from 34 ppt at high water slack to 27 ppt at low water slack (Figure 3.29b), contrasting with SPM concentrations of 40 mg l^{-1} at high water and 280 mg l^{-1} at low water (Figure 3.29d). Current velocities range from 1.4 m s^{-1} at 15:00 hrs (Figure 3.29c) and < 0.2 m s^{-1} at slack periods (12:30 and 18:30 hrs). Neither SPM concentration, salinity or current velocity show significant vertical structure, with the exception of the bottom 5 metres between 17:00 - 19:00 and 22:00 -24:00 hrs. Median particle sizes (Figure 3.29a) also exhibit little vertical structure with no indication of resuspension or settling. The largest median particle sizes measured (300 - 400 μm) occur towards the end of low water slack (280 mg l^{-1}, 27 ppt) and appear well distributed throughout the water column. There is no evidence for the rapid flocculation and settling which occurs in the upper estuary, albeit in far greater SPM concentrations, indeed the dominant particle behaviour appears to be advective.

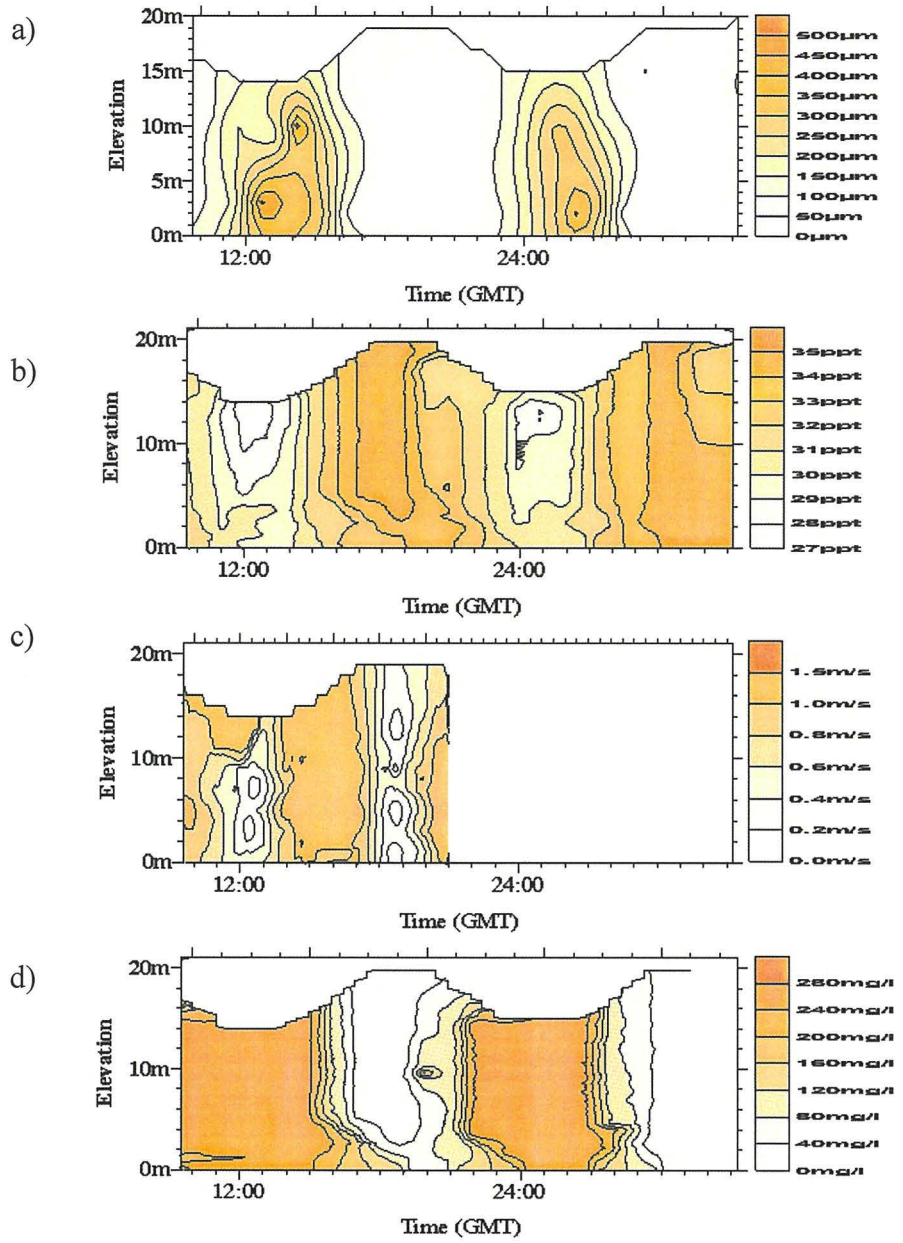

Figure 3.29 Time and spatial series of contoured data from HW5, November 1994. Data comprises, a) particle size, b) salinity, c) current velocity and d) SPM concentration.

3.4.1.13 HW5 - 22nd January 1995

Station HW5 was surveyed during Challenger cruise CH117A for a period of 12 hours on a 5.0 m tide (spring + 3 days). In comparison with HW5 surveyed during CH115C (4th November 1994), the salinity variation is comparable, 34 ppt to 24 ppt, high to low water (Figure 3.30b). However, the size of particles, the SPM concentration and current velocities encountered are all significantly lower. Current velocities range from 0.2 m s^{-1} at high and low water slack to 1.2 m s^{-1} during the flood tide (3-4 hours before high water slack) (Figure 3.30c). SPM concentrations were observed to vary little over the tidal cycle, maintaining an 80 to 100 mg l^{-1} background (Figure 3.30d) except for the surface waters around high water slack (20 to 40 mg l^{-1}). Measured median particle sizes exhibit a similar variation to that seen on the 4th November (CH115C), with the largest particles seen over low water slack (150 to 200 μm median diameter) (Figure 3.30a). Particle sizes were also observed to increase towards the end of high water slack (100 to 150 μm, at 22:30 hrs).

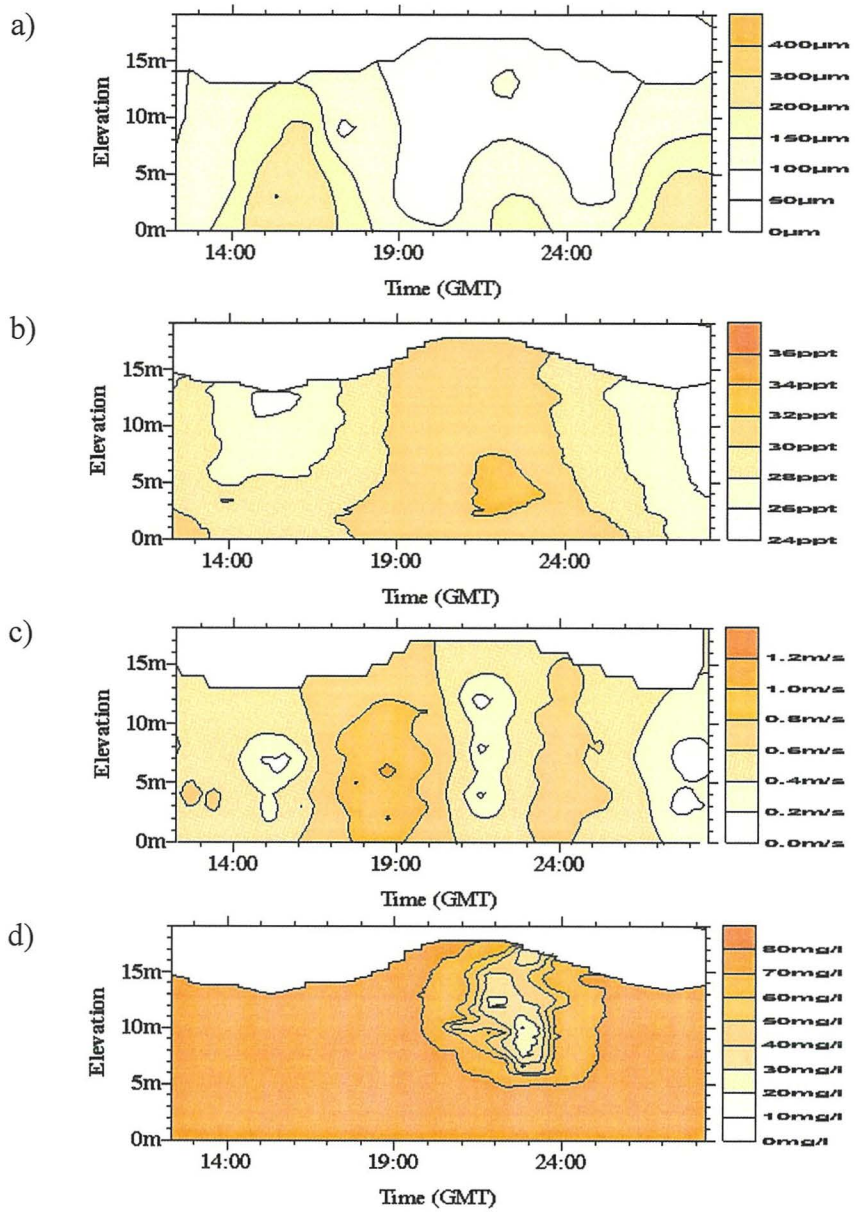

Figure 3.30 Time and spatial series of contoured data from HW5, January 1995. Data comprises, a) particle size, b) salinity, c) current velocity and d) SPM concentration.

3.4.1.14 HW7 - 7th November 1994

Station HW7 is the most easterly and southerly site (Figure 3.4) included in this work and also the site at which the least variation in salinity was observed (33.6 ppt at low water, 34.2 ppt at high water). SPM concentrations remain low throughout the tidal cycle, peaking at 10 mg l^{-1} during low water (Figure 3.31c), although high water SPM concentrations only fall to 7 mg l^{-1}. Current velocities also remain low throughout most of the tidal cycle, mid ebb tide velocities rising to only 0.6 m s^{-1} (Figure 3.31b), 3 hours after high water slack (22:00 hrs). SPM concentrations on the ebb tide rise marginally at 2 - 8 m from the bed. Current velocities upon the early morning flood tide appear to be considerably larger (1.2 m s^{-1} at 07:30 hrs) than the ebb tide and preceding flood tide. However, SPM concentration data is not available for this period. Median particle sizes range from 65 μm (03:00 hrs) over low water slack to 100 μm (23:00 to 24:00 hrs) near to the bed during the ebb tide (Figure 3.31a). The coincidence of increased near bed current velocities, SPM concentration and particle sizes, suggests a degree of resuspension on the ebb tide. As was the case at SG24, this resuspension event appears to be characterised by the entrainment of low numbers of relatively large particles. The same may be true of the flood tide, however the lack of SPM concentration data, precludes any such conclusion.

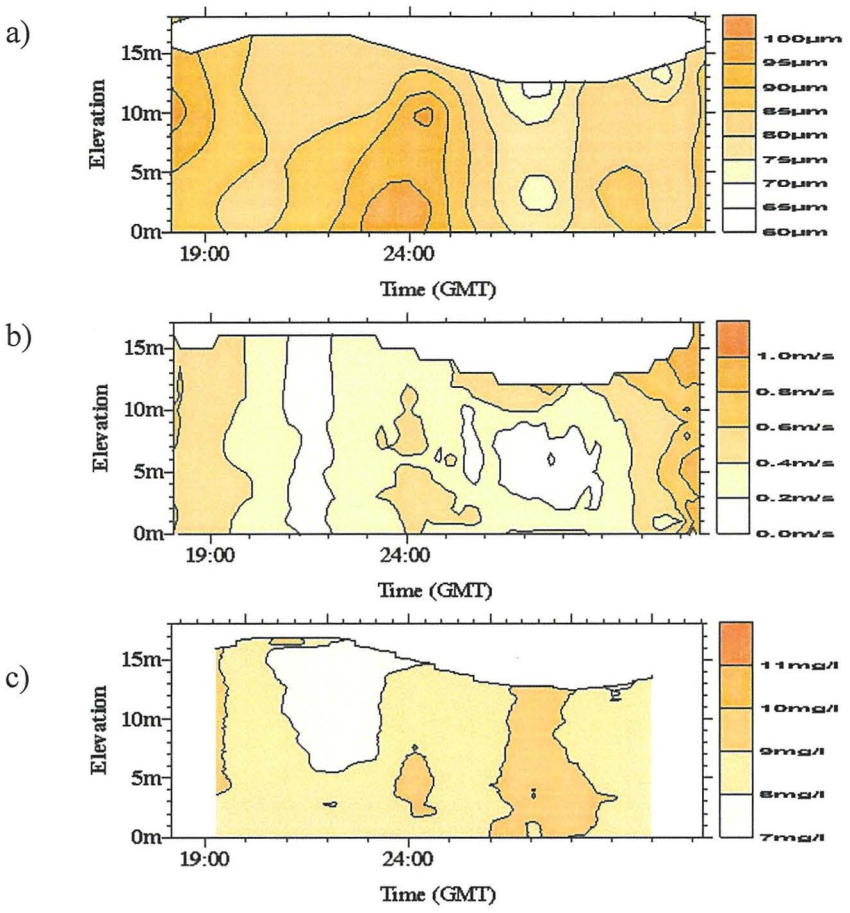

Figure 3.31 Time and spatial series of contoured data from HW7, November 1994. Data comprises, a) particle size, b) salinity, c) current velocity, d) SPM concentration and e) shear.

3.4.2. Spatial Variation in Particle Sizes between Spurn Head and Naburn

3.4.2.1. Introduction

The sediment within estuarine systems exhibits considerable variation in its characteristic physical behaviour and movement, due not least to the short and long term changes which occur in the dominant hydrodynamic regime. The semi-diurnal tidal cycle, the spring - neap cycle, land runoff, storms and biological activity are all factors which have the potential to affect the patterns of sediment movement within an estuary. Added to this is the complication that all these factors operate upon different time scales. In order at any given moment to faithfully represent the spatial distribution of sediment and its characteristics, it would be necessary to simultaneously measure the chosen characteristic at several points along the estuary axis. In the case of in-situ particle size analysis, this is not yet feasible (from a monetary standpoint only). However by carefully choosing data to provide a representation of the system for a given set of conditions, it is at least possible to attempt an understanding of the spatial distribution. Therefore, several of the anchor stations carried out between Naburn weir and Spurn Head have been chosen based upon the close proximity of a spring tide (+/- 2 days). Although they cover several seasons (March to September), the biological contribution is not regarded as important given the very high particle concentrations involved. Organic content within the Humber system shows little variation at 12 to 10 % of total sediment weight (Uncles et al., 1997). Rather than present the spatial variation in terms of distance from the head of the estuary at Naburn, it has been presented in relation to salinity. The location of features such as the turbidity maximum may vary by up to 10s of kilometres during the during spring-neap cycle and according to runoff, but varies considerably less within the salinity gradient of

the estuary. In using salinity as the spatial descriptor, seasonal and tidal factors are minimised.

3.4.2.2. Spatial Variation of Particle Size and Concentration at High Water

With the incursion of the tidal wave during the flood tide, the location of the turbidity maximum is likely to be found in the upper reaches of the estuary, depending upon seasonality this will be around or below Selby. Uncles (1997) places the turbidity maximum between 0 and 10 ppt salinity, with the greatest concentration at 1 ppt and the lower salinity limit varying according to the semi-diurnal (0.5 ppt at low water and 1 ppt at high water). Figures 3.33a & 3.33b illustrate the particle size and SPM concentration variation from the combined dataset, with SPM concentrations in the region of 20 to 28 g l^{-1} at 1 to 2 ppt salinity. Up and down estuary of this concentrations fall off quickly, eventually reaching 100 mg l^{-1} at Spurn Head and a similar concentration at Naburn. The variation in particle size differs, in that maximum sizes (400 μm) are seen between 5 and 22 ppt salinity, i.e. down estuary of the turbidity maximum, whilst in the highest concentrations, particle sizes are relatively low (100 to 200 μm). Particle sizes appear largest in the mid to bottom region of the water column, which agrees with the evidence from the individual anchor stations, suggesting flocculation in the surface to mid water column translating into large floc sizes in mid column after settling out.

a)

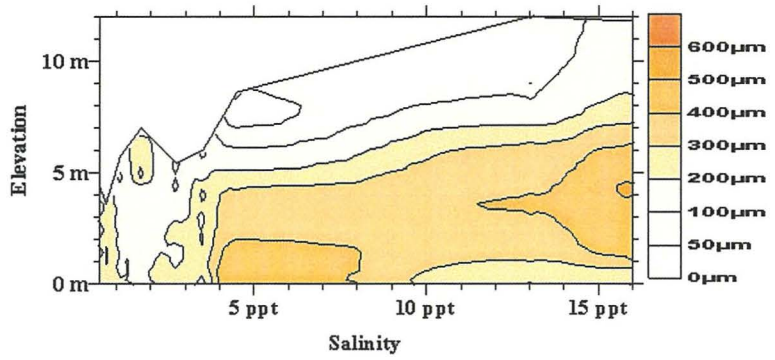

b)

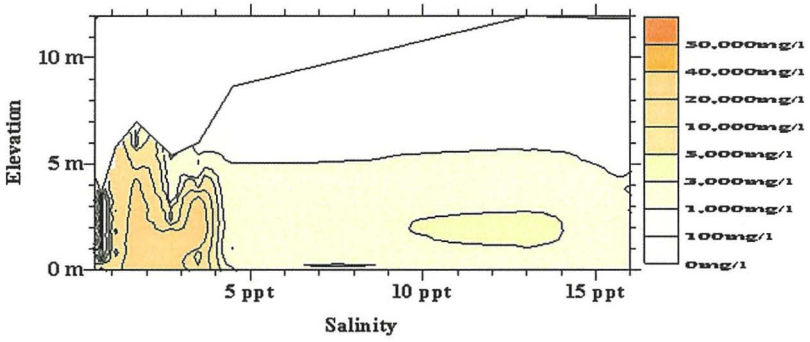

Figure 3.32 Profile of; a) median particle size and b) SPM concentration along the salinity gradient of the Humber Estuary. Values taken at High water on spring tides

3.4.2.3. Spatial Variation of Particle Size and Concentration at Low Water

The location of the turbidity maximum at low water may be >10 km down estuary of its location at high water, however, the salinity range within which it is found is still comparable. This is illustrated in the spatial variation of particle size and concentration at low water (Figures 3.34a & 3.34b). The maximum particle concentrations observed at low water are seen around 2.5 to 4 ppt salinity (12 to 19 g l^{-1}), somewhat lower than over high water and also contrary to Uncles' (1997) findings, they are to be found higher up the salinity gradient. Down estuary of the turbidity maximum, particle concentrations are greater than over high water with a shallower concentration gradient, although

concentrations still reduce to around 100 mg l^{-1} at Spurn Head. The particle sizes in the main body of the estuary, up and down estuary of the turbidity maximum, are considerably lower (150 to 175 μm) than over high water. Although sizes within the turbidity maximum remain low.

a)

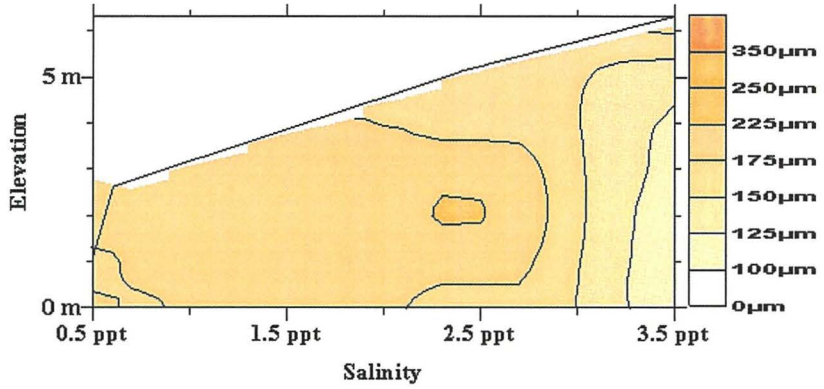

b)

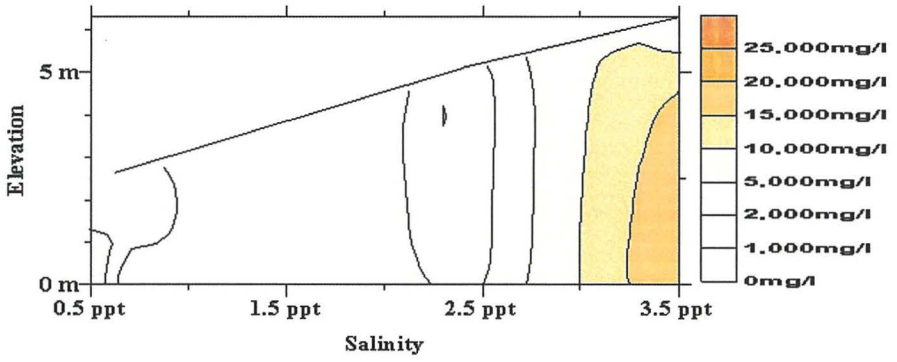

Figure 3.33 Profile of; a) median particle size and b) SPM concentration along the salinity gradient of the Humber Estuary. Values taken at Low water on spring tides

3.5. Discussion

Systematic deployment of the Par-tec100 in the Ouse - Humber system was carried out in order to characterise particulate matter in suspension and evaluate the Par-tec100's capabilities in extremes of water quality. During the deployment program, a wide range of estuarine conditions were encountered, allowing the collection of particle size data in association with other variables such as SPM concentrations, shear etc.

Particular attention was paid to the turbidity maximum and its role in the distribution of suspended sediment along the estuary axis. It was also intended to elucidate the possible effects which seasonality may have upon the nature of suspended matter, its spatial distribution and its tidal behaviour. The large variability in the concentration of the suspended sediment in the Ouse - Humber provided a unique insight into suspended particle behaviour, particularly in relation to flocculation processes. Anchor stations were sampled throughout the year at five key points along the estuary.

Of the stations, which were sampled, two were located up estuary of the turbidity maximum and the remainder located down estuary. No stations experienced the turbidity maximum peak, despite the very high particle concentrations encountered. Most stations, with the exception of Blacktoft, exhibited similar particle behaviour patterns, in particular over high water slack. It was observed that the high water slack period was characterised by particle flocculation and settling, it was during this period that the largest particle sizes were observed at mid depth in the water column. In the region of the Humber plume, the reverse was true, although large particles did form over high water slack, it was over low water slack that the largest particles and largest SPM concentrations occurred. It would appear that the upper water column, which clears rapidly as particles settle out, acts as a seeding ground for the growth of large flocs in the mid water column, once current

velocities and shear have slackened sufficiently. The settling of large flocs from the mid water column creates high solids concentrations at the bed, over high water slack. Settling velocities, particularly at Whitton channel during high water slack appear conservative when compared with direct measurements from video tracking devices (Fennessey, 1994), although at Selby the comparison is more favourable. Commencement of the ebb tide saw the entrainment of near bed flocs into the upper water column, where their disruption, rather than dilution resulted in a considerably finer suspended population which existed until the following high water slack. Entrainment of flocs from high concentration near bed layers appeared to be driven by shear (Selby, August & September). This being particularly evident at Blacktoft (August), although this was from a fluid mud layer, rather than a high water slack deposition event. Although shear was largely seen to result in smaller floc sizes owing to disruption, the derivation of a mathematical relationship is complicated by conflicting incidents during which increased shear induced the resuspension of large flocs.

Particle sizes in the turbidity maximum were considerably smaller (90 μm) than in comparable particle concentrations during other events (Blacktoft, August 1995 at neap, 800 μm). Whilst this supports observations by Bale et al (1989) in the turbidity maximum of the Tamar estuary, it conflicts with Eisma's (1991) observations in the Ems. At low water there is no totally slack period in the upper estuary, owing to river flow. Despite this, the current velocities and shear are sufficiently low that flocculation should be possible. Based upon similar conditions occurring at high water, the lack of such large flocs suggests an inability to generate flocs of sufficient strength to withstand either the low levels of shear, or particle-particle collisions. However, the most likely suggestion is that the binding strengths of particles, principally flocs, or the amount of polysaccharide material available to bind flocs in the turbidity maximum is important in determining the

natural size of the particle population. One contributing factor could be the mobilisation of long chain molecules (Carbohydrates) from particles within this region (Eisma et al, 1991b), reducing the potential for particle-particle binding.

In order to further the understanding of sediment dynamics in estuarine conditions it is necessary that objective measurements of particle characteristics be carried out in as wide ranging environmental conditions as possible. Subsequent dynamic models may then either use such data to provide a basis for a model or use it to test the accuracy of model predictions. The Par-tec100 during this study has been used in conditions, which far in a way exceed previous investigations using alternative methods of particle size measurement. The range of particle concentrations (0.01 to 100 gl^{-1}), salinity (0 to 24 ppt) and current velocities (0 to 1.6 ms^{-1}), in which particle size was measured, has provided an extremely valuable data set.

The Par-tec100's measuring capabilities were found to be unaffected by the range of conditions encountered in the upper estuary and coastal zone. Current speeds were encountered which approached the Partec laser beam's rotational speed, 2 ms^{-1}, yet no discernible effect was observed. This may be explained by the orientation of the probe directly into the current. Whilst there appears to be a general relationship between floc size and SPM concentration, during certain high particle concentration events the relationship is inverse. This primarily occurs within the region of the TM where small particle sizes are to be found coincident with very high particle concentrations. Therefore, there is no dependence of the Par-tec100 upon particle concentration within the range encountered during this study, borne out by the earlier laboratory experiments.

With the exception of two aborted anchor stations, as a result of failure in the modified remote focussing mechanism, deployments at these sites were on the whole successful. The instrument proved to be easy to deploy and due to the rapid measurement

cycle and small measuring volume it was able to provide a high degree of temporal as well as vertical spatial resolution. The manner of it's deployment does not end with vertical profiling, as the instrument was also successfully deployed using the same rig on tow along the Tamar estuary (Author, unpublished data).

Particle size relationships in the Ouse-Humber Estuary

4.1 Introduction

As we attempt to explain the behaviour of suspended particulate matter in the natural environment, it becomes increasingly evident just how complex is the nature of the interactions between particles. The cause for this lies not only with the changes in the hydrodynamic regime, which can occur on many scales, but also in the variability of the floc components. The survey of sites along the Ouse - Humber estuary serves to illustrate the degree to which the frequency and magnitude of transport processes, such as settling, entrainment, flocculation and de-flocculation, occur. There are two approaches to the elucidation of particle behaviour concerning these transport processes. The first approach is to look for patterns and relationships between the direct measurements of particle size and water quality / hydrodynamic variables, such particle concentration and fluid shear. By using direct correlation and multivariate analysis we can highlight the strongest relationships and provide simple models for predictive behaviour. In the second approach, we consider the physics of particle-particle interactions. Based upon the observations and relationships from multivariate analysis, models may be generated which predict not only simple particle size distribution descriptors, but also evolve the size distribution according

to changes in dynamic variables (shear, concentration etc.), collision kernels and cohesion / disruption probabilities.

The benefits of accurate determination of particle size in estuaries from modelling are manifest in the difficulties and expense of continual in-situ particle size monitoring. If the basics of particle-particle interactions in response to environmental changes can be developed and worked into a general estuarine model, this will greatly benefit the planning which goes into the maintenance of navigable waterways and emergency responses to pollution incidents. Whilst such models already exist, they are based upon laboratory experimentation and not field observations. Indeed we are only beginning to understand the variability of suspended particulate matter and the processes involved in particle size generation. Which is why in this chapter we will look at the relationships between particle size and the controlling environmental factors.

4.2 Causes of Aggregation & Disaggregation in Natural Flocs

Several authors have suggested mechanisms that are predominantly responsible for the generation and maintaining of suspended particle size distributions in estuaries. Salinity was reputed to cause flocculation of riverine particles upon contact with the low salinity (0.2 ppt) region of an estuary (Gibbs, 1989). The size of particles measured at Naburn weir, the limit of the tidal influence, revealed a very fine population of 19 μm median diameter. During low water at Selby, where salinity fell to 0.5 to 0.4 ppt, the size of particles in suspension was considerably greater, > 100 μm. However, this does not indicate that salinity is necessarily the cause of the particle size increase. The bed sediments change from approximately 90% silt and clay at Naburn, to 80% very fine sand

at Selby (Uncles, 1997) and it is the entrainment of this bed sediment which accounts for the increase in particle size. However, the large particle sizes which occurred at salinities approaching 1 ppt over high water, with sediment sourced from the turbidity maximum zone, where the silt and clay content was higher (60 - 70%, Uncles, 1997) and the particles are flocs rather than distinct grains. Gives the impression of increased flocculation due to salinity, but, is more likely due to increased collision frequencies between particles due to higher concentrations and possibly, an improved sticking efficiency due to the presence of mucopolysacharide coatings and tendrils (Neihof & Loeb, 1974; Hunter & Liss, 1982; Eisma, 1986 & 1991a).

The size of the smallest turbulent eddies is reported to limit floc growth (Eisma, 1991b). The largest flocs that exist in the water column approximate to the Kolmogorov microscale (Equation 3.3), either in response to particle stripping or due to total particle rupture, as the forces across the particle exceed its binding strength (Bache, 1989; Ani; 1991). The largest particles encountered within this study occurred within the fluid mud layer at Blacktoft (August), where the Kolmogorov scale would be expected to be large due to the very low current velocities and shear. However, in the water column where the Kolmogorov scale is likely to be of the order of 600 - 1000 μm at 0.5 m s^{-1}, 200 - 800 μm at 1.0 m s^{-1} (van Leussen, 1988), the size of the largest particles measured around slack water (< 800 μm) fit comfortably within the minimum eddy sizes.

The importance of the biological component of bed sediment and flocs in determining their size and behaviour was highlighted by the results of the LISP (UK) experiment. It was seen that the given the same hydrodynamic conditions, the size of particles resuspended from the bed was dependent upon the sediment critical shear threshold. This was affected greatly by the spatial distribution of biota and the associated

extracellular polymeric substances (EPS) that they produce. The same is also reported to be true of suspended particles in the low salinity region, where the polymeric substances (mucopolysacharides), which form a coating upon grain surfaces, aid the flocculation process (Eisma, 1986). Eisma (1986 & 1991a) reports upon the observation of a peak in dissolved carbohydrates within the low salinity region during winter. The peak is purportedly derived from mobilisation of the SPM particulate carbohydrate component from decaying algae. The reduction in particulate carbohydrates (mucopolysacharide) has the effect of reducing the binding strength of the flocs, seen in the low particle sizes from discrete particle size measurements. Despite this reduction in binding strength, Eisma (1986) suggests that this does not affect the size of flocs measured in-situ. Whilst this study did not include carbohydrate measurements in the upper estuary, the evidence from particle size data indicates that the turbidity maximum is characterised by a fine population mobilised from silt and clay deposits in the upper estuary and present in suspension at very high concentrations. The increased probability of particle collisions within the turbidity maximum do not appear to result in particle flocculation producing large flocs such as those at Balcktoft (August). This suggests that their sticking efficiency is lower than particles up and down-estuary, resulting in a low cohesion probability. Alternatively, the lower floc strengths within this region combine with high collision probabilities and turbulence to control the particle size population. In either case, both are directly attributable to a probable mobilisation of particulate carbohydrates.

4.3 Relationship Between Particle Size and Controlling Environmental Factors for the Ouse-Humber Estuary

4.3.1 Results of Simple Regression Analysis

Regressions of Median diameter (D_{50}) against particulate concentration and each of the relevant hydrodynamic variables were undertaken in order to assess the relevant dependence of particle size upon each of these variables. The regressions would also reveal the nature of the dependence seen in the scale and sign of the coefficients, as well as the type of model that best fits the data. All of the data from the Ouse-Humber Estuary deployments were used, providing a minimum of 1138 data points.

Independent	R^2	R^2 Adjusted	Std Error of Estimate	P-Value	Df	Model	Coeff A	Coeff B
Shear	2.383	2.295	141.31	0.000	1104	Y = A + B*(Sqrt(X))	+219.8	-63.23
Kolmogorov	3.604	3.515	0.47	0.000	1079	Y =A * X^B	+241.7	-0.089
Speed	11.794	11.713	90.05	0.000	1082	Y = A + B/X	+160.3	+3.423
Salinity	17.797	17.725	0.003	0.000	1137	Y = 1 / (A + B*X)	+0.006	+0.0002
SPM	34.898	34.840	79.41	0.000	1137	Y = A + B*X	+149.8	+0.006

Table 4.1 Regression analysis of D_{50} against calculated and measured master variable data for all stations along the Ouse-Humber Estuary. Results represent the best fit model. SPM represents particle concentration and K the Kolmogorov microscale length.

The variability in Median particle size for all samples taken during the Ouse-Humber survey was explained to varying degrees by individual master variables. The variables considered in the analysis were designed to reflect the probable influences upon particle size generation processes, such as flocculation, breakup and entrainment / resuspension. Salinity was included as a means of distinguishing the importance of the advective component.

The particle concentration exerts the strongest influence upon Median particle diameters (Table 4.1) in explaining 35% of the variability in D_{50}. It is also the only linear

relationship, with all other variables posessing square, square-root or inverse relationships. The ranking of Salinity as the second strongest relationship does not necessarily mean that salinity exerts a strong influence upon particle size generation, rather it supports the degree to which concentration plays a role in particle behaviour. This is seen from the nature of the relationship, whereby larger particles will be seen at lower salinities coincident with the higher suspended loads of the upper estuary. The poor relationship between size and the hydrodynamic variables, speed, shear and the Kolmogorov scale length at first appear to indicate a lack of influence. However, as was seen from the tidal stations during the processes of flocculation / settling and entrainment / resuspension a considerable lag time in the response of the particle population may be present.

A similar treatment of the 95th percentile diameters (D_{95}) was also carried out where in particular a relationship between D95 and the Kolmogorov microscale indicator was sought for.

Independent	R^2	R^2 Adjusted	Std Error of Estimate	P-Value	Df	Model	Coeff A	Coeff B
Shear	2.067	1.973	245.61	0.000	1104	Y = A + B*(Sqrt(X))	+429.4	+102.05
K	4.874	4.789	0.465	0.000	1079	Y =A * X^B	+532.3	-0.103
Speed	9.717	9.634	171.69	0.000	1082	Y = A + B/X	+329.2	+5.860
Salinity	24.872	24.806	0.001	0.000	1137	Y = 1 / (A + B*X)	+0.003	+0.0001
SPM	37.782	37.73	195.25	0.000	1137	Y = A + B*X	+307.2	+0.011

Table 4.2 Regression analysis of D_{95} against calculated and measured master variable data for all stations along the Ouse-Humber Estuary. Results represent the best fit model. SPM represents particle concentration and K the Kolmogorov microscale length.

Relationships between D_{95} and master variable data exhibits similar trend to that of D_{50} , in both the scale and mode of the relationship. The nature and weakness of the relationship between D_{95} and K agrees with the theory that particles are enveloped within eddies. Once enveloped within an eddy the floc may limited by the Kolmogorov microscale but does not have to grow to such an extent, although as concentration increases this may be the case. Therefore K may limit the upper scale of suspended flocs

but only at heightened levels of particulate concentration, at SPM levels of 5 gl^{-1} to 20 gl^{-1} the relationship becomes stronger with K describing 30% of the variation in D_{95}.

4.3.2 Particle Size Dependence by Station : Ouse-Humber Estuary

As well as looking at the data set as a whole, multivariate analysis was carried out for each individual station. Given the variability in observed processes and the magnitude of some variables, in particular particle concentration, and the seasonal changes throughout the survey program, it was felt that correlations might prove stronger over one station than for the complete survey. Multivariate analysis was carried out with both median particle size and the 95th percentile as the dependants. A set target of a 95% confidence level was used in determining the statistical significance of independent variables. In order to achieve a 95% confidence level, the P-values of each independent variable must be no greater than 0.05. Independent variables considered for the analysis included, shear, speed, salinity, particle concentration and an indication of the Kolmogorov microscale. The set of independent variables that provided the best fit was achieved by considering all variables and then removing the least statistically significant members based upon their P-value.

Multivariate analysis results exhibit considerable differences from station to station in terms of correlation and independent variables used. At Whitton Channel correlation between size (D_{50} & D_{95}) and independent variables is poor, with only 9 to 14% of the variability explained by a linear model containing K and SPM. In some cases all five independent variables combine to provide a relationship at the 95% confidence level. Whilst some stations show a high degree of correlation, the results appear to be site specific with no appearance of a seasonal or geographical pattern developing.

Station	Independent	R-Squared	R-Squared (adjusted)	Std Error of Estimates	P-Value	ANOVA				Model	
							Σ of Squares	Df	P-Value	Intercept	Coefficient
ALL	Salinity	9.257	8.997	91.63	0.000	Model	896736	3	0.000	242.3	-3.1642
	Shear				0.029	Residual	8.8	1047			-9.396
	Speed				0.000						-47.746
SE1	Shear	51.994	50.554	39.98	0.000	Model	173100	3	0.000	36.3	-39.992
	SPM				0.000	Residual	159824	100			+0.0015
	Salinity				0.000						+164.451
SE2	Kolmogorov	35.247	32.794	42.21	0.025	Model	129253	5	0.000	83.248	-0.0385
	Salinity				0.000	Residual	237450	132			+344.79
	Shear				0.002						-13.101
	Speed				0.001						-42.879
	SPM				0.000						-0.009
BT1	Shear	45.259	44.258	105.96	0.016	Model	$1.5x10^6$	3	0.000	235.6	+93.789
	Speed				0.000	Residual	$1.8x10^6$	164			-182.42
	SPM				0.000						+0.00686
BT2	Salinity	46.762	45.841	62.75	0.017	Model	798911	4	0.000	225.3	+4.962
	Shear				0.003	Residual	909522	231			-11.949
	Speed				0.000						-156.315
	SPM				0.042						-0.0031
WC1	Kolmogorov	11.256	8.566	86.35	0.0971	Model	62429	2	0.019	139.48	+0.026
	SPM				0.007	Residual	492216	66			+0.012
WC2	Kolmogorov	17.158	14.428	88.34	0.042	Model	147111	3	0.001	-42.04	-0.028
	Salinity				0.000	Residual	710249	91			+13.085
	SPM				0.035						+0.010
HB	Kolmogorov	42.803	40.637	74.85	0.000	Model	553497	5	0.000	304.57	-0.183
	Salinity				0.008	Residual	739628	132			+4.571
	Shear				0.000						-120.871
	Speed				0.000						-120.309
	SPM				0.000						+0.039
SG10	Kolmogorov	31.071	25.556	9.493	0.004	Model	1015	2	0.010	108.16	-0.016
	Speed				0.008	Residual	2253	25			-29.276
SG13	Salinity	66.464	58.079	9.063	0.001	Model	2604	4	0.001	-1176.5	+36.072
	Shear				0.035	Residual	1314	16			+219.94
	Speed				0.014						-15.387
	SPM				0.007						+4.464
SG23	Kolmogorov	46.492	42.033	14.651	0.004	Model	8952	4	0.000	-209.54	-0.009
	Salinity				0.000	Residual	10303	48			+9.362
	Speed				0.006						-29.399
	SPM				0.000						+0.494
SG24	Kolmogorov	56.558	51.128	12.797	0.004	Model	5116	3	0.000	-1155.8	-0.030
	Salinity				0.000	Residual	3930	24			+38.987
	Speed				0.002						-60.484

Table 4.3 Multivariate analysis of Ouse-Humber Estuary stations with Median particle diameter as the dependent variable.

Station	Independent	R-Squared	R-Squared (adjusted)	Std Error of Estimates	P-Value	ANOVA				Model	
							Σ of Squares	Df	P-Value	Intercept	Coefficient
ALL	SPM	14.301	14.143	167.35	0.000	Model	$5.1x10^6$	2	0.000	372.2	+0.0046
	Salinity				0.000	Residual	$3.0x10^7$	1081			-4.431
SE1	Kolmogorov	64.287	62.460	95.05	0.018	Model	$1.6x10^6$	5	0.000	-69.3	+0.582
	Speed				0.007	Residual	885376	98			+118.926
	Shear				0.008						-73.067
	SPM				0.000						+0.009
	Salinity				0.0138						+266.915
SE2	Kolmogorov	35.786	33.354	82.89	0.016	Model	505469	5	0.000	129.11	-0.081
	Salinity				0.000	Residual	906991	132			+719.425
	Shear				0.001						-28.324
	Speed				0.004						-74.701
	SPM				0.000						-0.0162
BT1	Salinity	48.115	46.842	178.78	0.023	Model	$4.8x10^6$	4	0.000	361.2	+11.321
	Shear				0.002	Residual	$5.2x10^6$	163			+230.53
	Speed				0.000						-343.82
	SPM				0.000						+0.0125
BT2	Salinity	46.476	45.549	118.59	0.011	Model	$2.8x10^6$	4	0.000	434.2	+9.987
	Shear				0.002	Residual	$3.2x10^6$	231			-23.618
	Speed				0.000						-300.04
	SPM				0.099						-0.0049
WC1	Kolmogorov	12.192	9.532	139.96	0.032	Model	179525	2	0.014	302.35	+0.056
	SPM				0.000	Residual	$1.3x10^6$	66			+0.019
WC2	Kolmogorov	20.028	18.290	169.47	0.025	Model	663131	2	0.000	59.88	-0.059
	Salinity				0.000	Residual	$2.6x10^6$	92			+21.620
HB	Kolmogorov	41.638	39.427	132.51	0.000	Model	$1.6x10^6$	5	0.000	600.09	-0.326
	Salinity				0.009	Residual	$2.3x10^6$	132			+7.986
	Shear				0.000						-230.647
	Speed				0.000						-219.122
	SPM				0.000						+0.061
SG10	Kolmogorov	37.164	29.309	21.901	0.034	Model	6809	3	0.010	169.19	-0.026
	Speed				0.033	Residual	11502	24			-54.635
	SPM				0.023						+2.122
SG13	Speed	38.643	36.087	27.406	0.001	Model	11353	1	0.001	231.77	-59.255
						Residual	18026	24			
SG23	Kolmogorov	39.328	34.272	36.367	0.002	Model	41150	4	0.000	-369.28	-0.027
	Salinity				0.001	Residual	63483	48			+17.713
	Speed				0.002						-82.814
	SPM				0.002						+0.890
SG24	Kolmogorov	48.985	42.608	31.402	0.000	Model	22723	3	0.001	-2330.0	+78.408
	Salinity				0.006	Residual	23665	24			-128.40
	Speed				0.030						-0.054

Table 4.4 Multivariate analysis of Ouse-Humber Estuary stations with the 95th Percentile diameter as the dependent variable.

4.4 Modelling of Suspended Particle Size Distributions

Particle transport behavior in response to the hydrodynamic regime, in its simplest form, is determined by physical characteristics such as settling velocity. This may take the form of the modified Stokes equation which describes the settling velocity of a floc (McCave, 1984), or alternatively, an empirically derived formulae such as the relationship between W_s and SPM concentration (Equation A2.5) (van Leussen, 1988). However, the behaviour described by these equations does not take flocculation into account. Flocculation models, such as that proposed by Krishnappan (1991) have limited use in transport modelling beyond the examination of water clearance because they lack a floc disruption component. Following laboratory experiments by Tsai (1987) concerning the effect of shear and concentration upon floc size, Lick & Lick (1988) proposed a model which allowed for deflocculation along with flocculation (Equation 4.1). It describes the loss and gain rate of particles of diameter k, from collisions between particles of diameter i and j.

$$\frac{dn_k}{dt} = \tfrac{1}{2} \sum_{i+j=k} A_{ij}\beta_{ij}n_i n_j - n_k \sum_{i=1}^{\infty} A_{ik}\beta_{ik}n_i - B_k n_k + \sum_{j=k+1}^{\infty} \gamma_{jk}B_j n_j$$

$$- n_k \sum_{i=1}^{\infty} C_{ik}\beta_{ik}n_i + \sum_{j=k+1}^{\infty} \gamma_{jk}n_j \sum_{i=1}^{\infty} C_{ij}\beta_{ij}n_i \qquad [4.1]$$

Each term on the right hand side of the above equation represents a loss / gain term for the number rate of particles in particle size interval k. The number of particles in each size class is represented by n, γ_{jk} is the probability that a floc of size k will form from the breakup of j, A_{ik} and C_{ik} are the probabilities of aggregation / disaggregation (respectively) following collision of i and k. B represents the loss (B_k) and gain (B_j) of flocs size k due

to breakup caused by shear. Burban (1989), who uses the model in the analysis of particle size as a function of shear, concentration and salinity, assumes B to be 0, as it is not yet possible to calculate B. The term β, represents the collision frequency functions for (McCave, 1984):

$$\beta_{ij} = \frac{2}{3}\frac{kT}{\mu}\frac{(d_i + d_j)^2}{d_i d_j} \qquad \text{Brownian motion} \qquad [4.2]$$

$$\beta_{ij} = (G/6)(d_i + d_j)^3 \qquad \text{Fluid shear} \qquad [4.3]$$

$$\beta_{ij} = \frac{\pi g}{72\mu}(d_i + d_j)^2 \left| \Delta p_i d_i^2 - \Delta p_j d_j^2 \right| \qquad \text{Differential settling} \qquad [4.4]$$

and for a 26 μm particle they take the form shown in Figure 4.1.

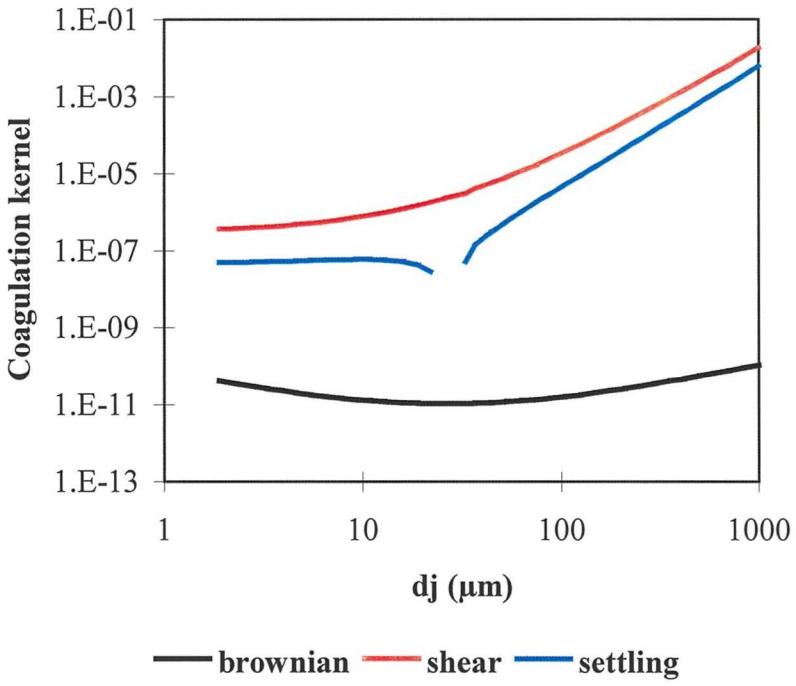

Figure 4.1 Coagulation kernels (probability) for differing modes of collision for a particle d_j colliding with d_i (26 μm). β_{ij} is the sum of each kernel.

The laboratory experiments of Tsai (1987) and their subsequent inclusion in the above model by Lick & Lick (1988) and Burban (1989), indicate that median particle size

is inversely proportional to particle concentration and shear. Burban (1989) justifies this observation by considering tri-particle collisions to be the dominant disaggregation mechanism, rather than shear or binary collisions. The output from the model agrees well with the experimental results, but both are in opposition to the conceptual model of particle size put forward by Dyer (1989). This states that particle size is proportional to concentration and inversely proportional to shear stress. This has also been the finding from deployments of the Par-tec100 in the Humber estuary. From a simple linear regression of median particle size against particle concentration ($R^2 = 34.90$, $n = 1138$) for all particle size measurements obtained in the Humber estuary, it can be seen that concentration is the principal determinant of particle size (addition of current velocity and shear to the regression improved it marginally). This can be seen from the reconstruction of Dyer's (1989) conceptual model using the in-situ particle size data collected in this work (Figure 4.2). The multiple regression was achieved using SYSTAT, a statistical package running under Windows, with the surface fitted using the distance weighted least squares method. The result is comparable to Dyer's (1989) model, although the scale of the flocs seen in-situ is greater than predicted by Dyer. This is not consistent with Burban's (1989) conclusion that tri-particle collisions are dominant over binary, in the disaggregation process. The discrepancy may be due to the experimental setup of Tsai (1987) and Burban (1989), where particles were extracted from a couette viscometer before analysis in a Malvern laser diffraction particle sizer. The transfer from a constant shear regime in the viscometer to a differing regime during analysis may effect an increase in flocculation which would be proportional to the particle concentration; their placement in a higher shear regime would cause rapid deflocculation and bias the results.

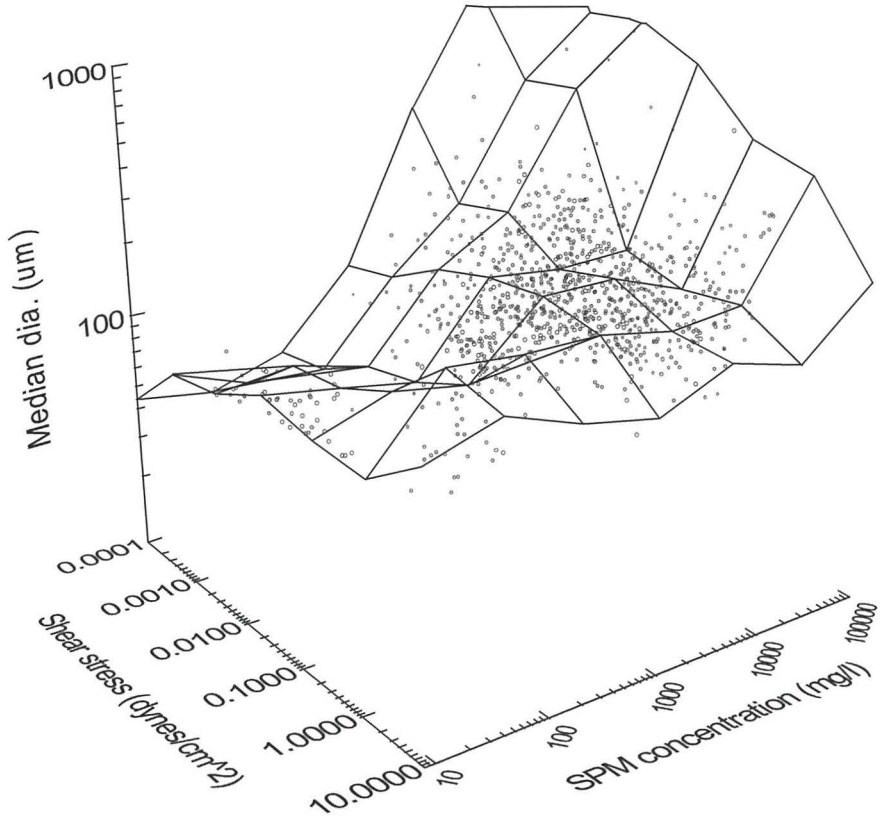

Figure 4.2 Plot of Median particle size against shear stress and SPM concentration. All in-situ particle size measurements within the Humber estuary and plume region have been included.

Suspended Particle Dynamics over an Intertidal Mudflat.

5.1. Introduction

Much of the research associated with characterisation of particulate matter in suspension has centred on the estuarine and coastal water column. To date, little effort has been applied to the intertidal region. This is mainly due to the limitations of previous instrumentation in dealing with the high particle concentrations and shallow water depths involved. However, intertidal areas act as sources or sinks for much of the suspended particulate material in estuaries. They therefore have the potential to act as long or short term storage areas for particle borne pollutants. Mudflats and salt marshes also provide important coastal defences for vulnerable low lying lands as well as being of vital importance to migratory and over-wintering wild fowl. The study of sediment transport processes in such areas is vital not only for their management but also to bring about a fuller understanding of estuarine processes.

Despite their environmental importance, the processes that affect sediment transport and therefore the temporal stability of the mudflats are poorly understood. Previous studies of water and sediment transport over intertidal mud flats (Collins et.al., 1981; Carling, 1977; Handyside 1978; Amos & Long, 1980) have highlighted some of the principal factors influencing sediment transport and hydrodynamics in shallow tidal areas.

Following a successful multidisciplinary experiment, LISP (Littoral Investigation of Sediment Properties), on the Bay of Fundy, Canada, a similar field investigation was set up in the UK under the auspices of LOIS RACS (C) (Black & Patterson, 1996). A site located in Spurn Bight at the mouth of the Humber estuary was chosen for this investigation into the processes affecting the intertidal habitat from the perspective of biological communities, bed sediment processes and water column dynamics. The object of LISP (UK) was to study the relationships between, biota, sediment stability and sediment dynamics through in-situ observations, within the same area and carried out within the same time scale using a multi-disciplinary approach. The opportunity to deploy the Par-tec 100 as part of LISP (UK) provided an ideal opportunity for further field evaluation of the instruments capabilities and flexibility and the collection of particle sizing data in association with biological and flume data.

The net movement of sediment (accretion or denudation) on or off the mudflat surface, is controlled by sediment stability and the magnitude of the shear stresses induced by the flow of water over the bed. The erosion thresholds of intertidal surfaces, which are described by the critical shear stress value, can be measured in-situ with the use of portable annular flumes (Widdows et.al., 1997; Amos, 1992). The use of such flumes has highlighted the importance of benthic organisms in the stabilisation of bed sediments, through pelletisation (faeces) or extrusion of long chain molecules which bind inorganic material (Widdows et.al., 1997). In so far as bulk sediment movements are concerned, research has tried to evaluate the net flux of material transported on the ebb and flood tides, through the use of simple turbidity and current meters from moored boats or masts (Collins et.al., 1981). The high spatial and temporal resolution of Collins' (1981) observations showed that the dominant processes affecting the bulk of sediment movement appeared to be dominated by episodic events. During the flood and ebb tides, rapid

changes in current velocity occur which are directly related to sediment stability, these events generate large amounts of particulate resuspension (Collins, 1981). The highest SPM concentrations, coincident with the highest current velocities, have been found to occur during the initial stages of the flood tide (water depth < 0.5m) and during the remnants of the ebb tide (water depth < 0.5m) (Collins, 1981).

5.2. Procedure & Site

The LISP (UK) experiment was carried out at Spurn Bight, which is located on the northern shore of the Humber Estuary and is a large intertidal embayment, extending approximately 3 miles from shore and 7 miles in width and is bounded to the east by Spurn Point (Figure 5.1). The intertidal area of Spurn Bight, like that of the rest of the lower estuary, displays a marked variability in the nature of bed sediments, which range from mud to sand within the bight.

Measurements were concentrated on four stations on a line extending normal to the shore at Skeffling (Figure 5.1). The near shore stations (A & B) could be accessed by foot, but not by the vessel which was used for waterborne tidal surveys. The outer stations (C & D) were surveyed from a beachable barge located on site between morning and evening high water. As 240v power for the instrument was not available at sites A and B, the Par-tec100 was only deployed from the barge at sites C and D. With all sites experiencing considerable periods of aerial exposure, approximately 5 hours for the outer stations, particular attention was paid to measuring the rapid variations in SPM characteristics during the progression of the tidal wave over the mudflat upon the ebb and flood tides. The configuration of the Par-tec100 meant that particle size measurements could be taken within 10cm of the bed, allowing particle size determination to be made in very shallow

waters during the critical periods when sediment became exposed on the outgoing tide and flooded on the incoming tide.

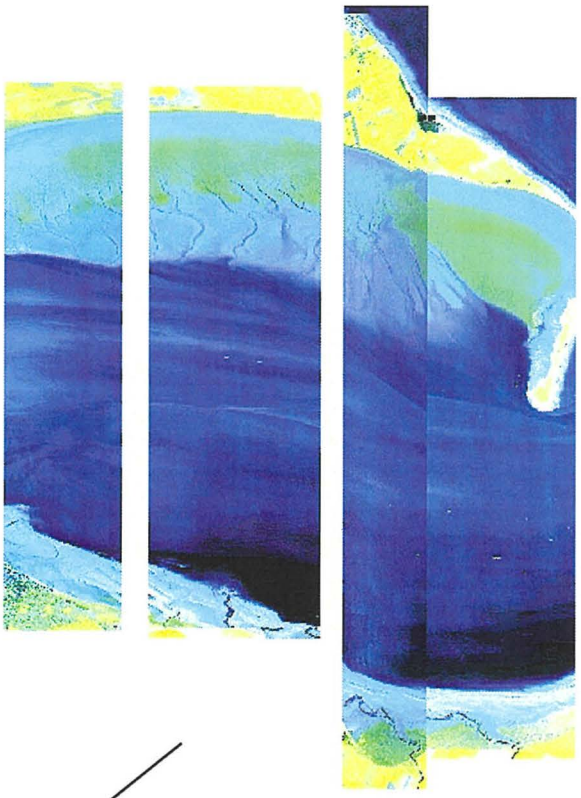

Figure 5.1a Composite of enhanced CASI images of the eastern Spurn Bight, 14:00 GMT on 28/06/94, altitude 3.05 km, bearing SW.

Figure 5.1b Location of the LISP UK site in Spurn Bight. Indicating the positions of the surveyed sites along the shore normal transect. Particle size measurements using the Par-tec100 were made at the outer stations, C and D between the 4th and 7th April 1995.

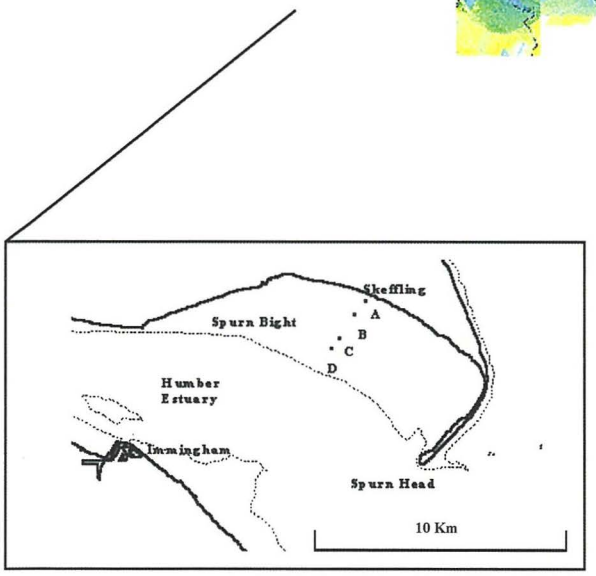

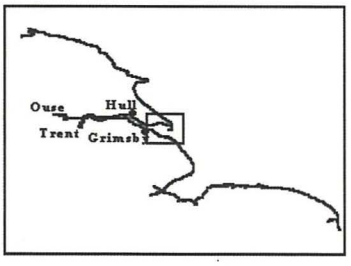

Station	Latitude	Longitude
A	N 53°38.50	E 0°4.25
B	N 53°38.40	E 0°4.10
C	N 53°37.45	E 0°3.80
D	N 53°37.45	E 0°3.86

The composition of the sediments progressed from mud at station A through to sandy mud at station C. Large ridges and runnels, running approximately normal to the shore occurred between stations B and C. At station D the sediment progressed to muddy sand with an altogether flatter topography.

The Par-tec100 was lowered from a davit extending 1m from the barge using a hand winch. In order to minimise interference from the hull, the instrument was placed on the shoreward side of the vessel during the ebb and moved to the seaward side prior to the flood tide. When the water column depth was sufficient to allow vertical profiling, the instrument was lowered through the water column and measurements were taken at various depths. When the water shallowed to < 1 m, the instrument was rested upon the bed, with the sensing zone approximately 10 cm above the bed. In this position measurements were taken every 30 s.

Current velocity measurements were provided by a Velocity Gradient Unit (VGU), (C. Jago, School of Ocean Sciences, Bangor). This consisted of vertically arranged, logarithmically spaced Ott current meters on a 2 m mast. The mast was anchored to the bed with the Ott current meters positioned normal to the expected current direction, i.e. normal to the shore. One set were directed shoreward and the second set seaward to allow measurements upon both the flood and ebb tide. The height of the meters above the bed were, 10, 25, 45, 85, 150 cm for the flood tide and 5, 20, 40, 80, 145 cm for the ebb tide. The result from the lowest current meter is used in this study, as it corresponds with the height of the Par-tec100 above the bed. A solid state logger was used to record VGU data for 1 minute in every 10 minutes and the values obtained over each minute were subsequently averaged. The VGU was installed on the 4th of April, which means that current velocity data for station C1 are only available for the evening flood tide at this site.

Suspended solids concentrations were provided by gravimetric samples taken from the surface waters and filtered onto tared 0.45 μm GF/C filter papers (C. Bull, School of Ocean Sciences, Bangor, Appendix 1).

5.3 Results

5.3.1 Use of the Par-tec100 in Generating SPM Concentration Data

Comparison of gravimetric values for suspended particulate concentrations with Par-tec100 particle count values, revealed that a strong correlation existed. The Par-tec100 has a high frequency sampling rate, during this deployment particle size measurements were taken in a matter of seconds rather than minutes. It seemed feasible then that if it were possible to obtain a good regression of the Par-tec100's particle count versus suspended solids concentration, that the Par-tec100 could be utilised for high frequency suspended solids concentration measurements.

In order to relate particle numbers (or counts) to solids concentration some attention must be paid to the nature of the particles. If we assume, that particle density remains relatively consistent irrespective of particle size. Then for a given mass concentration, the number of particles present would be inversely proportional to their size, as indicated in Table 1.1. The Par-tec100 derived particle count is therefore also dependent upon particle size. In order to account for particle size variation, the Median, Modal and Mean particle diameters were considered in the search for the best model for predicting particle concentrations. As these only describe one aspect of the particle size spectrum, other factors such as skewness, kurtosis, standard deviation and the coefficient of variance were also taken into consideration. The intention here was to take into account the spread of the particle size spectra and the likely effect that this would have upon the

particle count. Multiple regressions were carried out using all of the aforementioned variables. The only variables that exhibited a significant contribution to the relationship were a combination of the particle count value and either the Mean, Modal or Median particle size. The highest degree of correlation was found to occur with the product of the Median particle size and particle count, a simple regression involving this value revealed that the model proving the best fit was a Double Reciprocal model (Figure 5.2a).

The relationship between SPM concentration (S) and Par-tec100 particle counts (C) takes the form:

$$S = 1 / (0.000445 + (2847.9 / (C*D_{50})) \quad [5.1]$$

Where D_{50} represents the Median particle diameter. Data included in this analysis are from stations C & D on the 4th, 6th and 7th April, 1995, n=30. The correlation coefficient returned by the model was 0.928, with an R^2 value of 86.025%, adjusted to 85.526% for Df.

Analysis of Variance					
Source	Sum of squares	Df	Mean Square	F-Ratio	P-Value
Model	0.000596	1	0.000596	172.36	0.000
Residual	0.000097	28	0.0000035		
Total (Corr)	0.000693	29			

Table 5.1 ANOVA table for relationship between observed SPM concentration and Par-tec100 particle counts.

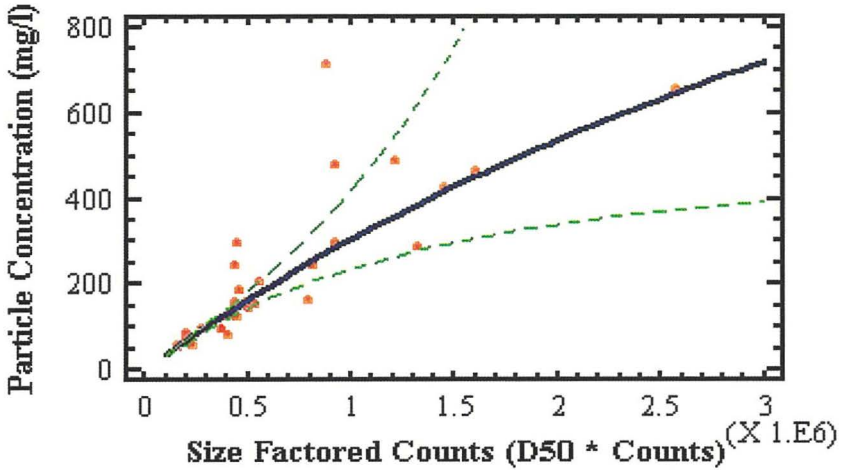

Figure 5.2a Plot of suspended solids concentration against Par-tec100 particle counts, factored for particle size (median diameter x particle count). The solid line represents the best fit to the data, whilst the dashed line indicates the 95% confidence limit.

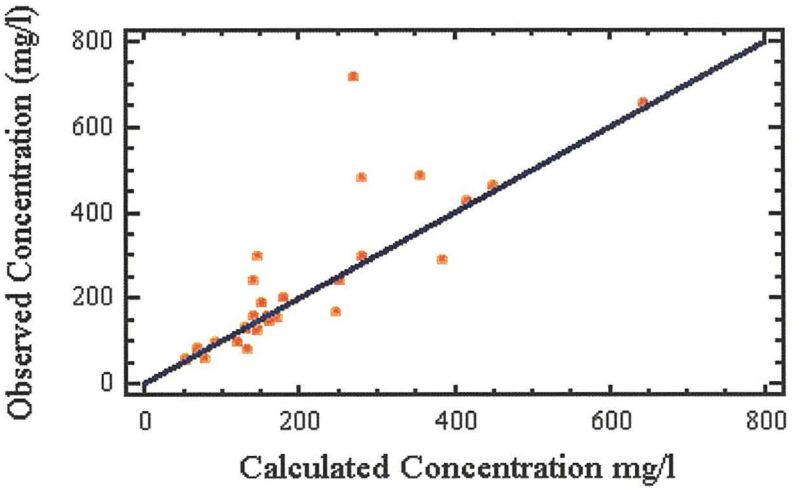

Figure 5.2b Plot of Observed Gravimetry values against values calculated from a double reciprocal regression based upon Par-tec100 particle counts. Allowing the calculation of suspended solids concentrations from the higher frequency Par-tec100 response.

The statistical significance of the correlation is high, given that the P-value (Table 5.1) is lower than 0.01, indicating a relationship with a 99% confidence level. The R^2 value indicates that this model explains 86% of the variability in suspended solids concentrations as measured by gravimetry. Due to such a strong correlation (Figure 5.2b), it was felt that the modelled values which could be provided by the Par-tec100, represented the most accurate source of high frequency SPM measurements during the course of the LISP project.

5.3.2 Field Observations

Particle sizes in the water column were measured by laser reflectance at station C on the 4th and 7th April and at station D on the 6th April. Tidal predictions for the nearby port of Immingham (Table 5.2) show that sampling was carried out from spring tide +1 day till the midpoint of the spring-neap cycle. The survey of site C, on the 4th April, being carried out only one day after a 5.79m spring tide.

Station	Date	Tidal Range (Immingham)	High Water Times
Spring tide:	3rd April	5.79m	
C1	4th April	5.40m	0810 / 2030
D	6th April	4.33m	0940 / 2230
C2	7th April	3.67m	0910 / 2140
Neap Tide:	10th April	2.50m	

Table 5.2 Sampling station details for LISP-UK, 1995.

The observations were carried out during predominantly light northerly winds, 2 to 4 m s^{-1} (Figure 5.2), veering south and then northwesterly over the course of the deployment. Wind strength on the 7th (station C2) decreased from a high of 8 m s^{-1} to 2 m s^{-1}, over the course of the afternoon as the tide ebbed, also changing direction from

northwesterly to northerly. On the subsequent flood, the direction reverted to northwesterly, although winds remained light (Figure 5.2).

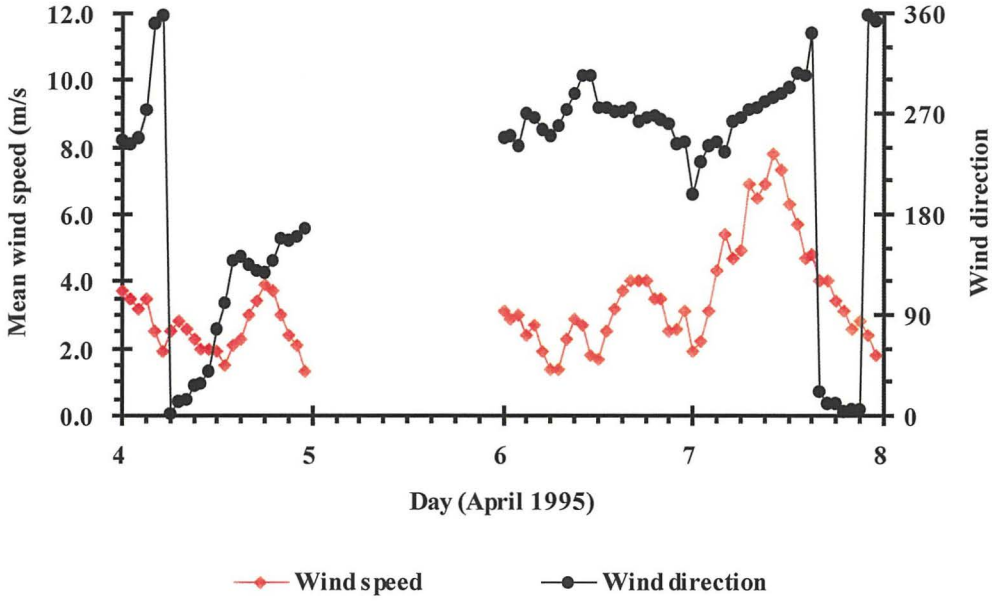

Figure 5.2 Meteorological data during the deployment of the Par-tec100 at the site of the LISP (UK) survey.

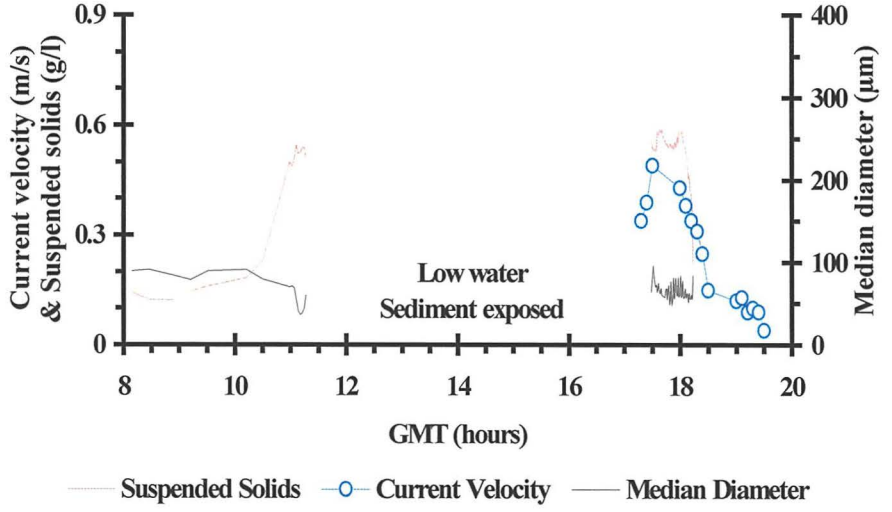

Figure 5.3 Time series of particle size, concentration and current velocity at station C (04/04/95).

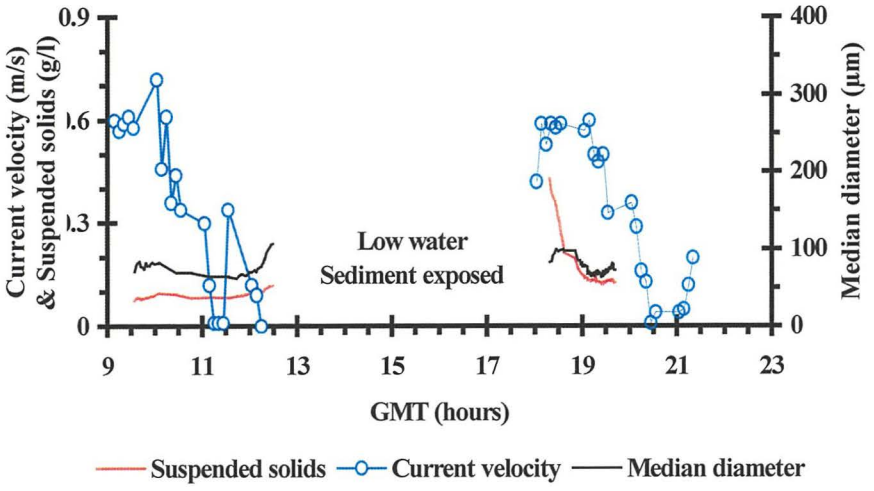

Figure 5.4 Time series of particle size, concentration and current velocity at station D (06/04/95).

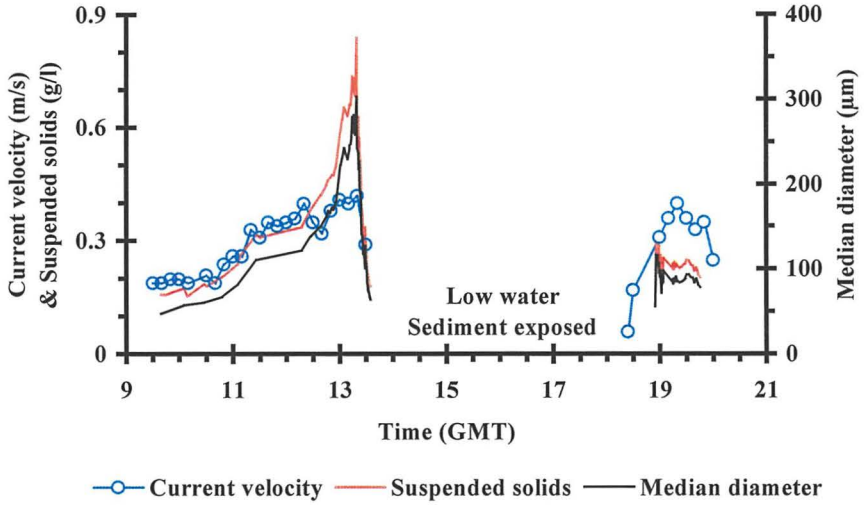

Figure 5.5 Time series of particle size, concentration and current velocity at station C (07/04/95).

The flood tide, or inundation of the exposed tidal flat, was generally characterised by a sharp rise in current velocity, coincident with high levels of suspended solids (600 mg l^{-1} (C1), 400 mg l^{-1} (D), 300 mg l^{-1} (C2), Figure 5.3 to 5.5). During the ebb tide, current velocities exhibit a markedly different behaviour between stations C and D. This is seen as a steady increase (C) or decrease (D), prior to the moment when the bed became exposed. Whereas particle concentration and size increased steadily with the ebbing tide,

until water depth was no more than 0.5 to 0.25 m, the SPM concentration rose significantly in the last moments before exposure (550 mg l^{-1} (C1), 125 mg l^{-1} (D1), 800 mg l^{-1} (C2)).

With the exception of the flood tides at stations C1 and D2, the size of particles in suspension is prone to large variation over a very short period. Particle sizes appear largest at the end and beginning of the ebb and flood tides, respectively. Whilst there appears to be a common pattern of variation in particle size during the flood tides for each station, the ebb tides differ greatly. There is little variation in particle size during the ebb tides of C1 and D2. Although, at C1 there is a noticeable decrease in size prior to sediment exposure. This is opposed to the pattern observed at C2, where the largest particles (450 μm median diameter) were seen at the end of the ebb tide. Prior to the bed sediment becoming exposed, current velocities appeared to be decreasing and particle sizes appeared to have peaked (200 μm median diameter). However, as the ridges became exposed, the drainage of the mudflat was dominated by runnels in which current velocities increased and particle sizes continued to rise

In general, after the initial passing of the tidal wave on the flood, particle sizes decrease to a minimum of 75 to 100 μm for the tide (all stations). This precedes a peak in the 10 minute averaged current data of around 0.4 m s^{-1}, at which point particle sizes rise, marginally, to over 100 μm. During this period of high current velocities the size of particles in suspension appears to fluctuate rapidly (Figures 5.3 to 5.5).

Examination of particle size spectra taken from particular stages of each tide (Figure 5.6) reveals that these are characteristically unimodal with a spread of roughly one order of magnitude (Figures 5.7 to 5.12). The particle size variation is seen to be greatest at C2, where the current velocities exhibited the least variation, maximising at 0.4 m s^{-1} (Figure 5.5) rather than 0.5 – 0.6 m s^{-1} at C1 (Figure 5.3) and D (Figure 5.4).

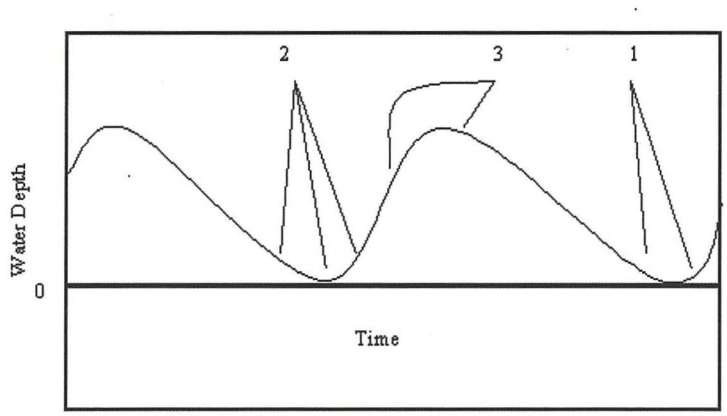

Figure 5.6 Illustration of temporal location of particle size spectra mentioned above and shown in Figures 5.7 to 5.12.

With reference to Figure 5.6 above;

1) At maximum suspended solids concentration at the tidal front (ebb and flood),

2) Prior to or after the front, i.e. at the leading edge of the tidal inundation / exposure and post front,

3) During the lower concentrations and currents experienced at the beginning of the ebb or approaching 1m water depth on the flood (mid tide, post high water and post front).

For the majority of measurements taken during the ebb, there was very little material below 20 μm or above 300 μm (Figures 5.10 to 5.12). This was also the case for the flood tides, where the maximum current velocity was marginally greater than on the ebb and the size of the particles changed little between stations (Figures 5.7 to 5.9). The only exception to this being C2 during the ebb where particles up to 1000 μm were seen, despite lower current velocities.

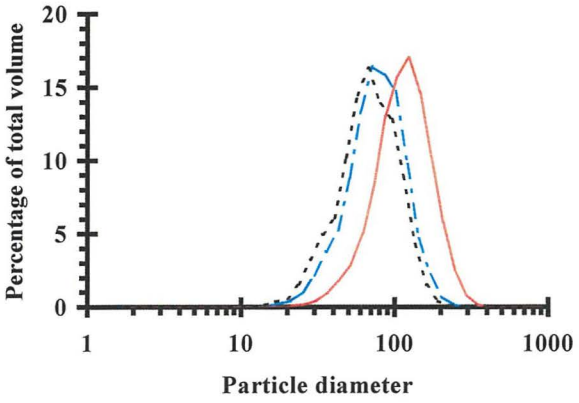

Figure 5.7 Particle size spectra during the initial stages of the flood event at station C, 4th April.

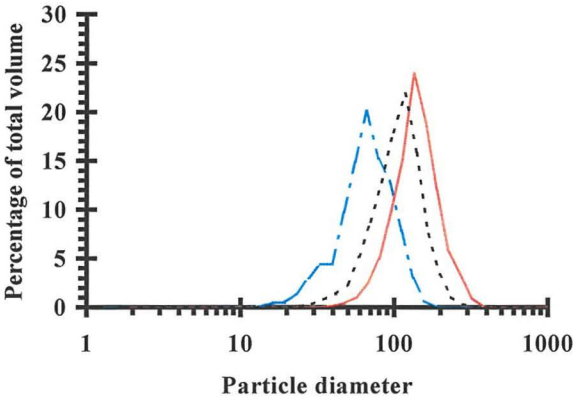

Figure 5.8 Particle size spectra during the initial stages of the flood event at station D, 6th April.

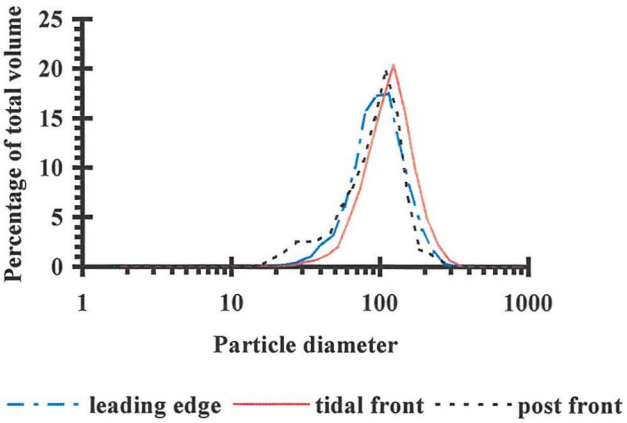

Figure 5.9 Particle size spectra during the initial stages of the flood event at station C2, 7th April. Legend applicable to 5.8 and 5.7.

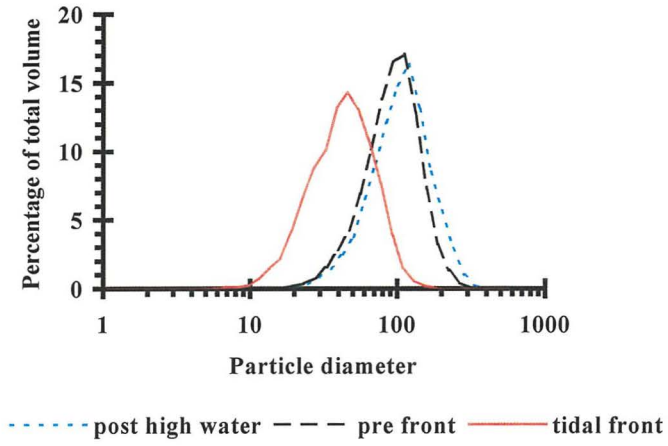

Figure 5.10 Particle size spectra measured during the final stages of the ebb tide at station C1, 4th April.

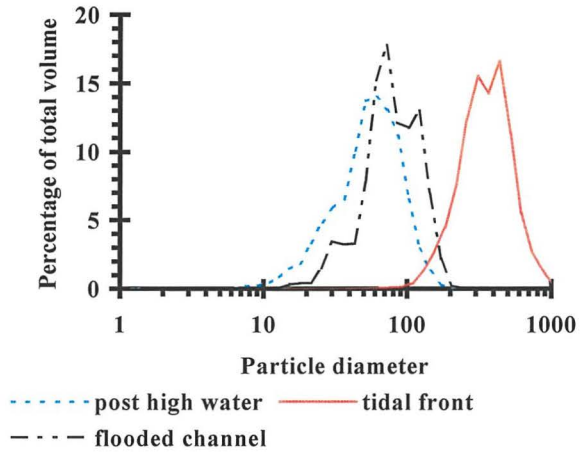

Figure 5.11 Particle size spectra measured during the final stages of the ebb tide at station D, 6th April.

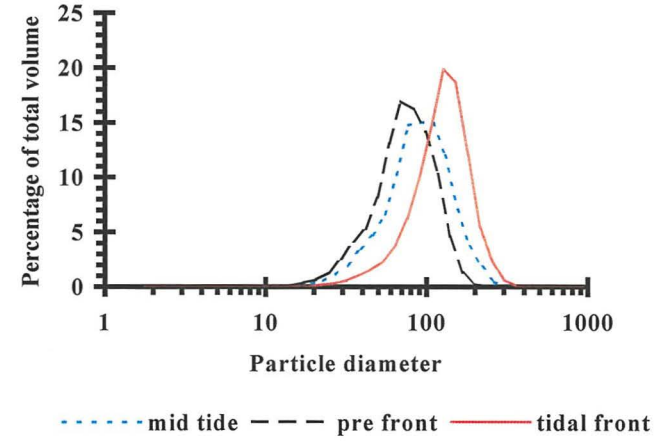

Figure 5.12 Particle size spectra measured during the final stages of the ebb tide at station C2, 7th April.

5.4 Discussion

The size of suspended particles over an intertidal flat was determined as part of a multidisciplinary study of a shore normal transect at Skeffling. Particle size measurements were taken at the seaward end of the transect, at stations C and D and were supported by suspended solids and current velocity data. Other studies carried out at the same time, or shortly thereafter, were consistent with the patterns of particle behaviour observed through the size measurements.

Bed characteristics, in terms of erosion thresholds, bioturbation, granulometry and sedimentation history, play a significant part in the mode of sediment resuspension and therefore the size of the resuspended particles. The bed form of the tidal flat at Skeffling exhibits significant changes between stations B and C, where a system of ridges and runnels take over from a relatively flat intertidal area. In the case of Skeffling, this tidal flat is characterised by a general coarsening of the bed sediment seaward (A to D), seen in the increased sand component, > 63 μm (Figure 5.13). Exceptions to this trend are evident between stations B and C. Station B has a relatively high sand content, >40% compared to A's <10%, which is more than matched by the runnels found between stations B and C. In these runnels, the sand content at station C is approximately 60%, yet the ridges separating the runnels and the flatter areas are characterised by having only 20% sand.

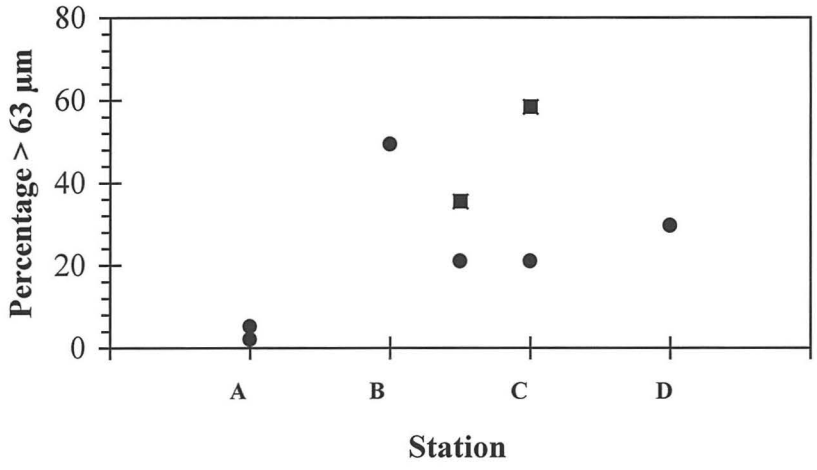

Figure 5.13 Sand content of bed sediments along the shore normal transect at Skeffling. Square symbols denote that the sample point was in a runnel or pool, whilst circles denote a ridge or flat area.

The differences between the ridges and runnels were reflected in their respective erosion thresholds. Critical erosion thresholds, for all sites and the midpoint between B and C, were measured using a portable flume (Widdows, pers comm). Critical erosion velocities were seen to decrease from 30 cm s^{-1} at A to approximately 20 cm s^{-1} at D, in opposition to the trend in grain size. Spatial variations in the erosion threshold at A, B and D were found to be negligible. In the ridge / runnel system erosion thresholds varied according to bed form, values for the runnels were significantly lower (by 10 cm s^{-1}) than the runnels (Figure 5.14). Several factors would appear to contribute to this observation, not least the pattern of bioturbation and the pooling of water in the runnels over low water, when the ridges are exposed.

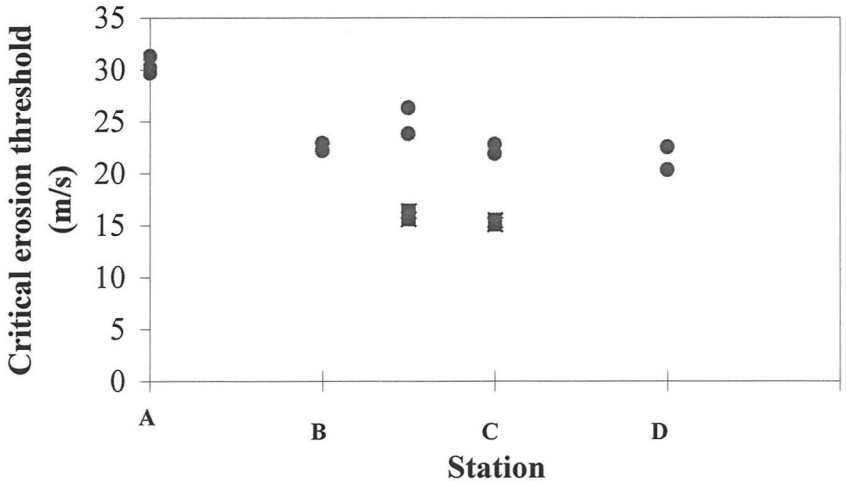

Figure 5.14 Critical erosion thresholds for surface sediment along the shore normal transect at Skeffling (Widdows, pers comm). Square symbols represent the gullies and pools, whereas the circles represent the ridges and remainder of the mudflat.

Benthic organisms are recognised as having an important role in sediment stability (Black, 1994). Excretion of extracellular polymeric substances (EPS), commonly termed mucus, provides a mechanism for binding inorganic particles. This has been recognised as being important in the aggregation and stability of suspended sediments in the low salinity regions of estuaries (Eisma, 1991) as well as in the stabilisation of bed sediments.

Increased critical erosion thresholds, which indicate improved sediment stability, may not be due solely to the binding strengths inherent between inorganic grains coated in polymeric substances. Secretions of such material may reduce surface drag and effectively increase the critical erosion stress (Paterson, 1997). EPS is carbohydrate rich; measurements of carbohydrate concentrations (Figure 5.15) in the surface sediments along the Skeffling transect, indicate a significant peak (0.188 mg g^{-1}) between stations B and C (Amos, pers comm). However, this does not necessarily indicate high binding strengths. Difficulties have been encountered in quantitatively relating total biomass, or some biological parameter to sediment stabilisation, in part due to species variations and the variable effectiveness when considering differing sediments. At present, sediment

stabilisation appears to owe more to the mechanism of stabilisation , for example, coatings or threads (Paterson, 1997), rather than any easily quantifiable bio-product, such as EPS.

The higher levels of carbohydrates between B and C, coincide with a high spatial variability in the critical erosion velocity (Widdows, pers comm). The degree of bioturbation, using *Macoma balthica* and *Nereis diversicolor* as indicators, between these stations follows the general trend in decreasing from a peak at B to D, where the contribution from *Nereis* is minimal and *Macoma* is three times less effective (Davey, pers comm). The resuspension behaviour of sediment within the ridge / runnel system (B / C) reflects the variability in the biological and morphological characteristics of this zone. This is seen in the differences between the ebb tides at station C on the 4th and 7th April. Whereas the tidal range and current velocities for C2 are lower than C1, both the particle concentration and size are greater (Figure 5.5). Although wind strength and direction differ significantly from the 4th (C1), the bed morphology, was also found to be different and is likely to contribute more to the sediment behaviour observed at C2.

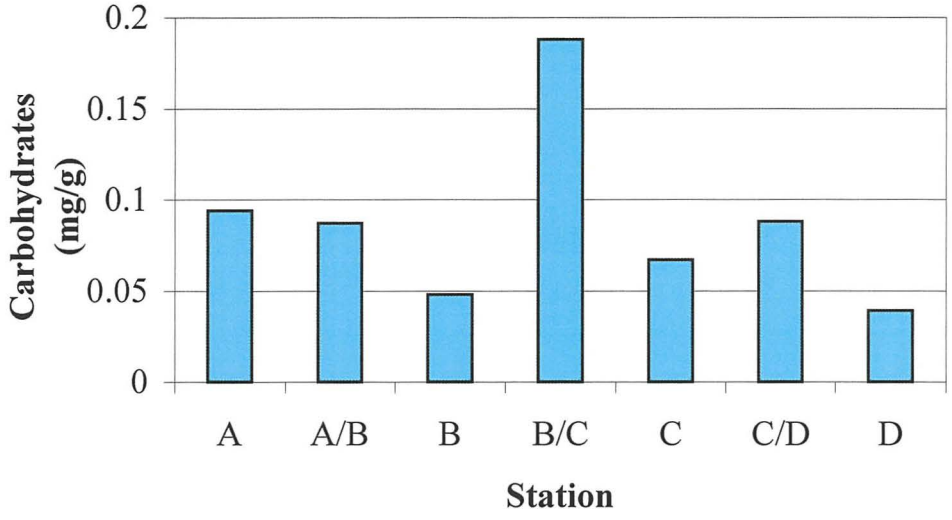

Figure 5.15 Surface sediment carbohydrate concentrations along the shore normal transect at Skeffling (Amos, pers comm).

Station C was located at the edge of the ridge / runnel system which extended from station B to station C. At stations on the edge of the ridge / runnel system, minor differences in the location of the barge when positioned on site led to marked differences in the underlying bed topography, depending upon whether the barge was on or off the ridges. Station C1 was situated over a relatively flat intertidal area, but C2 was located between a series of runnels to the north and a flatter expanse to the south. This difference in topography resulted in a differing maximum particle concentration from station C1 (0.55 g l^{-1})to C2 (0.7 - 0.8 g l^{-1}). Particle size increased from 50 μm (C1) to 300 μm (C2), with particles up to 1000 μm being observed (Figure 5.5). This is in contrast to the size of particles measured using a laboratory based Coulter Counter. The range of sizes being determined as 8 to 22 μm (Widdows, pers comm), indicating an inherently fragile particle population. It is likely that this reflects the localised source of material within the runnel system. The runnels remain waterlogged throughout the aerial exposure of the intertidal flat at low water, the sediments are characteristically sandier, with lower critical erosion thresholds. They may also be a form of sink during high water slack for large aggregates

and faecal pellets, whilst also providing a low energy environment for the settling of material over low water, depending upon the runnel's water content. Therefore, despite lower current velocities, resuspension of material on the ebb is greater on the 7th (C2) due to the localised bed topography and its influence upon the nature of the bed and resuspended sediment, elements absent at C1 and D.

The anomalous observations during the ebb tide of C2 contrast with the lack of size variation at stations D and C1, for the flood as well as ebb. With the tides changing from spring to neap, the current velocities upon the flood tide are seen to fall (0.5 m s^{-1} to 0.35 m s^{-1}, station C). This is also seen in the lessening of suspended particle concentration during these events (0.6 g l^{-1} falling to 0.3 g l^{-1}, station C). During this period median particle sizes at stations C and D, ranged between 60 and 100 μm, with no significant change in response to resuspension events. Away from the influence of the runnels, the background advective component is comparable in size to the material observed during resuspension events, such as the initial incursion of the flood tide. Comparable observations were carried out using POST, a sediment transport instrumentation package comprising EM current meters and MOBS, one week after the Par-tec100 deployment. This also indicated that the initial flood (prior to 0.3 m water depth) is characterised by high current velocities (0.5 to 0.6 m s^{-1}) and suspended solids (0.8 g l^{-1}) (M. Christie, pers comm). Similar particle size information was also gathered during the deployment of INSSEV, a video based size and settling velocity determination system. It's deployment at station D during the flood tide of the 20th April showed the existence of a relatively fine particle population, extending between 30 μm (20 μm being the limit of INSSEV's resolution) and 200 μm, with settling velocities in the range 0.2 to 3 mm s^{-1}. Two samples collected during the flood when current velocities were 0.13 and 0.31 m s^{-1}, show little variation in the spread of particles. The size range of the particles

observed with INSSEV and the stability of their size distribution is in agreement with the Par-tec100 findings.

Unlike the ebb, the aerial exposure of the sediment during low water means that there is no easily mobilised sediment source. Photic migration of biota upon exposure of the intertidal flat and the subsequent excretion of polymeric substances will contribute to Bio-stabilisation of the sediment surface, sometimes taking the form of algal mats. Such processes were observed at Skeffling. Given the nature of the material available for resuspension, the mode of resuspension, particle stripping for example, under such conditions will differ from that seen at C2 on the ebb and could account for the lack of large particles seen over the ridges at C and at station D.

Discussion

6.1 Introduction

The study of suspended particle characteristics and sediment transport behaviour has important environmental and economic implications, as outlined in Chapter 1. Because of its importance in the mechanics of estuarine floc aggregation and disaggregation processes, the measurement of particle size is fundamental to the modelling of cohesive sediment transport (Teisson, 1997). By providing high spatial and temporal measurements of undisturbed floc size, the data presented in this work represents not only a valuable source of material for the quantitative determination of flocculation processes, but also represents a means for the future development of flocculation and transport models.

6.2 Instrument Capabilities and Performance

6.2.1 Suitability Based upon Laboratory Evaluation

The Par-tec 100 is principally an instrument designed for the process industries. As such it is not necessary that it be as accurate as other forms of particle size analysis, it's purpose being purely to detect changes in particle populations rather than provide definitive size comparisons. However, because it is focussed upon industries whereby high particle concentrations are involved, with particles possessing a wide variety of compositions and shapes, this provides considerable potential for it's use in the estuarine environment. Initial evaluation of the instrument highlighted some key benefits, such as the rapidity of analysis, the range of particle concentrations that it could work reliably in and it's similar treatment of diverse particles. Despite discrepancies in its absolute sizing capabilities in comparison to other techniques, a calibration technique was devised which considerably improved the Par-tec 100 response. This method of calibration has also been applied successfully to the Partec200 (Phillips & Walling, 1998), an FBRM instrument which differs in the optical arrangement. Following the development of the calibration technique and given the considerable advantages over existing in-situ techniques, the Par-tec 100 was modified for use in the field.

Adaptation of the Par-tec 100 for in-situ operation took the form of transferring the power supply and signal processing circuit boards to the submersible unit. The boards were extracted from the control unit and secured around a steel frame, which was then connected to the stripped down probe unit (Figure 3.9). The modified probe unit and associated electronics were housed in a cylindrical, water tight PVC casing. Connections to the surface PC and power supply were provided by a 32 core cable. Pressure testing of

the instrument housing was carried out for depths down to 200m, subsequent deployments from RRS Challenger attained depths of 100m without water ingress and with good communication with surface instrumentation.

6.2.2 Field Performance

Part of this study has involved the evaluation, adaptation and construction of a focused beam reflectance based in-situ particle sizing instrument. The deployment of this instrument in estuarine and coastal waters allowed the acquisition of suspended particle size data, from the low salinity region of a macro tidal estuary, to marine conditions at the estuarine limit. Particle size characterisation was also carried out as part of the LISP (UK) experiment. This novel sizing method proved capable of making non-disruptive measurements of fragile aggregates in waters with SPM concentrations extending from 4 mg l^{-1} to 100 g l^{-1}.

Problems of floc breakage have been avoided by using the in-situ Par-tec 100 and comparisons between in-situ particle size distributions and discrete samples analysed after storage (Figure 6.1) clearly show that fragile aggregates are disrupted during manipulation. Calibration of the Par-tec 100 instrument using a number of calibration standards was undertaken and proved to be valid for a number of calibration materials. The instrument was found to be capable of accurate and repeatable size determination over a wide range of SPM concentrations, 10 mg l^{-1} to > 50 g l^{-1}. Such particle concentrations as these and those encountered in the Humber estuary (100 g l^{-1}), lie beyond the scope of any other in-situ particle sizer are present (Bale & Morris, 1987; Eisma et al, 1990; Fennessey et al, 1997). One other advantage lay in the rapid real time analysis. Analysis of in-situ particle size and the production of a size distribution could be carried out in 8 to 25 s depending upon particle number. Allied with the small volume of the sensing zone, this provides a

high degree of spatial and temporal resolution and makes it possible to measure rapid fluctuations in the size distribution of particles brought about by a change in the turbulent regime. These high frequency size measurements are compatible with high frequency turbulence and sediment monitoring instrumentation such as POST (Christie, pers comm).

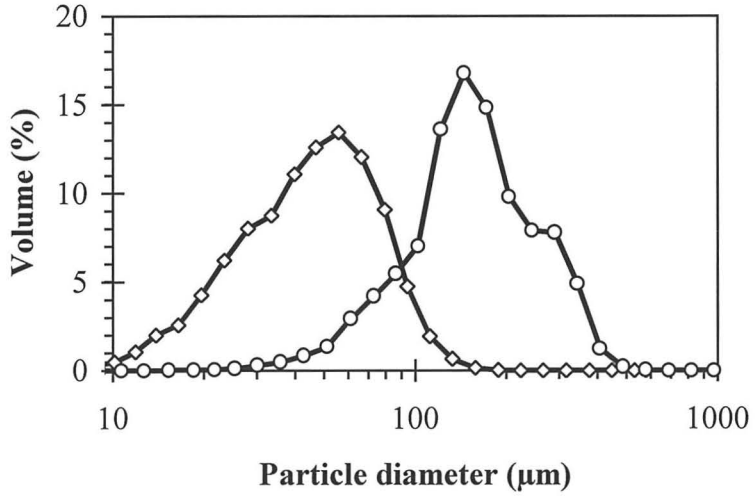

Figure 6.1 *Particle size distributions obtained from the Ouse turbidity maximum at Selby in September 1995. The solid circles represent an in-situ measurement and the open diamonds a laboratory measurement of a discrete sample using the same instrument. The distribution median values are 442 and 49 µm, respectively.*

6.3 Ouse - Humber Estuary Deployments

Deployment of the Par-tec 100 in the Humber estuary and in Spurn Bight provided a comprehensive suite of data describing the spatial and temporal variation in suspended particle size. The physical factors which influence particle size distributions, SPM concentration, shear, salinity and current velocity, were also determined (R. Uncles & J. Stephens, Plymouth Marine Laboratory). Previous studies in the Tamar, Scheldt and

Gironde estuaries (Bale, 1987; Eisma, 1991; Gibbs, 1989) revealed that the size of the largest particles encountered over a tidal cycle were consistently around 500 μm. The only exception occurred in the Ems, where particles up to 1 to 4 mm were observed (Eisma, 1983; van Leussen, 1993). Eisma (1991b) also reports maximum floc sizes in the Rhine and Gironde to be 600 to 800 μm, with the majority of flocs being greater than 200 to 300 μm. Our observations in the Humber estuary, showed that maximum floc sizes over a tidal cycle vary from 300 to 600 μm in the upper estuary and from 150 to 200 μm in the lower estuary (Station HW5) and plume region (Table 6.1). There is considerable variation in the size of the largest particles for each tidal cycle, with the largest being seen around high or low water depending upon the position of the turbidity maximum relative to the station. The largest particles overall, were seen in the fluid mud layer situated at Blacktoft (August), where median particle sizes in excess of 1000 μm occurred.

Station	**Date**	**Range of 95th percentiles (μm)**	**Peaks in 95th percentiles (μm)**
Selby	24th August 1995	200-600	700
Selby	28th September 1995	350	650
Blacktoft	21st August 1995	400-600	> 1000
Blacktoft	26th September 1995	300	600-800 ca. HW
Whitton channel	18th July 1995	200 LW-800 HW	
Whitton channel	17th March 1995	350-400	600-800 ca. HW
Humber bridge	16th March 1995	300-400	600-700
SG23	8th June 1995	100-200	
SG10	7th June 1995	150-200	
SG13	3rd June 1995	175-200	
SG24	4th June 1995	150-250	
HW5	4th November 1994	150	400-800 ca. LW
HW5	22nd January 1995	150-200	300-400 ca. LW
HW7	7th November 1994	140-160	

HW - High water, LW - Low water.

Table 6.1 Variation in the 95th percentile particle diameters at stations along the Ouse-Humber Estuary, November 1994 to September 1995.

6.4 Particle Size Variations at Stations along the Ouse-Humber Estuary

Based upon the observed pattern of SPM concentration and particle size there exist five distinct regions within the estuary:

1. The upper estuary, above the turbidity maximum. (Selby, August & September)
2. The turbidity maximum. (Blacktoft, September)
3. The upper estuary, below the turbidity maximum. (Blacktoft, August; Whitton, Humber Bridge & SG23)
4. The lower estuary. (HW5)
5. The Humber plume.(SG10, 13 & 24; HW7)

Sediment transport surveys were carried out in the early part of 1994 (Uncles, 1996) and axial surveys carried out at the time of Par-tec 100 deployments (Uncles, pers comm). These revealed that the turbidity maximum in the Humber estuary extends from salinities of 1 ppt to 10 ppt at high water and from 0.5 ppt to 10 ppt at low water. Although the central peak of the turbidity maximum was not encountered during the course of this work, Blacktoft (September) was located marginally down-estuary where salinity's of 3.4 ppt at low water were encountered, whilst Selby (September) was located up-estuary with salinities of 0.7 ppt at high water.

Particle settling and resuspension was evident at all stations within regions 1 and 3, occurring around high water slack. In region 1, SPM concentrations were seen to rise on the flood tide following a tidal bore (more pronounced in September) which generated intense near bed current shear. However, maximum SPM concentrations on the flood occurred one hour after maximum current velocities and maximum near bed shear, as was observed by Uncles (1996), this indicates advection of material from down-estuary. Despite high concentrations close to the bed, the largest particles were seen in the mid

waters, away from high levels of shear. As currents decreased towards slack water, clearance of the water column began, larger flocs were generated in the mid waters and settled into the near bottom waters by the end of slack water (Figure 6.3). The surface waters were thus left with low concentrations of SPM of small size. Resuspension of particles from the bottom waters upon the ebb tide lagged current velocity. As near bottom shear rises, large particles are resuspended into the upper water column, as near bed SPM concentration increases. A shear pulse was observed at Selby (September, 12:30 hrs) extending into the surface waters and coincident with a near bottom SPM concentration peak and floc size minima, suggesting a high degree of floc disruption. Figure 6.2 shows the variability in floc size distributions over high water slack. Most significant is the difference between 11:25 hrs, the end of settling and 11:56 hrs, the onset of resuspension, with a 118 μm shift in the median particle diameter from 289 μm to 407 μm, as large flocs are resuspended. The ebb tide was characterised by decreasing SPM concentrations and floc sizes, with intense current shear present in the mid to bottom waters. No settling occurred over low water slack.

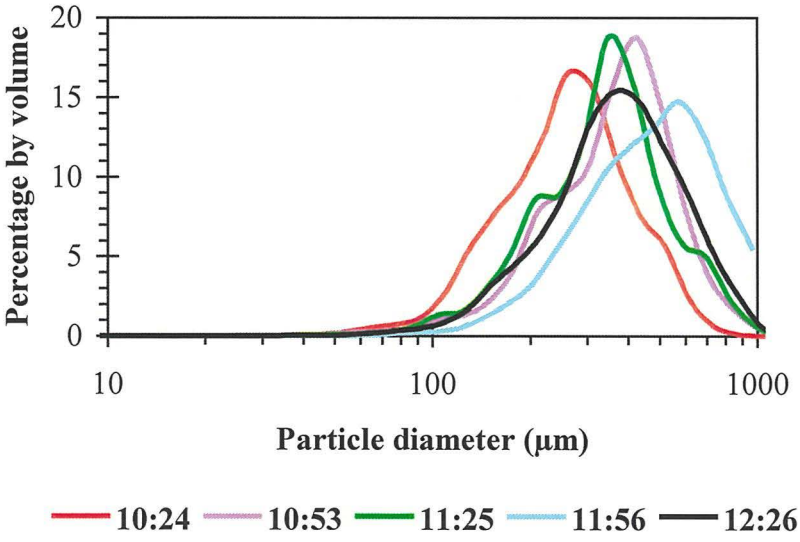

Figure 6.2 Temporal variation in particle size spectra at Selby (September) around high water slack (11:00 hrs) at 1.75 m above the bed.

The characteristics of suspended particles in the main body of the turbidity maximum may be inferred from the observations made at Blacktoft in September. This site was located relatively close to the turbidity maximum's peak SPM concentration at Booth Ferry Bridge, 20 km up-estuary (Uncles, pers comm). SPM concentrations were seen to rise from 1 - 2 g l^{-1} at high water to 26 g l^{-1} close to the bed over low water. There was no stratification of SPM or salinity observed and poor indication of particle settling. The size of suspended particles was found to be inversely proportional to SPM concentration and although this relationship had been seen at other stations, it was generally related to high shear causing floc disruption (Selby, September). Whereas at Blacktoft, shear remained low throughout. The size of particles over high water slack reached 400 μm, whilst over low water particles of 90 μm were measured. This agrees well with laser diffraction particle size measurements from the turbidity maximum of the Tamar estuary (Bale, 1989), where particle sizes on the ebb tide fell to 64 - 84 μm (at < 1 ppt, 1 g l^{-1}) from 400 μm around high water slack (at 11 ppt). Other studies in the Tamar, Gironde and Ems estuaries have also shown that smaller flocs exist in the turbidity maximum than exist down-estuary (Gibbs, 1989; Eisma, 1991a; McCabe, 1992), although the floc sizes in the turbidity maximum for these studies range from 6 & 160 μm in the Tamar, 20 μm in the Gironde and 125 -160 μm in the Ems.

The stations of Whitton channel (March & July) and the Humber bridge all have features in common with regions 1 and 2. Over high water the process of particle settling / water column clearance followed by resuspension upon the ebb tide was observed. This differed from the pattern seen at Selby, in that the initial stages of resuspension were characterised by a greater number of small particles than seen at the onset of settling (Figure 6.3). The size distribution of particles was also found to be multimodal, with four distinct component populations, P0, P1, P2 & P3. The modal peak P1 (440 μm) exhibits

the largest reductions over high water, contributing most to water column clearance (Figure 6.3). Resuspension upon the ebb modifies the distribution such that P3 and P2 are replaced by R3. The cause of the size distribution multimodality is due to the source of the component modes. The difference between high and low water particle size distributions (Figure 6.4) reflects upon the source material for the respective particle populations. Smaller particles exist in the turbidity maximum tail during low water with larger particles in less turbid waters outside of the turbidity maximum's influence (salinity > 5 - 10 ppt), during high water. This pattern of larger flocs seaward of the turbidity maximum has also been reported in the Tamar, Gironde and several other European estuaries (Gibbs, 1989; Eisma, 1991a; McCabe, 1992).

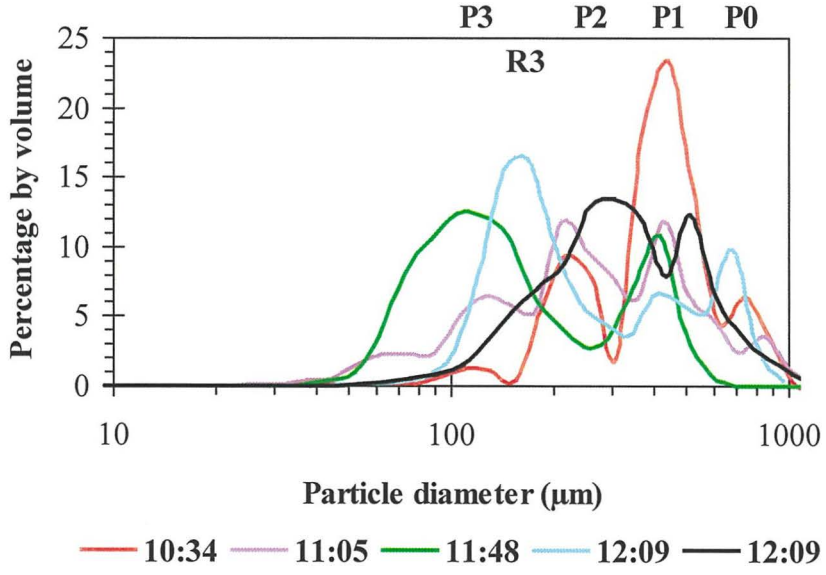

Figure 6.3 Temporal variation in particle size spectra at Whitton channel (September) around high water slack (11:00 hrs) at 3.2 m above the bed. P1, P2 & P3 represent component modes in the size distribution during settling (10:34 - 11:48). R1 & R2 represent component modes in the size distribution during resuspension (11:48 - 12:09).

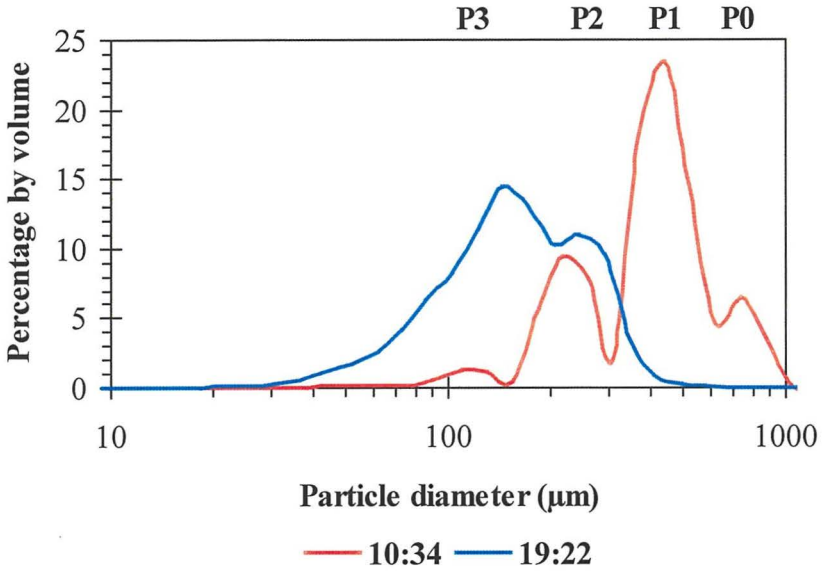

Figure 6.4 Variation in particle size spectra at Whitton channel (September) for high (11:00 hrs) and low water slack (19:00 hrs).

Particle sizes in the lower estuary (region 4) exhibit a pattern which is contrary to region 3, with the largest particles occurring over low water slack. In general however, the particles are smaller (200 -300 µm over high water) and present in lower concentrations, by an order of magnitude. The clearance of the water column over high water is less pronounced, there being no indication that particle settling and resuspension occurs. Beyond the mouth of the estuary, region 5, the variation in particle size and concentration over a tidal cycle is small (60 to 150 µm median diameters, 4 to 30 mg l^{-1}). Particle sizes near to the bed increase over high water, caused by the settling of low numbers of relatively large particles (up to 200 µm, median diameter), their resuspension occurring upon the ebb tide. SPM concentrations only began to rise when the front of Humber plume was encountered as low water approached. Particle sizes over low water were comparable with high water, with the exception of SG24 & HW7, where SPM

concentrations remained very low throughout the tidal cycle, an indication of the lesser influence of the plume in this region.

6.5 LISP (UK) Intertidal Mudflat Deployment

A further demonstration and evaluation of the Par-tec 100s capabilities was achieved during the deployments as part of LISP (UK). Deployment took place over the intertidal mudflat of Spurn Bight with two stations being sampled, each on two occasions. Of particular interest was the sediment behaviour during the inundation and exposure of the mudflat on the flood and ebb tides.

Due to the nature of the bed sediments and topographical features of the mudflat, there was a considerable variation between the size of suspended particles resulting from the inundation and exposure of an intertidal mudflat. These features also gave rise to a high degree of site specificity. Critical erosion thresholds exhibited a gradual decrease seaward from station C to D, though were considerably reduced by up to 50% with in the runnels of the pronounced ridge/runnel system between B and C. This was attributed to the effect of water cover over low water reducing the photic migration of biota to the surface. With reduced migration the excretion of extracellular polymeric substances (EPS) was also reduced. Given the importance of ESP in sediment stabilisation (Black, 1994) the effect upon the sediment of the runnels was observed in the lower critical shear stresses. This proved significant upon the ebb tide, when high concentrations of large particles were resuspended from runnels during the last 0.5 m of water and transported seaward. Over the flatter expanses of the ridge crests and at station D the particles brought into suspension during the flood and ebb tides were seen to be considerably smaller. This reflects the greater degree of biotic stabilisation of the bed sediment.

6.6 The Future of FBRM in Estuarine Particle Size Analysis

The Par-tec 100 represents a considerable advance in particle sizing techniques applicable to the estuarine and marine environment. It's deployment in the Ouse-Humber Estuary and on the intertidal mudflats of Spurn Bight has proven it to be highly adaptable. It has provided particle size information in a range of conditions that were beyond other techniques. Yet there is still the potential for further development. With advances in battery technology the instrument will prove readily adaptable to remote long term deployment given the ease of it's use and data storage / management. Having been already deployed under tow in the Tamar Estuary, it's incorporation into towed rigs and packages is also something which is easily achievable.

This work has highlighted several areas within this field of research that are important in bringing about a better understanding of the role of particle flocculation in sediment transport. The high spatial variability of particle behaviour, on the scale of mm's and km's requires that measurements of particle characteristics and their driving forces (current velocity, shear and SPM concentration) are measured on similar scales. The combination of focused beam reflectance technology with miniature optical backscatter sensors and 3D electro-magnetic current velocity measurements in systems such as POST (Christie, pers comm), could provide unparalleled information regarding the variability of particle size and behaviour on small temporal and spatial scales. This would provide the information for the development of the second topic of future research that of particle size modeling. The data gathered in this field program showed a high degree of similarity with Dyer's (1989) conceptual model, but disagreed with the laboratory findings of Tsai (1987) and Burban (1989). Further research in this area is required which combines the control of

the laboratory experimentation with the validity of the field measurements. This could be carried out, again through the combination of focused beam reflectance technology with other existing technologies, in this case the type of portable flumes used by Widdows (1988). This would effectively take the very same laboratory experiments carried out by Tsai (1987) and Burban (1989) into the field. Particular attention needs to be drawn to the quantification of the shear induced aggregation and disaggregation processes, which have not been included in previous models (Equation 6.1). One other relationship that requires improved understanding is the role of particular mucopolysacharide compounds in determining particle size through their effect upon the mode of aggregation and the floc binding strength.

CONCLUSIONS

7.1 Laboratory and Field Evaluation of the Par-tec100

A commercially available FBRM instrument which can measure particles within the range 2 to 1,000 μm has been successfully adapted to allow in-situ measurements of particle size distributions in estuarine waters. Following evaluation and calibration, particle size measurements using this device compared well with existing sizing technology. FBRM technology offers significant advantages over other systems for in-situ particle sizing. Reproducible and accurate particle size determination is possible between 10 mg l^{-1} and 50 g l^{-1}. From field deployments no discernible degradation in the quality of analysis was seen at up to 100 gl^{-1}. There was no indication of floc breakage as a result of the FBRM technique irrespective of current velocities. A high degree of spatial and temporal resolution was achieved using this technique due to the small measuring volume and rapidity of analysis.

7.2 Particle Size Variation in the Humber Estuary

Deployment of the Par-tec100 in the Humber Estuary confirmed the presence of large macro-flocs (200 to 700 μm diameter) over a semi-diurnal tidal cycle which were similar in size to those observed in the Rhine and Gironde Estuaries by Eisma et al (1991a) using an in-situ photographic technique.

Five distinct regions were identified within the Humber Estuary from in-situ particle size data and SPM behaviour. These are located in:

A. **The upper estuary above the turbidity maximum**. Characterised by high concentrations of large (up to 500 μm median diameter) particles derived from the turbidity maximum region, these readily flocculate and settle over high water, but are resuspended upon the ebb tide. At low water, small particles at relatively low concentrations are seen which do not flocculate or settle.

B. **The turbidity maximum**. Characterised by very large concentrations of small particles (24 gl^{-1}, 90 μm median diameter). At low water (<4 ppt) no flocculation or settling occurred. At higher salinities, over high water large particles (400 μm median diameter) were seen at low (2 gl^{-1}) concentrations.

C. **The upper estuary below the turbidity maximum**. Essentially the same as above, with the exception that the particle concentrations and sizes were larger over low water.

D. **The lower estuary**. Characterised by particle concentrations an order of magnitude lower than C (gradual decrease). Particle sizes were also lower than C over low water (200 to 300 μm median diameters). Particle concentrations and sizes were lowest over high water.

E. **The Humber plume**. Characterised by low particle concentrations and size (4 to 30 mg l^{-1}, 60 to 150 μm median diameters). Particle sizes and concentrations were generally highest over low water.

7.3 Size Characteristics of Suspended Particulates on an Intertidal Mudflat

The size of suspended particles resulting from the inundation and exposure of an intertidal mudflat showed strong site specificity. The local ridge / runnel topography at station C gave rise to spatial variation in bed sediment critical erosion thresholds. This proved significant upon the ebb tide, when high concentrations of large particles were resuspended from runnels during the last 0.5 m of water and transported seaward. Resuspension of smaller particles on the ridges of station C and at station D during the ebb and flood tides, reflects the greater degree of biotic stabilisation of the bed sediment. In the runnels, the effect of maintaining water cover over low water reduces photic migration of biota to the surface. This hinders bed stabilisation and causes the runnels to posses low critical erosion thresholds.

7.4 Predictors of Particle Sizes in Estuaries and Coastal Waters

The size distribution of suspended particles showed great spatial and temporal variability. Multivariate analysis indicated the relationship between median particle diameter and the controlling environmental factors to be site specific and too complex for such a simple treatment. However, median particle diameter did vary proportionally with particle concentration and inversely with shear stress. The manner of this relationship is seen to confirm the conceptual model of Dyer (1989). Elucidation of the factors which control natural particle size distributions will require more detailed observations and the use of modelling techniques to resolve the various inter-related processes which influence particle size in natural waters.

7.5 Suggestions for Future Work

In-situ focused beam reflectance particle sizing provides a method to study the size characteristics of estuarine particles at high temporal and spatial resolution and will contribute to a better understanding of the factors that influence estuarine particle characteristics and transport. The instrument could be readily adapted for use on longer-term and wide area deployments either as a bottom lander or on towed instrumentation packages.

The small measuring volume and resolution of the Par-tec 100 lends itself to further research into particle flocculation / breakup dynamics. In association with small-scale measurements within in-situ flumes incorporating MOBS and EMS current detectors, considerable advances in the understanding of particle dynamics may be achieved.

APPENDICIES

APPENDIX 1 Methods

Gravimetric Determination of Suspended Particle Concentration.

Samples for the determination of suspended solids concentration in the field, were taken as close as was possible to the probe tip of the Par-tec100. This helps to minimise errors induced by fluctuations in the suspended load, or from instantaneous bursts of resuspended material. The size of the sample was determined by the amount of material in suspension. In the case of work carried out in the upper reaches of the Humber estuary, a 50ml sample was sufficient, whereas along the Holderness coast samples in excess of 500ml would be required.

Determination of suspended solids requires a filter paper of pre-determined dry weight, through which a sub-sample is filtered. The paper and residue are subsequently dried until all water has been evaporated, determined by checking the weight of the drying paper, such that when there is no further decrease in its weight, it can be said to be dry. In practice, not all of the papers are repeatedly checked, rather a paper with significantly more in the way of residue is used as an indicator. Once dried the papers are re-weighed, the difference from the pre-filtered weight divided by the volume filtered determines the concentration (C) (Equation A1.1).

$$\frac{W_1 - W_2}{V_s} \qquad [A1.1]$$

The weights W1 and W2 represent the dried pre-filtered and dried filtered weight of the filter paper, respectively, in mg. Vs, represents the volume of the filtered sub-sample,

litres. The papers used during this study were nominally 0.45um Whatman GFC papers. Filtration took place over a conical flask, a vacuum was applied to this flask in order to assist gravitational filtration.

Production of Natural Particle Calibration Materials.

In the earliest determination of the Par-tec100's effectiveness, it was necessary to use as many particle types and sizes as possible. These took the form of polystyrene beads, pollen grains, glass beads and natural sediments. Whilst the size of the commercially available standards could be used as a calibration check for the Par-tec100, they did not represent the nature of naturally occurring estuarine sediments. In order to provide a useful means of size comparison, directly related to the intstruments intended use, a series of standards were produced from estuarine bed sediment gathered in the low salinity regions of the Tamar and Plym estuaries, Devon. It was necessary to fractionate these sediments, narrowing their naturally diverse size distribution to provide a number of well sorted, unimodal standards. These, when analysed with proven sizing techniques would provide a means to quantify the Par-tec100's accuracy in sizing natural particles. The sediment was subjected to ultrasonic and hydrogen peroxide treatment, in order to eliminate aggregation and reduce the population to inorganic primary constituents.

Production of samples with narrow size distributions followed a simple method of settling fractionation. The settling velocities of particles corresponding to the upper and lower size limits of the desired size fractionations were calculated (Equation A1.2).

$$W_s = \frac{(\rho_s - \rho_w)\, g\, d^2}{18\, \eta} \qquad [A1.2]$$

As an example, if the fraction 10 to 20 μm was to be produced, then the settling velocities of the lower and upper, 10 and 20 μm respectively, would be 6.682×10^{-3} cm s^{-1}

and 2.672 x 10^{-2} cm s^{-1}. Where, in the above equation, Ws representing settling velocity is derived using the particles effective density (ρ_s - ρ_w), with ρ_w, the density of water being equal to 1 g cm^{-3}, ρ_s, the density of the particle being equal to 2.2 g cm^{-3}. The gravitational constant, g, is taken as 981 cm s^{-2}, the liquid viscosity, η, is taken as 0.009779 cp and d represents the particle diameter (cm).

Fractionation of a relatively dilute (< 1000 mg l^{-1}), well mixed sample took place in a metre long settling column. The sediment was allowed to settle for periods determined from the settling time of the upper size limit over 50 cm. Once this period had elapsed, then the upper 50 cm of the column could be classed as being less than a given size. The column was first left to allow all particles greater than 6 μm to settle out of the first 50 cm, this portion was siphoned off and stored, with the process being repeated for the remaining fluid (the lower 50 cm in the column) after further dilution. After four repetitions, the decanted fluid was added to one vessel and allowed to settle out over 2 days, the volume was then reduced by siphon, to one litre without disturbing the sediment, this sub-sample being classed as <6 μm. The process of settling over 50 cm was repeated for the remainder of the original sample, using a period appropriate for 10 μm particles. In this way, by sub-sampling and decreasing the settling time in increments a series of size fractions were produced, these being; <6, 6-10, 10-20, 10-30, 20-40, 40-60, 60-100, 100-200, 200-300, 300-600 & >600 μm.

Calculation of Particle Settling Velocities from Particle Size Data

There are several empirically derived formulae for the derivation of particle settling velocities from particle size (Section 2.5). Without confirmation in the form of field derived in-situ particle settling velocities, the application of such formulae to this dataset may lead to mis-interpretation. However, it was possible to derive particle settling

velocities from water clearance rates. This was done with the aid of SURFER, a mapping and contouring application for Windows. Periods in spatial and temporal particle size profiles were selected for application of the method based upon the criteria that the dominant mechanism affecting the observed size of suspended particles at a given moment was particle settling. Only periods that were affected by settling were chosen, so as to exclude possible confusion with advection and resuspension.

Once the station and period were chosen, only two meeting the specified criteria (Figures 3.5 & 3.15), vertical slices through the contoured data were taken for 600 second time intervals. These produced ASCII files, 'time files', containing depth (10 cm increments) with the corresponding median particle size (μm) for a given time. Using a set of particle settling velocity channels extending from 150 μm to 400 or 300 μm in increments of 25 μm, the depth of the median particle size corresponding to the settling velocity channel (for example 150 μm) was calculated for each time file. This provided, for each channel, a change in depth of the median size corresponding to the channel with time (Table A.1).

		time (0 = 17:20) (s)						Ws
	Depth (m)	0	600	1200	1800	2400	3000	(mm s^{-1})
median	150				0.04	0.07	0.1	0.058
diameter	175		0	0.08	0.15	0.19	0.26	0.106
(μm)	200	0.03	0.12	0.19	0.27	0.46	0.86	0.179
	225	0.16	0.25	0.39	0.81	0.95	1.1	0.329
	250	0.34	0.54	0.89	1.05	1.19	1.34	0.354
	275	0.66	1	1.16	1.3	1.5	1.61	0.350
	300	1.24	1.51	1.87	1.94	1.94	1.94	0.389

Table A1.1 : Calculation of particle settling velocities from Par-tec100 data. Humber Bridge 16/03/95 at high water (18:00 hrs)

Using this information, an example of which is seen above (Table A.1), the settling velocity of each channel may be calculated as;

$$w_s = \frac{(D_1 - D_2)}{(T_2 - T_1)} \qquad [A.1.3]$$

where D_1 is the depth at time T_1, D_2 is the depth at time T_2 and w_s is the settling velocity.

APPENDIX 2 Supplementary Particle Characteristics

Determination of Particle Effective Densities

Several workers have demonstrated the inverse relationship that exists between a particles equivalent spherical diameter (ESD) and its density. With increasing floc size, the floc density approaches that of water, indeed Gibbs (1983b; 1989) observed that estuarine flocs consist of up to 90% pore water (50 to 90% for marine aggregates (McCave, 1984).

McCave (1984) proposed a power-law expression for a flocs effective density (ρ_e) and the ESD (d_f), assuming that at <1 μm, ρ_e = 1gcm^{-3} whilst at >1200 μm, ρ_e = 0.003gcm^{3}. ρ_e may then be given by :

$$\rho_e = d_f^{0.42} \qquad \text{for } d_f < 50\ \mu m \qquad [A2.1]$$

$$\rho_e = d_f^{-1.3} \qquad \text{for } 50\ \mu m < d_f < 1200\ \mu m \qquad [A2.2]$$

These relationships are based upon Tambo and Watanabe's (1979) results concerning clay-iron, clay-magnesium and biological flocs. Ani et al (1991) proposed a similar relationship ;

$$\rho_e = a\, d_f^{-k} \qquad [A2.3]$$

with values for a and k of 1.02×10^{-4} to 8.3×10^{-4} and 0.76 to 1.92, respectively, for floculated Tamar sediment. For a 500 μm floc this would provide an effective density of, 0.26 to 9.94×10^{-4} gcm^{-3}, compared to that of McCave's, 9.58×10^{-4} gcm^{-3}. However all experimental results are prone to deviations in flow through the floc, surface texture and shape (Gibbs et al, 1985), resulting in a considerable scatter of floc densities (for a 500 μm ESD, 0.76 to 0.999 gcm^{-3} (Ani et al , 1991) or 0.994 gcm^{-3} (McCave, 1984)). Also, equation 2.5 is valid only in the range 200 μm < df < 800 μm.

Using sediment from the Chesapeake Bay, Gibbs (1985) demonstrated that; assuming a particle sphericity of 0.8 (Tambo & Watanabe, 1979) or 1 , caused an over-estimation of floc densities. A cylinder of length to width ratio of 1.6:1 was found to provide the best fit.

Determination of Particle Settling Velocities

For a spherical particle, diameter d, in a laminar flow regime, its settling velocity (ws) is described by Stoke's law;

$$w_S = \frac{g\,(\rho_S - \rho)\,d^2}{18\mu} \qquad [A2.4]$$

where; g = gravitational constant (980 cms^{-2}), $(\rho_S - \rho)$ = effective density (gcm^{-3}, μ = viscosity ($g\ cm^{-1}\ s^{-1}$). However, Stoke's law is relevant only at Reynolds numbers (Re) of less than unity ($Re = d\ \rho_S\ w_S/\mu$ (Lerman et al , 1974) and is invalid for particles with ESD's > 1000 μm (Re = 0.98 at 1000 μm) (McCave, 1984).

Settling velocity models were derived experimentally (Whitehouse, 1960; McLaughlin, 1961; Migniot, 1968; van Leussen, 1988) through the use of settling velocity

tubes (SVT's). A general relationship between w_s and the SPM concentration (C) was found (van Leussen, 1988):

$$w_S = k\, C^m \qquad [A2.5]$$

The constants k and m are attributed with various values according to the author, although early results placed m between 1.33 and 1. In the field, Owen tubes and other hybrid SVT's have revealed similar power-law relationships (Barton et al , 1991; van Leussen, 1988 and references therein) with k and m values varying between 0.15 to 35.8 and 0.92 to 2.9, respectively, independent of salinity and showing high site and temporal specificity. Such wide variations in the constants may be due to the removal of natural shear upon capture and the spatial/temporal variability of particle nature.

Additional floculation is found to occur in SVT's (Puls, 1988) and correction is needed, hence Puls' m values are considerably greater than those of other workers (uncorrected data). Barton's data which shows a wide scatter of m values for SPM in the Tamar estuary (2.9 to 0.92) may have been brought about through variations in the sticking efficiency of particles upon collision. Such that particles with a high efficiency show pronounced aggregation, resulting in an m value of 0.92, whilst low efficiency particles exhibit limited aggregation and return a high m value consistent with Puls. Variations in sticking efficiency may be brought about either by changes in the nature of the particle organic coatings (Barton's data was collected over several seasons) or the quantity of organic material present. Kranck and Milligan (1980) observed variations in settling velocity related to organic content, with a 1:1 ratio of inorganic to organic matter volume providing the largest settling velocities, and assuming equal collision efficiencies, the greatest degree of aggregation.

Recent *in-situ* evaluation of a drifting video-microscope system, has yielded floc settling velocities in the Ems, of 0.5 to 2.0mms^{-1} for 200-500 μm flocs (at 20-50 mgl^{-1}) and 1 to 7mms^{-1} for 400-1100 μm flocs (van Leussen, 1993).

Determination of Floc Binding Strength

The size of suspended particulates is determined by their physical strength in response to the hydrodynamics of the suspending medium. The binding strength of the floc components, in relation to the magnitude of the turbulent field, thus determines whether aggregate breakage will occur. The maximum floc size (d_{max}) generally takes the form (van Leussen, 1988) ;

$$d_{max} = a\ v_o^{-m} \qquad [A2.6]$$

where; v_o is the void fraction, a is dependent upon the total shear strength of the floc and b upon the breakage mechanism and floc strength. A further dependence being; as to whether $d_f \gg l$. Van Leussen supposes that because floc porosity increases greatly in line with size, the shear strength decreases significantly. Krone (1963) observed such a decrease in the shear strength of flocs, in relation to their degree of aggregation, i.e. primary particles > floculi > flocs > floc aggregates (aggregation orders 0,1,2 & 3, respectively) (van Leussen, 1988).

More recently, Ani et al (1991) observed that floc strength actually increases in line with floc size, whereas the strength per particle bond decreases. Tambo & Hozumi (1979) describe the binding strength of a floc (B) as ;

$$B = s\ (1 - e)\ d^2 \qquad [A2.7]$$

where; s is the strength parameter and e the floc void ratio. As individual flocs settled in a column of variable energy dissipation rate (ε), Ani et al (1991) calculated the

average stress (B/d^2) at the point of rupture. At this point the energy dissipation rate becomes critical (ε_c) (Eqn. A2.8). They were able to show that whilst large flocs have more brittle bonds and thus break rapidly at ε_c, they rupture at higher levels of shear stress.

$$B/d^2 = r\,(\varepsilon_c\, d)^{2/3} \qquad [A2.8]$$

The provision of greater shear strength by organic material in the binding of flocs, over the suppression of the electrical double layer and subsequent binding by Van der Waals forces, has been recognised (van Leussen, 1988 and references therein). Hence within the low salinity region of an estuary, the mobilisation of mucopolysaccharides from bacteria and algae, is of greater importance than the increase in cations, across the salt water interface, in the flocculation of riverine material (Eisma et al, 1986; 1991; 1991a).

References

Abarnou A., Avoine J., Dupont J.P., Lafite R. & Simon S. 1987. Role of suspended sediments on the distribution of PCB in the Seine estuary (France).- Cont. Shelf Res. 7 (11/12): 1345-1350.

Agrawal Y.C. & Pottsmith H.C. 1994. Laser diffraction particle sizing in STRESS. Continental Shelf Research 14 (10/11): 1101-1121.
Agrawal Y.C., McCave I.N. & Riley J.B. 1991. Laser diffraction size analysis..- in: Principles, methods and application of particle size analysis, Ed. J.P.M. Syvitski. p.209-221, Cambridge.

Ahrens M.A. & Peters R.H. 1991. Patterns and limitations in limnoplankton size spectra.- Can. J. Fish. Aquat. Sci. 48(10): 1967-1978.

Alldredge A.L. & Gotschalk C.C. 1988. In-situ settling behaviour of marine snow.- Limnol. Oceanogr. 33: 339-351.

Alldredge A.L. & Silver M.W. 1988. Characteristics, dynamics and significance of marine snow. Prog. Oceanogr. 20(1): 41-82.

Allen G.P. 1973. Etude des processes sedimentaires dans l'estuaire de la Gironde.-Mem. Inst. Geol. Bassin D'Aquitaine No. 5.

Allen G.P., Courtois G., Jeaneau B. & Klingbiel A. 1980. Etude des deplacements des sables sur une barre d'estuaire - Banc de Plassac, Gironde - a l'aide d'un traceur radioactif.- in: Bull. Instit. Bassin D'Aquitaine, 11 (2): 281-315.

Amos C.L. & Long B.F.N. 1980. The sedimentary character of the Minas Basin, Bay of Fundy.- in: The coastline of Canada: Littoral processes and shore morphology, Ed. S. McGann. Geological Survey of Canada.

Ani S. Al, Dyer K.R. & Huntley D.A. 1991. Measurement of the influence of salinity on floc density and strength.- Geo-Marine Letters 11: 154-158.

Asper V.L., Deuser W.G., Knauer G.A. & Lohrenz S.E. 1992. Rapid coupling of sinking particle fluxes between surface and deep ocean waters.- Nature 357(6380): 670-672.

Bale A.J. & Morris A.W. 1987. *In-situ* measurement of particle size in estuarine waters.- Estuarine, Coastal and Shelf Science 24: 253-263.

Bale A.J. & Morris A.W. 1991. *In-situ* size measurements of suspended particles in estuaries and coastal waters using Laser Diffraction.- in: Principles, Methods and Applications of Particle Size Analysis, Ed. J.P.M Syvitski: 197-208, Cambridge.

Bale A.J., Barret C.D., West J.R. & Oduyemi K.O.K. 1989. Use of *in-situ* Laser Diffraction particle sizing for particle transport studies in estuaries.- in: Developments in Estuarine and Coastal Study Techniques, EBSA 17 Symposia, Eds. J. McManus & M. Elliot, Olsen & Olsen.

Bale A.J., Morris A.W. & Howland R.J.M. 1984. Size distributions of suspended material in the surface waters of an estuary as measured by Laser Fraunhofer Diffraction.- in: Transfer Processes in Cohesive Sediment Systems, Eds. W.R. Parker & D.J.J Kinsman, Plenum.

Barretta-Bekker 1992. Encyclopedia of Marine Science.

Barton M.L., Stephens J.A., Uncles R.J. & West J.R. 1991. Particle fall velocities and related variables in the Tamar estuary.- in: Estuaries and Coasts: Spatial and Temporal Intercomparisons, Eds. M. Elliot & J.P. Ducrotoy: 31-36, Olsen & Olsen.

Bryant R. & Williams D.J.A. 1983. Characteristics of suspended cohesive sediment of the Severn Estuary, UK.- Can. J. of Fish. and Aquat. Sci. 40 (Suppl. 1): 96-101.

Burban P.Y., Lick W. & Lick J. 1989. Flocculation of fine-grained sediments in estuarine waters.- Journal of Geophysical Research 94 (C6): 8323-8330.

Carling P.A. 1978. The influence of creek systems on intertidal sedimentation. Unpublished PhD thesis. University of Wales.

Chanut J.P. & Poulet S.A. 1982. Short term variability of the size spectra of suspended particles in a rapidly changing environment.- Estuarine, Coastal and Shelf Science 15: 497-513.

Colijn F., Admiraal W., Baretta J.W. & Ruardij P. 1987. Primary production in a turbid estuary, the Ems-Dollard: Field and model studies.- Cont. Shelf Res. 7 (11/12): 1405-1410.

Collins M.B., Amos C.L. & Evans G. 1981. Observations of some sediment-transport processes over intertidal flats, the Wash, UK.,- Spec. Publ. int. Ass. Sediment. 5: 81-98.

Costello D.K., Carder K.L., Betzer P.R. & Young R.W. 1989. In-situ holographic imaging of settling particles: applications for individual particle dynamics and oceanic flux measurements.- Deep-Sea Res. 36A: 1595-1605.

Dobereiner C. & McManus J. 1983. Turbidity maximum migration and harbour siltation in the Tay Estuary.- Can. J. of Fish. and Aquat. Sci. 40 (Suppl. 1): 117-129.

Dyer K. 1988. Fine sediment transport in Estuaries.- in: Physical Processes in Estuaries, Eds. J Dronkers & W van Leussen, Springer-Verlag.

Dyer K.R. 1978. The balance od suspended sediment in the Gironde and Thames estuaries.- in: Estuarine Transport Processes, Ed. B.J. Kjerve, p.135-145, Uni. SC Press, Columbia.

Edzwald J.K., Upchurch J.B. & O'Melia C.R. 1974. Coagulation in estuaries.- E.S.T. 8 (1): 58-63.

Eisma D. 1986. Flocculation and de-flocculation of suspended matter in estuaries.- Neth. J. of Sea Res. 20 (2/3): 183-199.

Eisma D. 1991a. Particle size of suspended matter in estuaries.- Geo-Marine Letters 11: 147-153.

Eisma D., Bernard P., Cadee G.C., Ittekkot V., Kalf J., Laane R., Martin J.M., Mook W.G., van Put A. & Schuhmacher T. 1991b. Suspended matter particle size in some West-European estuaries; Part 1: particle size distribution.- Neth. J. of Sea Res. 28 (3): 193-214.

Eisma D., Bernard P., Cadee G.C., Ittekkot V., Kalf J., Laane R., Martin J.M., Mook W.G., van Put A. & Schuhmacher T. 1991c. Suspended matter particle size in some West-European estuaries; Part 2: A review on floc formation and breakup.- Neth. J. of Sea Res. 28 (3): 215-220.

Eisma D., Schuhmacher T., Boekel H., van Heerwaarden J., Franken H., Laan M., Vaars A., Eijgenraam F. & Kalf J. 1990. A camera and image-analysis system for *in-situ* observation of flocs in natural waters.- Neth. J. of Sea Res. 27 (1): 43-56.

Fennessy M.J., Dyer K.R. & Huntley D.A. 1994. INSSEV: An instrument to measure the size and settling velocity of flocs in-situ.- Marine Geology 117: 107-117.
Francois R.J. & van Haute A.A. 1985. Structure of Hydroxide flocs.- Water Research 19 (10): 1249-1254.

Gentien P., Lunven M., Lehaitre M. & Dunvent J.L. 1995. *In-situ* depth profiling of particle sizes. Deep-Sea Research 4 (8): 1297-1312.
Gibbs R.J. & Konwar L.N. 1983. Sampling of flocs using Niskin bottles.- Environmental Science Technology 17: 374-375.

Gibbs R.J. 1985. Estuarine flocs: Their size, settling velocity and density.- Journal of Geophysical Research 90 (C2): 3249-3251.

Gibbs R.J., Konwar L. & Terchunian A. 1983b. Size of flocs suspended in Delaware Bay.- Can. J. of Fish. and Aquat. Sci. 40 (Suppl. 1): 102-104.

Gibbs R.J., Tshudy D.M., Konwar L. & Martin J.M. 1989. Coagulation and transport of sediments in the Gironde Estuary.- Sedimentology 36: 987-999.

Handyside T. 1977 An investigation of hydrodynamical parameters of an intertidal sand flat in the Loughor Estuary using velocity gradient profiles. Unpublished Bsc disertation. Dept of Oceanography. University College of Swansea.

Hansen D.V. & Rattray M. Jr. 1966. New dimensions in estuarine classification.- Limnol. Oceanogr. 11: 319-326.

Harnby N. et. al. 1982.- in: Mixing in the Process industries, Eds. N. Harnby, A Nienow & M.F. Edwards, Butterworths, London.

Harnby N., Edwards M.F. & Nienow A. Mixing in the Process Industries, Butterworth and Heinemann.

Hart B.T. 1982. Uptake of Trace metals by sediments and suspended particulates: A review.- Hydrobiologia 91: 299-313.

Head P.C. 1976. Organic processes in estuaries.- in: Estuarine Chemistry, Eds. J.D. Burton & P.S. Liss: 54-92, Academic Press.

Hobbel E.F., Davies R., Rennie F.W., Allen T., Butler L.E., Waters E.R., Smith J.T. & Sylvester R.W. 1991. Modern Methods of On-Line Size Analysis for Particulate Process Streams,- Part. Part. Syst. Charact. 8: 29-34.

Hunter K.A. & Liss P.S. 1982. Organic matter and the surface charge of suspended particles in estuarine waters.- Limnol. and Ocean. 27 (2): 322-335.

Jantschik R., Nyffeler F. & Donard O.F.X. 1992. Marine particle size measurement with a stream scanning laser system. Marine Geology. 106(3): 239-250.

Jay D.A. & Smith J.D. 1988. Residual circulation in and classification of shallow stratified estuaries.- in: Proc. Int. Symp. Physical Processes in Estuaries, Eds. Dronkers & van Leuessen, p.21-41, Springer.

Jiang Q. & Logan B.E. 1991. Fractal dimensions of aggregates determined from steady state size distributions.- Env. Sci. Tech. 25: 2031-2038.

Jilan Su & Kangshan W. 1986. The suspended sediment balance in Chang Jiang Estuary.- Estuarine Coastal Shelf Science 23: 81-98.

Johnson R.G. 1974. Particulate matter at the sediment-water interface in coastal environments.- Journal of Marine Research 32 (2): 313-329.

Jones S.E., Bale A.J. & Law D.J. 1996. Temporal and spatial variability of in-situ suspended particle size in the Humber Estuary and Holderness coastal zone. NERC Final Report, December 1996. GR3/09469.

Jones S.E., Bale A.J. & Law D.J. 1995. Development of an instrument for in-situ particle sizing using laser backscatter spectrometry. NERC Final Report, March 1995. GST/02/665 SIDAL Special Topic.

Kolmogorov A.N. 1941. The local structure of turbulence in incompressible viscous fluid for very large Reynolds numbers.- C R Acad. Sci. URSS, 30: 301.

Kranck K. & Milligan T.G. 1980. Macroflocs: Production of marine snow in the laboratory.- Mar. Ecol. Prog. Ser. 3: 19-24.

Kranck K. & Milligan T.G. 1991. Grain size in Oceanography.- in: Principles, methods and application of particle size analysis, Ed. J.P.M. Syvitski. p.332-345, Cambridge.

Kranck K. & Milligan T.G. 1992. Characteristics of suspended particles at an 11-hour anchor station in San Fransisco Bay, California.- Journal of Geophysical Research 97 (C7): 11373-11382.

Krishnappan B.G. 1991. Modelling of cohesive sediment transport.- Int. Symp. on the transport of suspended sediments and its mathematical modelling, Florence, Sept.pp 433-466.

Krone R.B. 1963. A study of rheologic properties of estuarial sediments.- Techn. Bull. 7, Comm. of Tidal Hydraulics, US Army Corps of Eng. WES Vicksburg.

LASENTEC 1: Operations Manual for the PAR-TEC 100, LASENTEC, Bellevue, USA.

LASENTEC 2 : Preston Geren, LASENTEC Consultant, Statistical Study - Effect of variable chords on Particle Measurement, LASENTEC, Bellevue, USA.

Law. D.J. & A.J. Bale (1998). In-situ characterisation of suspended particles using focused-beam, laser reflectance particle sizing. In: Black, K.S., Paterson, D.M. & Cramp, A. (eds) Sedimentary Processes in the Intertidal Zone. Geological Society, London, Special Publications, 139, 57-68.

Law D.J., Bale A.J. & Jones S.E. 1997. Adaptation of focused beam reflectance measurement to in-situ particle sizing in estuaries and coastal waters. Marine Geology 140, pp47-59.

Lerman A., Lal D. & Dacey M.F. 1974. Stoke's settling and chemical reactivity of suspended particles in natural waters.- in: Suspended Solids in Water, Ed. R.J. Gibbs, p.17-47, Plenum.

Lick W. & Lick J. 1988. Aggregation and disaggreagtion of fine grained lake sediments.- J. Great Lakes Res. 14(4): 514-523.

Maddux W.S. & Kanwisher J.W. 1965. An *in-situ* particle counter.- Limnol. and Ocean. 10: R162-168.

McCabe J.C., Dyer K.R., Huntley D.A. & Bale A.J., 1992, The variation of floc sizes within a turbidity maximum at spring and neap tides.- in: Coastal Engineering, Proc. 23rd Int. Conf., Venice, Ch. 243.

McCave I.N. 1983. Particulate size spectra, behaviour and origin of nepheloid layers over the Nova Scotian Continental Rise.- Journal of Geophysical Research 88: 7647-7666.

McCave I.N. 1984. Size spectra and aggregation of suspended particles in the deep ocean.- Deep Sea Research 31 (4): 329-352.

McCave I.N. 1991. Laser diffraction size analysis.- in: Principles, Methods and Applications of Particle Size Analysis, Ed. J.P.M Syvitski: 119-128, Cambridge.

McLaughlin R.T. 1961. Settling properties of suspensions.- Trans. Am. Soc. Civ. Eng. 126: 1734-1767.

Migniot C. 1968. Etude des propietes physiques de differents sediments tres fins et de leur compartement sous des actions hydrodynamiques.- La Houille Blanche 7: 591-620.

Morris A.W., Bale A.J., Howland R.J.M., Millward G.E., Ackroyd D.R., Loring D.H. & Rantala R.T.T. 1986. Sediment mobility and its contribution to trace metal cycling and retention in a macrotidal estuary.- Wat. Sci. Tech. 19: 111-119.

Nakagawa H. & Nezu I. 1975. Turbulence of open channel flow over smooth and rough beds.- Proc. Jpn Soc. Civ. Eng. 241: 155-168.

Neihof R.A. & Loeb G.I. 1974. Dissolved organic matter in seawater and the electric charge of immersed surfaces.- Journal of Mar. Res. 32: 5-12.

Nienow A.. 1982.- in: Mixing in the Process industries, Eds. N. Harnby, A Nienow & M.F. Edwards, Butterworths, London.

Officer C.B. 1981. Physical dynamics of estuarine suspended sediments.- Mar. Geol. 40: 1-14.

Parker D.S., Kaufman W.J. & Jenkins D. 1972. Floc break-up in turbulent flocculation process.- J. San. Eng. Div. Proc. Am. Soc. 98: 79-99.

Paterson D.M.. 1997. Biological mediation of sediment erodibility: ecology and physical dynamics.- in: Cohesive Sediments, Eds. N. Burt, R. Parker & J. Watts. Wiley.

Phillips J.M. & Walling D.E., 1999. The particle size characteristics of fine-grained channel deposits in the River Exe Basin, Devon, UK, Hydrological Processes, 13 : 1-19

Phillips J.M. & Walling D.E.,. 1998. Calibration of a Par-Tec 200 laser back-scatter probe for in-situ sizing of fluvial suspended sediment, *Hydrological Processes,* 12 : 221-31.

Puls W., Kuehl H. & Heymann K. 1988. Settling velocity of mud flocs: results of field measurements in the Elbe and the Weser estuary.- in: Proc. Int. Symp. Physical Processes in Estuaries, Eds. Dronkers & van Leuessen, p.404-424, Springer.

Rowle A. 2000. Basic Principles of Particle Size Analysis. Technical Paper. Malvern Instruments, Worcestershire, UK.

Schubel J.R. & Kana T.W. 1972. Agglomeration of fine grained suspended sediment in Northern Chesapeake Bay.- Power Tech. 6: 9-16.

Sheldon R.W., Prakash A. & Sutcliffe Jr. W.H. 1972. The size distribution of particles in the ocean.- Limnol. and Ocean. 28 (3): 327-339.

Syvitski J.P.M. 1991. in: Principles, methods and application of particle size analysis, Ed. J.P.M. Syvitski, Cambridge.

Tambo N. & Hozumi H. 1979. Physical characteristics of flocs- II. Strength of floc.- Water Research 13 (5): 421-428.

Tambo N. & Watanabe Y. 1979. Physical characteristics of flocs- I. The floc density function and aluminium floc.- Water Research 13 (5): 409-420.

Teisson C. 1997. A review of cohesive sediment transport models.- in: Cohesive Sediments, Eds. N. Burt, R. Parker & J. Watts. Wiley.

Thorn M.F.C. & Burt T.N. 1983. Sediments and metal pollutants in a turbid estuary.- Can. J. of Fish. and Aquat. Sci. 40 (Suppl. 1): 207-215.

Tsai C.H., Iacobellis S. & Lick W. 1987. Flocculation of fine grained lake sediments due to a uniform shear stress.- J. of Great Lakes Res. 13 (2): 135-146.

Uncles R.J., Elliott R.C.A. & Weston S.A. 1985. Observed fluxes of water and suspended sediment in a partly mixed estuary.- Estuarine Coastal Shelf Science 20: 147-167.

Uncles R.J., Stephens J.A. & Harris C. 1997. Seasonal variability of subtidal and intertidal sediment distributions in the Humber-Ouse Estuary.- in: Sedimentary Processes in the Intertidal Zone, Eds. K. Black, D. Patterson & A. Cramp. Geological Society, London, Special Publications, 139.

Uncles R.J., Stephens J.A. & Plummer D.H. 1996. Sediment characteristics and transport in the Humber-Ouse Estuary, UK, during May 1994.- Physics of Estuaries and Coastal Seas, Ed. J. Dronkers. Proceedings PECS 96.

UNESCO 1988. River inputs to Ocean systems: Status and recommendations for research; Final report of SCOR Working Group 46.

van Leussen W. & Cornelisse J.M. 1993. The determination of the sizes and settling velocities of estuarine flocs by an underwater video system.- Neth. J. of Sea Res. 31 (3): 231-241.

van Leussen W. 1987. Aggregation of particles, settling velocity of mud flocs: A review.- in: Physical Processes in Estuaries, Eds. J. Dronkers & W. van Leussen.

van Leussen W. 1991. Fine sediment transport under tidal action.- Geo-Marine Letters 11 (3/4): 119-126.

Whitehouse U.G., Jeffrey L.M. & Debrecht J.D. 1960. Differential settling tendencies of clay minerals in saline waters.- in: Clays & Clay Minerals 7th, Ed. A. Swineford, Pergamon Press.

Williams R.A., Peng S.J. & Naylor A. 1992. *In-situ* measurement of particle aggregation and breakage kinetics in a concentrated suspension,- Powder Technology.

Winant C.D. & Bratkovich A. 1977. Structure and mixing within the frontal region of a density current.- in: Sixth Australian Hydraulics and Fluid mechanics Conf., Adelaide. p.68-69.